UNIVERSIDADE FEDERAL DO ESPÍRITO SANTO

CENTRO DE CIÊNCIAS DA SAÚDE

PROGRAMA DE PÓS-GRADUAÇÃO EM BIOTECNOLOGIA

EDUARDO DE ALMEIDA SOARES

PROTEÔMICA QUANTITATIVA, LIVRE DE MARCAÇÃO, DE *CARICA PAPAYA L.* EM RESPOSTA À DOENÇA MELEIRA DO MAMOEIRO

VITÓRIA

2016

RENORBIO

PROGRAMA DE PÓS-GRADUAÇÃO EM BIOTECNOLOGIA

EDUARDO DE ALMEIDA SOARES

PROTEÔMICA QUANTITATIVA, LIVRE DE MARCAÇÃO, DE *CARICA PAPAYA L.* EM RESPOSTA À DOENÇA MELEIRA DO MAMOEIRO

VITÓRIA

2016

EDUARDO DE ALMEIDA SOARES

PROTEÔMICA QUANTITATIVA, LIVRE DE MARCAÇÃO, DE *CARICA PAPAYA L.* EM RESPOSTA À DOENÇA MELEIRA DO MAMOEIRO

Tese de doutorado apresentada ao Programa de Pós-graduação em Biotecnologia da Rede nordeste de Biotecnologia (RENORBIO) do ponto focal Universidade Federal do Espírito Santo (UFES), como parte dos requisitos necessários à obtenção do título de Doutor em Biotecnologia.

Orientadores: Prof.ª Dr.ª Patricia Machado Bueno Fernandes e Prof. Dr. Silas Pessini Rodrigues

VITÓRIA

2016

Dados Internacionais de Catalogação-na-publicação (CIP)
(Biblioteca Setorial do Centro de Ciências da Saúde da Universidade Federal do Espírito Santo, ES, Brasil)

Soares, Eduardo de Almeida, 1985 -
S676p Proteômica quantitativa, livre de marcação, de *Carica papaya L.* em resposta à doença meleira do mamoeiro / Eduardo de Almeida Soares – 2016.
130 f. : il.

Orientador: Patricia Machado Bueno Fernandes.
Coorientador: Silas Pessini Rodrigues.

Tese (Doutorado em Biotecnologia) – Universidade Federal do Espírito Santo, Centro de Ciências da Saúde.

1. Proteômica. 2. Espectrometria de Massas. 3. Carica. I. Fernandes, Patricia Machado Bueno. II. Silas, Pessini Rodrigues. III. Universidade Federal do Espírito Santo. Centro de Ciências da Saúde. IV. Título.

CDU: 61

---

renorbio
rede nordeste de biotecnologia

Programa de Pós-Graduação em Biotecnologia

Ponto Espírito Santo - Universidade Federal do Espírito Santo

DEFESA DE TESE

ALUNO: EDUARDO DE ALMEIDA SOARES

TÍTULO DO PROJETO: "Proteômica quantitativa, livre de marcação, de *Carica papaya* L. em resposta à doença da meleira do mamoeiro".

PROFESSOR ORIENTADOR: Patrícia Machado Bueno Fernandes

BANCA EXAMINADORA:	**CONCEITO**	**ASSINATURA**
Profª. Drª. Patrícia Machado Bueno Fernandes RENORBIO/UFES (Orientadora)	Suficiente	
Prof. Dr. Silas Pessini Rodrigues UFRJ (Coorientador)	Suficiente	
Prof. Dr. José Aires Ventura RENORBIO/UFES (Titular)	Suficiente	
Profª. Drª. Diolina Moura Silva UFES (Titular)	Suficiente	
Prof. Dr. Wanderson Romão IFES (Titular)	Suficiente	
Profª. Drª. Russolina Benedeta Zingali UFRJ (Titular)	Suficiente	

TIPO DE SESSÃO: Aberta

DIA: 29 de Junho de 2016

HORÁRIO: 14h00

LOCAL: Universidade Federal do Espírito Santo – Núcleo de Biotecnologia, 2°andar, auditório.

AGRADECIMENTOS

À CAPES, CNPq, FAPES e FINEP, pelo financiamento do projeto.

À FAPES e ao Programa Ciências sem Fronteiras, pelas bolsas de estudo concedidas.

Ao Incaper e sua equipe, pela concessão da área em campo experimental de Sooretama-ES e auxílio no experimento de campo.

À RENORBIO e UFES, pelo oferecimento deste programa de pós-graduação.

Aos membros da banca examinadora, que aceitaram avaliar este trabalho.

Aos professores José Aires, Silas Rodrigues, Antonio Alberto e Patricia Fernandes, por toda orientação e oportunidades de aprendizado.

A todos os integrantes da equipe do LBAA.

À professora Leslie M. Hicks e toda sua equipe, por terem me recebido em seu laboratório e auxiliado com recursos financeiros, técnicos e intelectuais durante a execução das análises de LC-MS/MS.

A todos os familiares, amigos e colegas que, direta ou indiretamente, contribuíram para o meu processo de formação.

Ao meu irmão Renato e minha noiva Carolina, por toda cumplicidade e paciência nos períodos de ausência ou nas noites de lâmpada acesa.

DEDICATÓRIA

A Deus e à Santa mãe Maria, por todas as oportunidades oferecidas, pelas derrotas motivadoras de mudanças benéficas e promotoras da expansão da zona de conforto, e por todas as vitórias alcançadas.

À minha mãe Maria de Almeida, cujos esforços de guerreira me conduziram até aqui e me guiarão pela eternidade.

ESTRUTURA DA TESE

Esta tese é apresentada em formato de Artigo Científico. As listas de figuras e Referências contêm as ilustrações e referências bibliográficas apresentadas na introdução deste trabalho de tese.

RESUMO

Mamão (*C. papaya L*), uma fruteira de grande importância econômica mundial, vem sofrendo acentuados prejuízos na pré colheira, sobretudo pela doença da meleira do mamoeiro, caracterizada pela exsudação espontânea de látex aquoso e fluido que oxida e se acumula como uma substância pegajosa nos órgãos da planta. A meleira é causada por uma infecção sinérgica dos vírus PMeV e PMeV2, cuja sintomatologia manifesta-se apenas após a transição juvenil-adulto (florescimento) das plantas. Para entender os mecanismos de interação planta-vírus e a dependência fenológica da sintomatologia, o proteoma de *C. papaya* foi acessado, via proteômica quantitativa livre de marcação baseada em LC-MS/MS, para plantas infectadas e não infectadas (controle) em quatro diferentes idades (3, 4, 7 e 9 meses pós germinação). Este estudo possibilitou a identificação de 1.623 e a quantificação de 1.609 proteínas, cuja comparação de abundâncias revelou uma elevação nos níveis de proteínas relacionadas à fotossíntese e redução nos níveis de proteínas relacionadas à atividade de *caspase-like*, *26S-proteassomo* e remodelamento de parede celular no período assintomático e anterior ao florescimento. O surgimento dos sintomas após o florescimento (7 meses pós germinação) foi acompanhado de uma redução no acúmulo de proteínas relacionadas à fotossíntese e elevação no acúmulo de proteínas relacionadas ao metabolismo de carboidratos, lipídeos, aminoácidos, proteínas, nucleotídeos e ácidos nucléicos. Além do acúmulo de proteínas envolvidas em resposta a estresse, sinalização, transporte e parede celular. O somatório destes resultados aponta para a existência de um mecanismo de tolerância incompleto na fase assintomática e anterior ao florescimento, com uma sinalização por ROS via cloroplasto seguido de um sistema ineficiente na contenção da infecção sistêmica pela depleção da atividade caspásica, proteassomal, e de remodelamento de parede. Este mecanismo de tolerância incompleta no pré florescimento ganha novos elementos com a transição juvenil-adulto, que com uma infecção já instalada de forma sistêmica, origina os sintomas de resposta necrótica e clorótica tardios. A inibição nos processos de remodelamento de parede celular anteriores ao florescimento acarreta no enfraquecimento dos laticíferos, que se rompem quando em desequilíbrio osmótico, gerando o aspecto melado do mamoeiro doente.

Palavras chave: Proteômica quantitativa livre de marcação. Espectrometria de massas. *Papaya meleira vírus.*

ABSTRACT

Papaya (*C. papaya L*), a fruit of great economic importance worldwide, which has suffered huge preharvest losses, mainly by papaya sticky disease (PSD), characterized by spontaneous exudation of aqueous and fluid latex, which oxidizes and accumulates as a sticky substance in the organs of the plant. PSD is caused by a synergic infection by PMeV and PMeV2 viruses, whose symptoms arise only after the juvenile-adult transition (flowering) of the plants. To understand the plant-virus interaction mechanisms and the phenological dependence of the symptoms onset, the *C. papaya* proteome was accessed by LC-MS/MS-based label-free quantitative proteomic approach for infected and uninfected (control) plants in four different ages (3, 4, 7 and 9 months post germination). This study permitted the identification of 1,623 and quantification of 1,609 proteins, whose the abundances comparison showed an increased levels of photosynthesis related proteins and decreased levels of proteins related to caspase-like activity, 26S-proteasome and cell wall remodeling during asymptomatic stage (prior to the flowering). The onset of the symptoms after flowering (7 months after germination) was accompanied by a reduction in the accumulation of proteins related to photosynthesis and increase in accumulation of proteins related to the metabolism of carbohydrates, lipids, amino acids, proteins, nucleotides and nucleic acids. In addition, was observed the accumulation of proteins involved in response to stress, signaling, transport and cell wall. The sum of these results supports the hypothesis of an incomplete tolerance mechanism in the asymptomatic phase (prior to flowering), with a chloroplast ROS signaling followed by ineffectiveness in containing systemic infection by activity depletion of caspase-like, proteasome, and cell wall remodeling. This incomplete tolerance mechanism at pre flowering acquire new elements with the juvenile-adult transition, which the installed systemic infection, delivers the late and ineffective symptoms of necrotic and chlorotic response. Inhibition in cell wall remodeling processes prior to flowering weakens the latex vessels, which bursts during the PSD osmotic imbalance, leading the sticky aspect of the diseased papaya plants.

Keywords: Label-free quantitative proteomics. Mass spectrometry. *Papaya meleira virus.*

LISTA DE FIGURAS

Figura 1. Flores e frutos de mamoeiro masculino, feminino e hermafrodito 13

Figura 2. Imagens de microscopia eletrônica de varredura de látex de frutos de mamão 14

Figura 3. Micrografia eletrônica de vírions de PMeV purificados..... 15

Figura 4. Análise de preparação viral purificada de látex de plantas de mamão apresentando sintomas severos de meleira 16

Figura 5. Látex de frutos de mamão..... 17

Figura 6. Sintomas da meleira..... 18

Figura 7. Representação esquemática dos quatro modelos de imunidade vegetal .. 20

Figura 8. Esquema de amplitude de resistência ou susceptibilidade a doenças..... 22

Figura 9. Translocação de sinais imunológicos móveis 24

Figura 10. Representação esquemática da infecção viral em plantas 27

Figura 11. Visão esquemática de classes de proteínas que são moduladas 28

Figura 12. Reações luminosas da fotossíntese..... 29

Figura 13. Estrutura de UPS e tipos de proteólises proteassomo-dependente..... 31

Figura 14. Estrutura da parede celular primária 34

Figura 15. Fluxograma das técnicas mais utilizadas em proteômica 36

Figura 16. Diferenças entre proteoma quantitativo com e sem marcação 37

SUMÁRIO

1. INTRODUÇÃO 11

1.1. *Carica papaya L.*, uma fruteira de grande importância econômica 11

1.2. A doença meleira do mamoeiro 12

1.3. Mecanismos comuns na interação compatível planta-vírus 19

1.4. Fotossíntese na infecção viral de plantas 26

1.5. Sistema ubiquitina/proteassomo 26S na interação planta-vírus 30

1.6. Parede celular e o processo infeccioso 33

1.7. Proteômica quantitativa "*Gel-free, label-free*" 35

2. OBJETIVOS 38

2.1. Objetivo Geral 38

2.2. Objetivos Específicos 38

3. ARTIGOS DERIVADOS DA TESE 40

3.1. Manuscrito 1 40

3.2. Manuscrito 2 68

4. CONSIDERAÇÕES FINAIS 111

5. REFERÊNCIAS 114

ANEXO 1 118

ANEXO 2 124

ANEXO 3 128

1. INTRODUÇÃO

1.1. *Carica papaya L.*, uma fruteira de grande importância econômica

A fruticultura tropical é detentora de uma grande fatia da produção, comercialização e consumo mundial de alimentos. Dentre as fruteiras de maior produção mundial encontra-se o mamão (*C. papaya*), com uma produção de 12 milhões de toneladas de frutos frescos em 2013, sendo o Brasil o segundo maior produtor deste fruto (“FAOSTAT”, 2016).

Com uma fase juvenil de aproximadamente 3 meses e um tempo de geração de apenas 9 meses, o mamoeiro possui um genoma de 372 Mb organizados em 9 pares de cromossomos (ARUMUGANATHAN; EARLE, 1991). O mamoeiro é uma planta trióica, podendo produzir flores masculinas, femininas ou hermafroditas dependendo do sexo da planta (Figura 1), sendo as plantas hermafroditas de preferência agronômica no Brasil por sua maior produtividade e facilitações de pós-colheita. Quando o mamoeiro atinge a maturidade sexual, a produção de flores é continuada em paralelo à produção de frutos durante o ano inteiro (MING; YU; MOORE, 2007).

Originário da Bacia Amazônica Superior, o cultivo de mamão estende-se por toda região tropical e subtropical do planeta (KIM et al., 2002), cujos cinco maiores produtores são Índia, Brasil, Indonésia, Nigéria e México (“FAOSTAT”, 2016). As doenças, sobretudo as viroses, causam sérios prejuízos aos produtores de mamão, chegando a destruir por completo alguns pomares. Dentre as doenças de maior impacto para o mamoeiro está a meleira do mamoeiro (ABREU et al., 2015), de ocorrência oficialmente relatada no Brasil e México (KITAJIMA et al., 1993; PEREZ-BRITO et al., 2012). Somados, Brasil e México perfizeram o total de 19% (2,3 milhões de toneladas) da produção mundial de mamão em 2013. Somente no Brasil, cerca de 20% dos pomares de mamão são afetados pela meleira do mamoeiro, causando

grandes prejuízos pré-colheita (VENTURA et al., 2003), o que denota para a dimensão do impacto desta doença no cenário mundial.

1.2. A doença meleira do mamoeiro

Os primeiros relatos da sintomatologia da meleira do mamoeiro, como a exsudação espontânea de látex com alta fluidez, foram associados à estresse abiótico por déficit hídrico ou desbalanceamento de cálcio e boro no solo, resultando na deficiência de absorção destes elementos (CORREA et al., 1988; NAKAGAWA; TAKAYAMA; SUZUKAMA, 1987). Posteriormente, a etiologia biótica foi revelada e atribuída a partículas virais isométricas de aproximadamente 50nm de diâmetro, com a presença de fita dupla de RNA (dsRNA) e restritas às células dos laticíferos (KITAJIMA et al., 1993), onde encontram-se fortemente aderidas às partículas de látex (Figura 2). Posteriormente foi confirmada a transmissão dos sintomas pela inoculação destas partículas virais em mamoeiros sadios e realizada a descrição oficial do *Papaya meleira virus* (PMeV) como um vírus de partículas isométricas, sem taxonomia definida, com aproximadamente 45nm de diâmetro (Figura 3) e portador de um genoma de dsRNA de aproximadamente 12kbp e um capsídeo formado por duas proteínas de 14 e 25kDa (MACIEL-ZAMBOLIM et al., 2003). O sequenciamento do genoma de *C. papaya* possibilitou a criação de um banco de dados no portal *Phytozome* com aproximadamente 135 Mb organizados em 4.114 contigs contendo 27.332 loci e 27.796 transcritos codificantes para proteínas (MING et al., 2008).

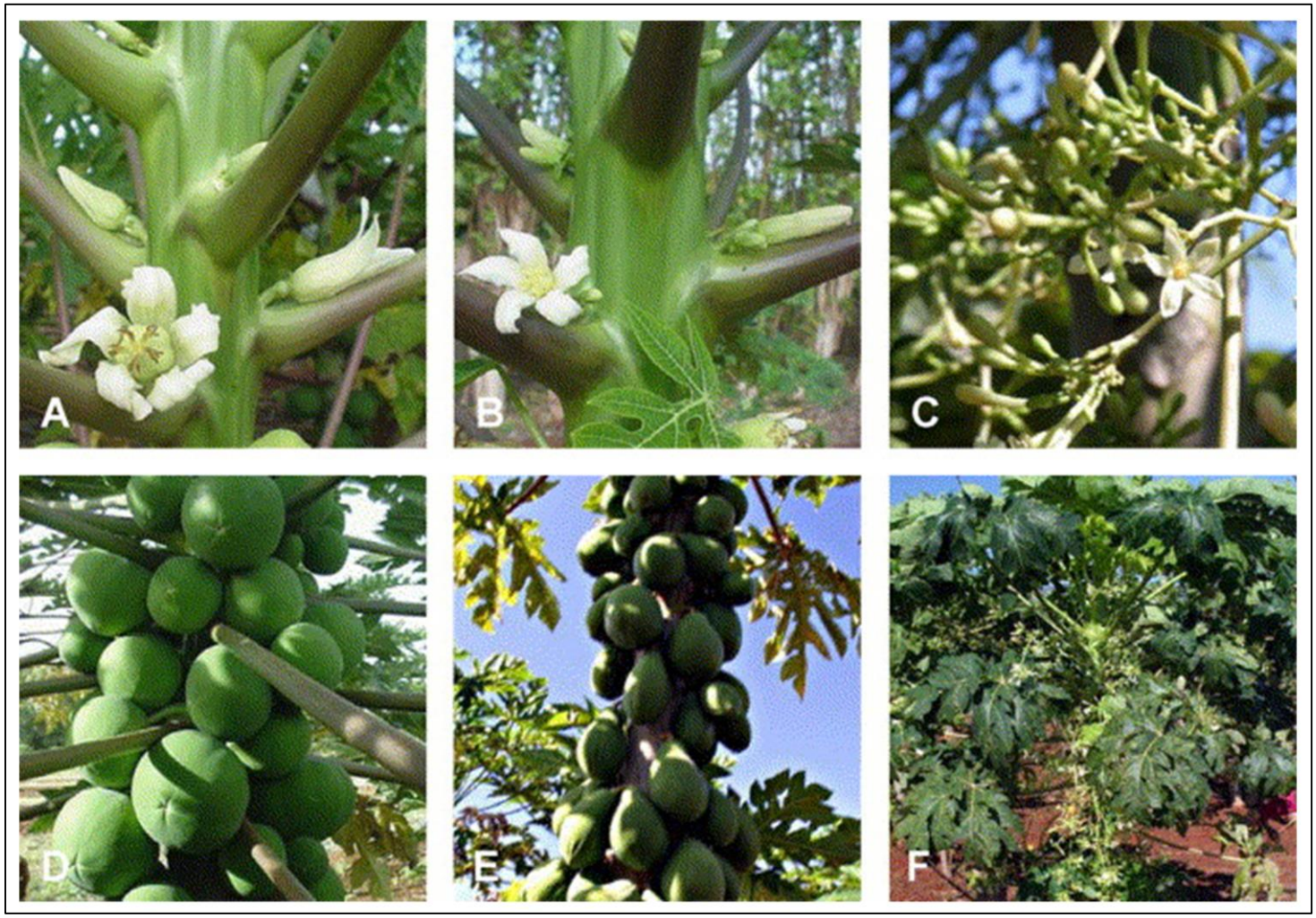

Figura 1. Flores e frutos de mamoeiro masculino, feminino e hermafrodito. (A) Flores femininas; (B) Flores hermafroditas; (C) flores masculinas; (D) fruto feminino; (E) fruto hermafrodito; (F) planta masculina (MING; YU; MOORE, 2007).

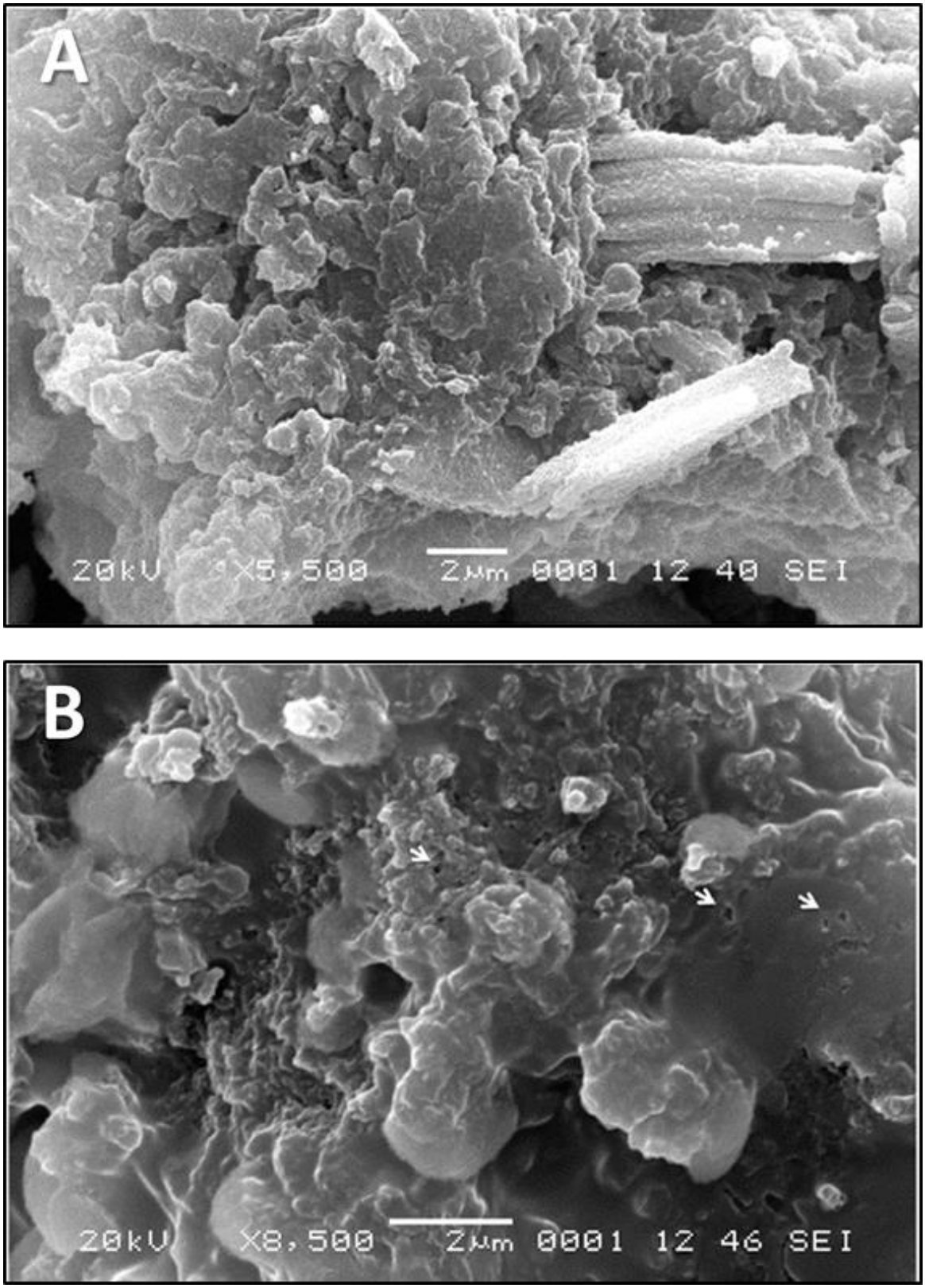

Figura 2. Imagens de microscopia eletrônica de varredura de látex de frutos de mamão. (A) Látex de frutos sadios; (B) látex de frutos com meleira. Pequenos círculos de aproximadamente 40 a 50nm e alterações na estrutura e possível degradação são evidentes no látex de frutos infectados e não observados em látex de frutos sadios (MAGAÑA-ÁLVAREZ et al., 2016).

Entretanto, um estudo recente revelou que a etiologia da meleira do mamoeiro consiste em uma infecção sinérgica pelo já conhecido PMeV, agora um *toti-like virus* em associação ao recém descrito *Papaya meleira virus 2* (PMeV2), um *umbra-like virus*. PMeV2 possui um genoma de fita simples de RNA (ssRNA) com aproximadamente 4,5 kb não codificante para proteína capsidial (Figura 4). A associação é proposta nos termos da montagem de PMeV2 com proteínas capsidiais de PMeV e montagem de PMeV com proteínas de movimento de PMeV2, permitindo que PMeV possa movimentar-se célula a célula no hospedeiro, enquanto o PMeV2 passa a ser transmitido pelo mesmo vetor de PMeV (SÁ ANTUNES et al., 2016).

O principal sintoma da meleira do mamoeiro é uma exsudação espontânea de látex muito aquoso e translúcido, principalmente de frutos (Figura 5) e folhas (RODRIGUES et al., 1989), cuja fluidez retarda a polimerização e o contato prolongado com o ar provoca oxidação e acúmulo deste látex como uma substância pegajosa (KITAJIMA et al., 1993). Uma particularidade desta doença está na dependência da transição juvenil-adulto (MACIEL-ZAMBOLIM et al., 2003), que ocorre aproximadamente aos 4-6 meses pós germinação e é marcado pela floração. Após a floração surgem os sintomas de queima ou necrose nas extremidades de folhas jovens, mancha zonada ou clorose nos frutos e o aspecto melado no mamoeiro (Figura 6) (VENTURA et al., 2003).

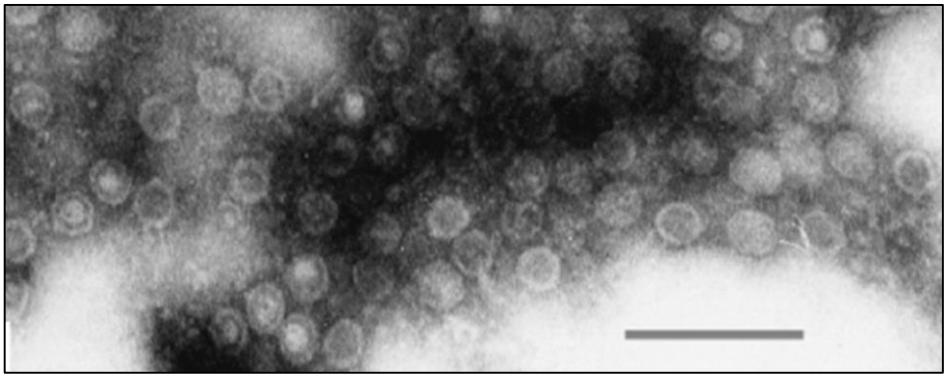

Figura 3. Micrografia eletrônica de vírions de PMeV purificados corados negativamente com 2% m/v de ácido fosfotungstico pH 6.9 (barra = 200 nm) (MACIEL-ZAMBOLIM et al., 2003).

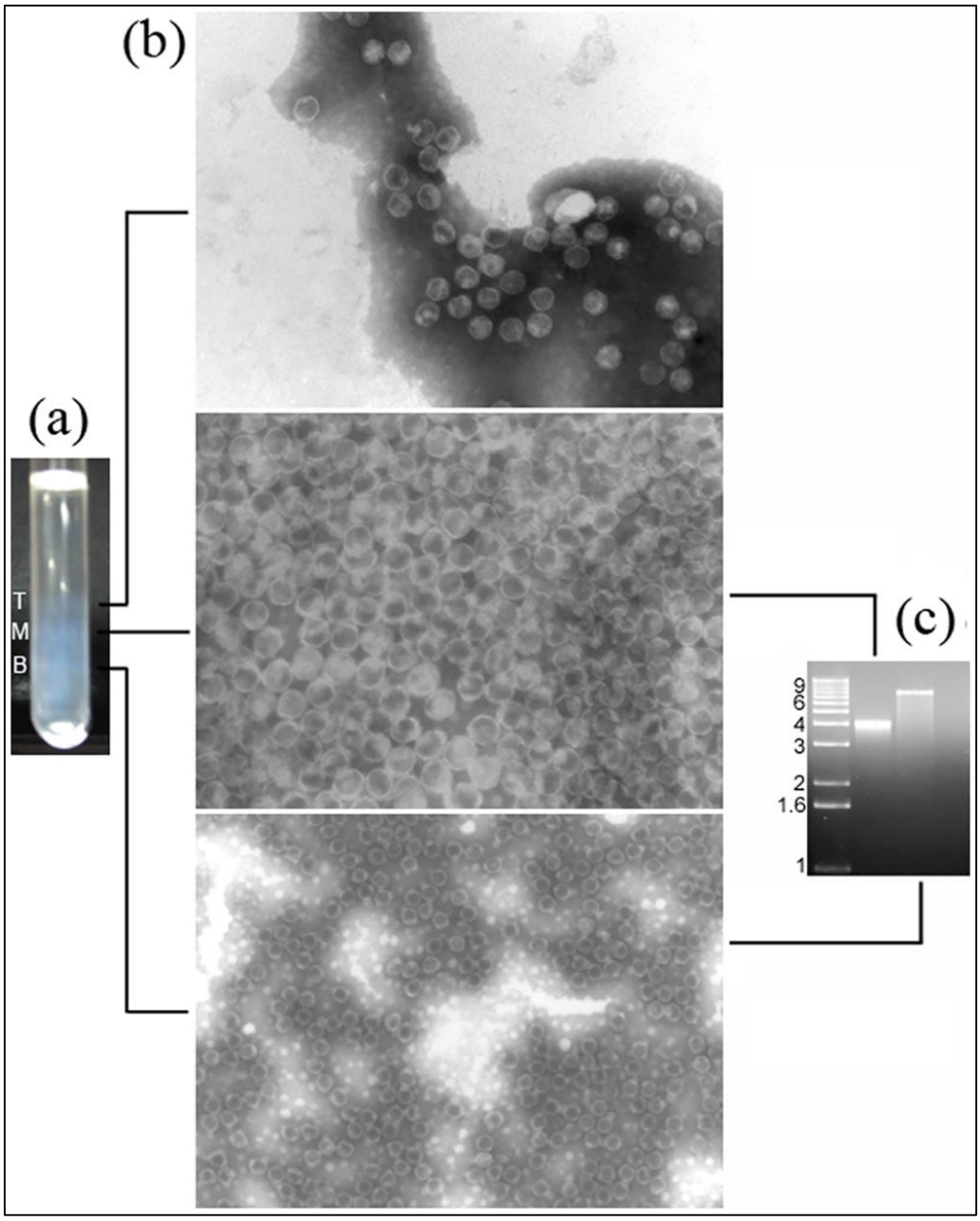

Figura 4. Análise de preparação viral purificada de látex de plantas de mamão apresentando sintomas severos de meleira. (a) Bandas virais após centrifugação em gradiente de densidade de sacarose. T, topo; M, meio; B, base. (b) Imagem de microscopia eletrônica de transmissão de partículas virais das frações T, M e B. T e M, 140.000x; B, 85.000x. (c) Eletroforese em gel de agarose de RNA extraído de partículas das frações M e B (SÁ ANTUNES et al., 2016).

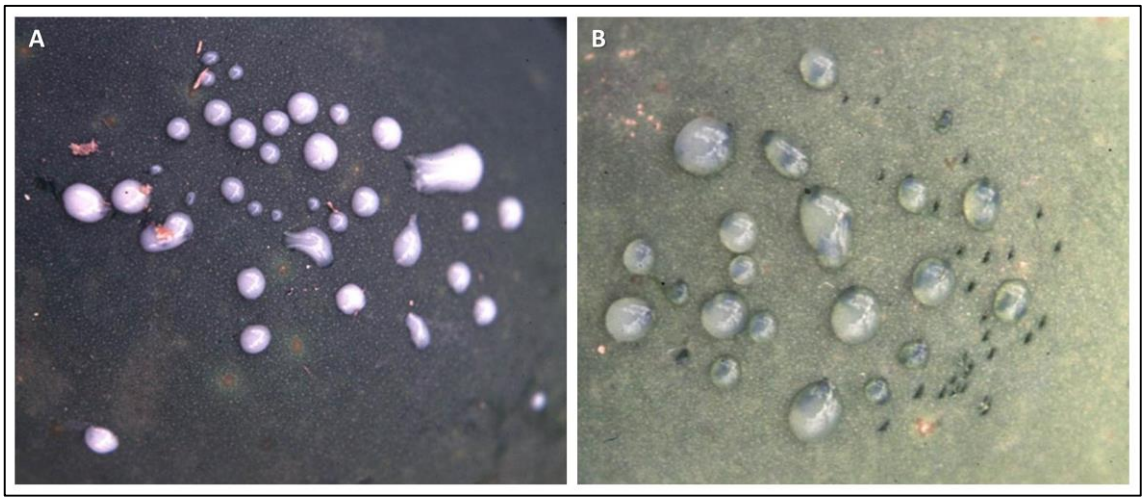

Figura 5. Látex de frutos de mamão. (A) Látex leitoso de fruto sadio; (B) látex aquoso de fruto com meleira. Adaptado de (LIBERATO JR; TATAGIBA, 2006. *Papaya meleira virus* - PmeV. Disponível online: PaDIL - http://www.padil.gov.au).

O diagnóstico de meleira em campo baseia-se na visualização dos primeiros sintomas e, como o vetor ainda é desconhecido, o controle existente é mediante a pratica de rouging (corte das plantas doentes) (VENTURA et al., 2003). Desta forma, a ausência de sintomas antes do florescimento mantém plantas infectadas e assintomáticas no campo, podendo agir como fonte de vírus na dispersão para outras plantas do pomar (RODRIGUES et al., 2009a). Já em laboratório, *primers* desenhados com base em fragmentos de sequência genômica do vírus permitem a utilização de técnica de reação em cadeia da polimerase (PCR) para a confirmação da infecção a partir de tecidos foliares e de forma independente da existência dos sintomas (ABREU et al., 2012). O desenvolvimento de técnicas de diagnóstico molecular deste vírus permitiu grande avanço nas pesquisas com plantas infectadas e assintomáticas.

Figura 6. Sintomas da meleira. (A) Queima ou necrose nas extremidades de folhas jovens; (B) mancha zonada ou clorose em frutos; (C) aspecto melado no mamoeiro. Adaptado de (VENTURA; COSTA; PRATES, 2004).

Dentre as alterações identificadas em mamoeiros portadores de sintomas de meleira estão as modificações na estrutura e composição do látex (MAGAÑA-ÁLVAREZ et al., 2016; RODRIGUES et al., 2009b), como elevação nos níveis de peróxido de hidrogênio (H_2O_2), redução no acúmulo de inibidor de serino protease e da cisteíno protease quimopapaina (RODRIGUES et al., 2012), além de um desequilíbrio osmótico provocado pela elevação nos níveis de fósforo, potássio e água nos laticíferos (DE ARAÚJO et al., 2007). Outras alterações observadas a nível foliar em mamoeiros com meleira são o acúmulo de calreticulina, proteínas relacionadas ao proteassomo e proteínas de resistência (PRs), ex. endoquitinase e PR-4 (RODRIGUES et al., 2011), diminuição na expressão de microRNAs cujos alvos preditos são proteínas relacionadas ao proteassomo (miR162, miR398 and miR408) e vários outros microRNAs envolvidos em vias de resposta a estresses (ABREU et al., 2014). Adicionalmente, foi identificada uma diminuição de integridade das nervuras foliares de mamoeiros portadores de meleira (MAGAÑA-ÁLVAREZ et al., 2016).

1.3. Mecanismos comuns na interação compatível planta-vírus

Organismos vegetais não possuem células especializadas em defesa, mas a ausência destas não impede a existência de uma maquinaria intrincada de defesa celular contra infecção por diversos patógenos. Estas defesas possuem um efeito imunológico local ou sistêmico, além de uma memória imunológica que pode transcender gerações (SPOEL; DONG, 2012). A identificação de diversos processos de defesa vegetal permitiu a formulação de quatro modelos de imunidade vegetal (Figura 7), relacionados diretamente à natureza e local da infeção e à predisponibilidade genética do hospedeiro para vias de resistência (MUTHAMILARASAN; PRASAD, 2013). O estádio do desenvolvimento fenológico do hospedeiro também pode exercer influência direta ou indireta nestes processos de defesa (WHALEN, 2005). A interação planta-patógeno pode ocorrer de duas formas básicas: incompatível (grande maioria dos casos), quando ocorre uma infecção local seguido do confinamento e eliminação do patógeno, sem que haja uma infecção sistêmica ou maiores prejuízos ao hospedeiro (resistente ao patógeno); ou compatível, quando o patógeno obtém sucesso no processo infeccioso do hospedeiro (susceptível). A determinação de tolerância depende do grau de comprometimento da fisiologia do hospedeiro (MANDADI; SCHOLTHOF, 2013; MUTHAMILARASAN; PRASAD, 2013).

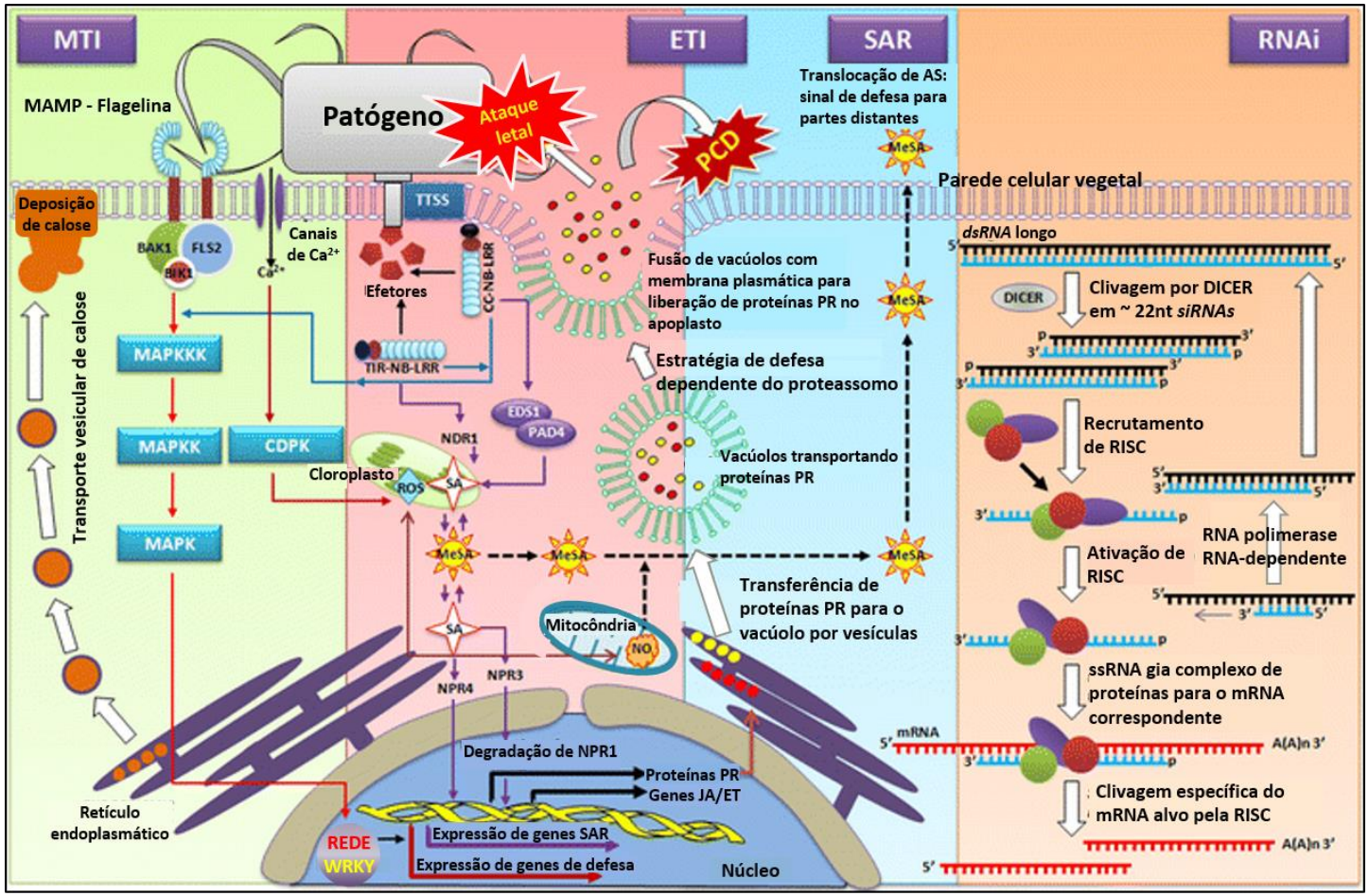

Figura 7. Representação esquemática dos quatro modelos de imunidade vegetal. (i) Imunidade disparada por MAMP (MTI); (ii) imunidade disparada por efetores (ETI); (iii) resistência sistêmica adquirida (SAR); (iv) silenciamento gênico (RNAi). A ilustração de ETI inclui os eventos envolvidos no sistema imunológico autônomo de células, baseado na fusão de membranas, para combater bactérias intracelulares, induzindo necrose local (morte celular programada por resposta hipersensível) (MUTHAMILARASAN; PRASAD, 2013) adaptado.

A efetividade e amplitude do sistema imune vegetal é um somatório de várias possibilidades (Figura 8), que se inicia com o reconhecimento, por parte da planta, de um padrão de moléculas associadas a micróbios/patógenos (MAMPs/PAMPs) por intermédio de proteínas receptoras (PRRs) e ative a imunidade disparada por PAMP (PTI). Alguns patógenos superam esta primeira defesa, produzindo efetores que interferem com PTI ou que possibilitam sua nutrição, reprodução e dispersão, resultando em uma susceptibilidade disparada por efetor (ETS). Em seguida, existe uma nova possibilidade de defesa, onde uma destas moléculas efetoras é reconhecida por uma proteína NB-LRR, ativando a imunidade disparada por efetores (ETI), uma versão amplificada de PTI que frequentemente ultrapassa um limiar para indução de morte celular por resposta hipersensível (HR) e resulta no isolamento e eliminação do patógeno no local da primeira infecção. Entretanto, alguns patógenos acabam eliminando ou modificando suas moléculas efetoras através do fluxo gênico horizontal, o que os permite suprimir ETI (JONES; DANGL, 2006). Como esperado para processos coevolutivos, a seleção favorece vegetais com novos alelos de NB-LRR, que podem reconhecer um dos novos efetores do patógeno, resultando novamente em ETI em um verdadeiro cabo-de-guerra molecular (ALEXANDER; CILIA, 2016).

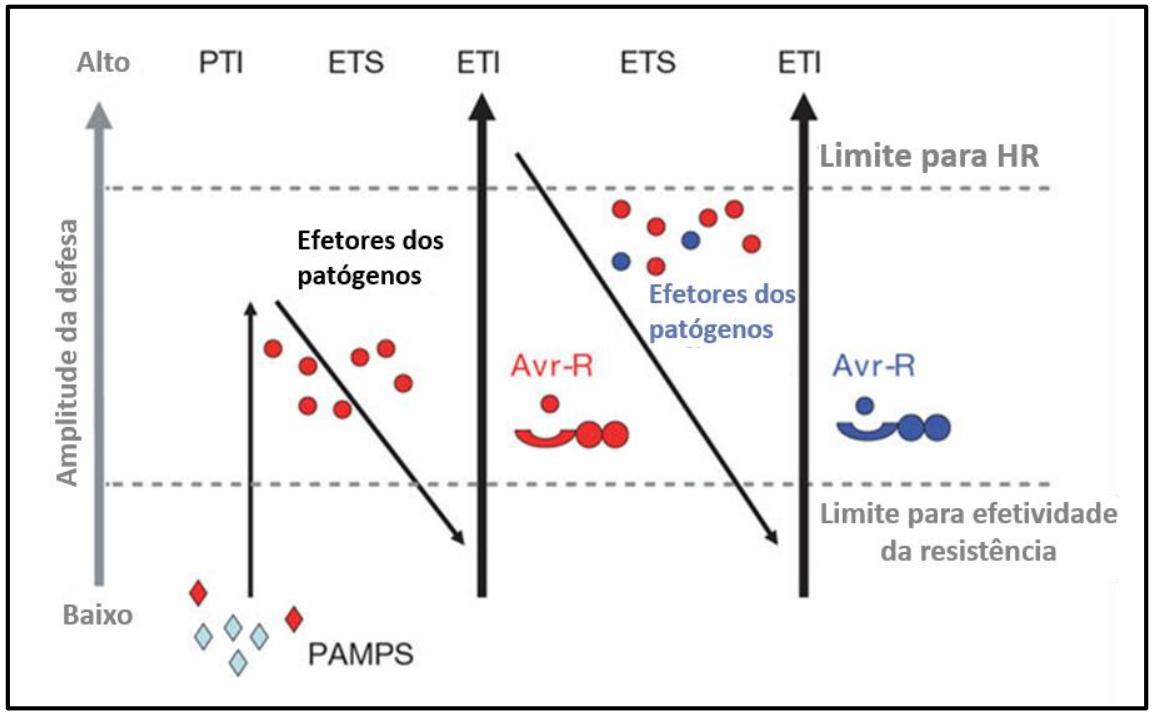

Figura 8. Esquema de amplitude de resistência ou susceptibilidade a doenças. O desfecho da imunidade vegetal é proporcional a [PTI - ETS + ETI]. Na fase 1, plantas detectam padrão de moléculas associadas a micróbios/patógenos (MAMPs/PAMPs, diamantes vermelhos) via PRRs para ativar a imunidade disparada por PAMP (PTI). Na fase 2, os patógenos bem sucedidos produzem efetores que interferem com PTI ou possibilitam a nutrição e dispersão do patógeno, resultando em uma susceptibilidade disparada por efetor (ETS). Na fase 3, um efetor (indicado em vermelho) é reconhecido por uma proteína NB-LRR, ativando a imunidade disparada por efetores (ETI), uma versão amplificada de PTI que frequentemente ultrapassa um limiar para indução de morte celular por resposta hipersensível (HR). Na fase 4, os patógenos bem sucedidos são aqueles que perderam o efetor vermelho, e possivelmente ganharam novos efetores através do fluxo gênico horizontal (em azul) – isso pode ajudar os patógenos a suprimir ETI. A seleção favorece novos alelos de NB-LRR vegetais que podem reconhecer um dos efetores recém-adquiridos, resultando novamente em ETI (JONES; DANGL, 2006) adaptado.

Para que células distantes do local inicial da infecção possam se preparar para a possível interação com o patógeno (*systemic acquired resistance*, SAR), sinais imunológicos móveis como ácido metilsalicílico (MeSA), ácido azelaico, glicerol-3-fosfato (G3P), proteína de transferência de lipídeos “DEFECTIVE IN INDUCED RESISTANCE (DIR1) e “AZALEIC ACID INDUCED 1 (AZI1) são produzidos no local da infecção e translocados através do sistema vascular para partes não infectadas da planta (Figura 9), induzindo um acúmulo de ácido salicílico, por um mecanismo ainda desconhecido, que induz: a secreção de proteínas relacionadas ao patógeno (PRs) com atividade antimicrobiana; somada à metilação de histonas e outras modificações da cromatina, que ativa os genes relacionados à imunidade para aumentar a expressão e estabelecer uma memória imunológica. O acúmulo de ácido salicílico ainda induz uma recombinação homóloga somática através da ação de “BREST CANCER SUSCEPTIBILITY 2 (BRCA2) e RAD51, com potencial de estabelecer uma memória transgeracional da imunidade (SPOEL; DONG, 2012).

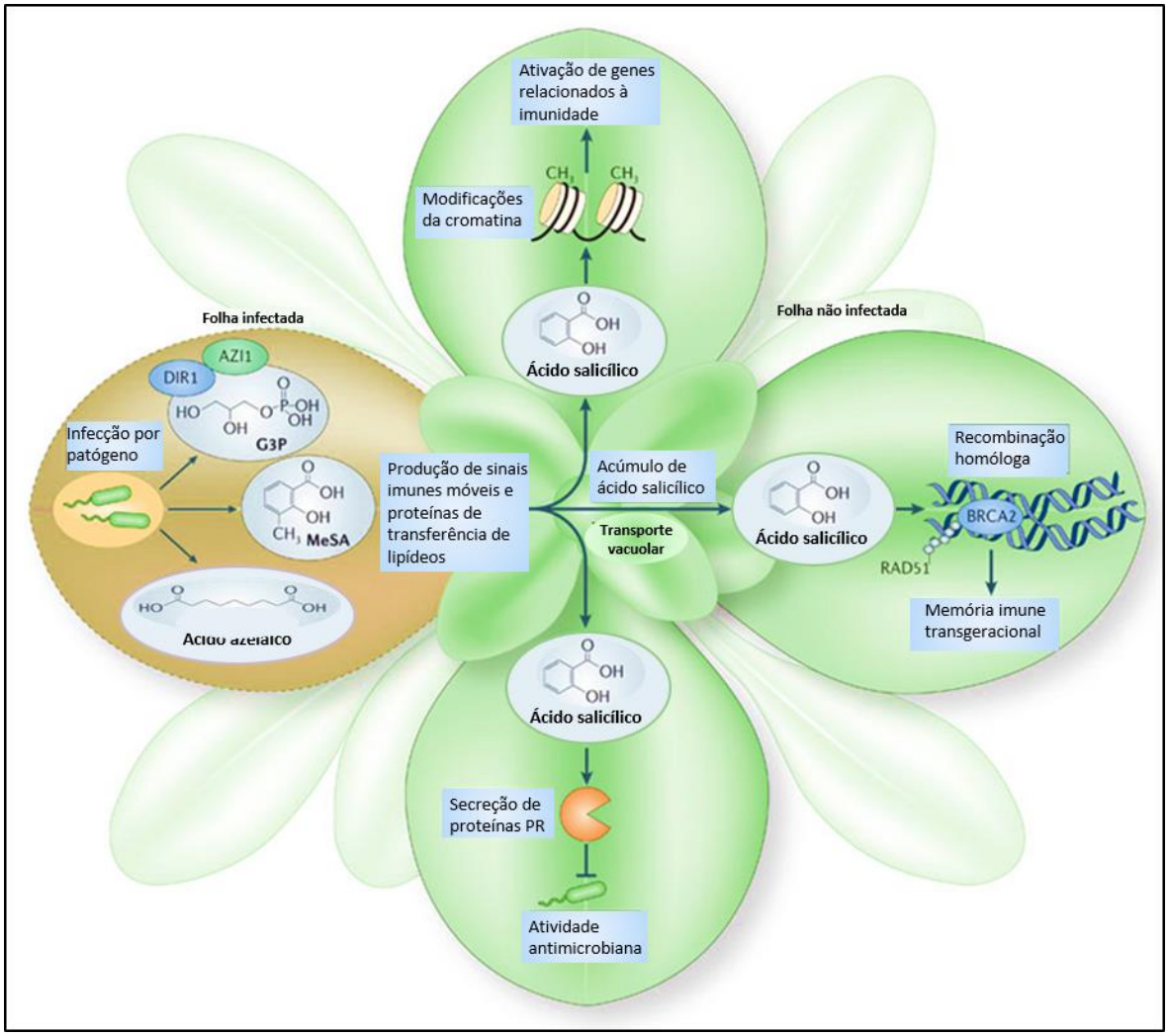

Figura 9. Translocação de sinais imunológicos móveis induzindo imunidade sistêmica e memória imunológica. Infecção local de um patógeno resulta na produção de sinais imunológicos móveis como ácido metilsalicílico (MeSA), ácido azelaico, glicerol-3-fosfato (G3P), proteína de transferência de lipídeos “DEFECTIVE IN INDUCED RESISTANCE (DIR1) e “AZALEIC ACID INDUCED 1 (AZI1). Estes sinais móveis são transportados através do sistema vascular para partes não infectadas da planta, onde, por um mecanismo desconhecido, induz o acúmulo de ácido salicílico (molécula sinalizadora para resistência sistêmica adquirida). Acúmulo de ácido salicílico induz: a secreção de proteínas relacionadas ao patógeno (PRs) com atividade antimicrobiana; metilação de histonas e outras modificações da cromatina que aprontam os genes relacionados à imunidade para aumentar a expressão e estabelecer uma memória imunológica; e uma recombinação homóloga somática através da ação de “BREST CANCER SUSCEPTIBILITY 2 (BRCA2) e RAD51 com o potencial de estabelecer uma memória transgeracional da imunidade (SPOEL; DONG, 2012) adaptado.

Uma vez que o comportamento do vírus é peculiar e apresenta várias distinções na interação planta-patógeno quando comparado a outros patógenos como fungos e bactérias, foi proposta uma equivalência analógica em termos de nomenclatura, com a inclusão de algumas definições para cada termo. Desta forma, um efetor viral consiste em uma proteína codificada pelo vírus que, em contato com células hospedeiras, interfere nos componentes de sinalização de defesa do hospedeiro, promovendo a virulência. Uma imunidade disparada por efetores (ETI) virais consiste em uma resposta disparada por proteínas de resistência (R) que reconhecem, direta ou indiretamente, os efetores codificados pelo vírus ou a atividade viral no hospedeiro. Uma imunidade disparada por PAMP (PTI) consiste em uma resposta imune basal disparada pelo reconhecimento de um padrão de moléculas conservadas do vírus (PAMP). O reconhecimento deste padrão de moléculas virais é realizado por proteínas específicas com atividade receptora aderidas à membrana plasmática (MANDADI; SCHOLTHOF, 2013).

A infecção viral em plantas tem início com a entrada do vírus baseada em injúria mecânica, seguida de descapsidação (para vírus portadores de capsídeo). Neste ponto a infecção pode se dar de forma incompatível (se PTI for suficiente), sessando o processo infeccioso, ou compatível, na qual o vírus realiza a tradução e replicação de seu material genético com posterior encapsidação (para vírus portadores de capsídeo) e dispersão (célula-célula ou sistêmica). Interações compatíveis comumente terminam por desenvolver sintomas no hospedeiro, tais como: mosaicismo; manchas anelares; clorose; necrose; murcha; e nanismo (Figura 10). O processo infeccioso como um todo promove uma modificação nos padrões de acúmulo de proteínas envolvidas no metabolismo de: açúcares; ROS; energia; e proteínas (síntese/turnover). O processo infeccioso promove o acúmulo diferencial das proteínas envolvidas em parede celular, metabolismo secundário, fotossíntese e patogênese.(Figura 11) (DI CARLI; BENVENUTO; DONINI, 2012).

1.4. Fotossíntese na infecção viral de plantas

A maquinaria fotossintética consiste na fonte primordial de energia e carboidratos para o vegetal (KANGASJÄRVI et al., 2014), sendo ainda parte integrante dos mecanismos de manutenção do estado REDOX, com a produção de ROS e atuação de enzimas antioxidativas (EDREVA, 2005). Tais fatos fazem da maquinaria fotossintética o alvo principal dos patógenos durante os processos infecciosos (KANGASJÄRVI et al., 2014). As reações luminosas da fotossíntese são realizadas em dois grandes complexos, fotossistema II (PSII) e fotossistema I (PSI), cujas atividades são interligadas através da plastoquinona (PQ), do complexo do citocromo b6f (Cytb6f) e do pool de plastocianina (PC). A funcionalidade plena de todo aparato fotossintético forma a cadeia de transporte de elétrons do cloroplasto (Figura 12).

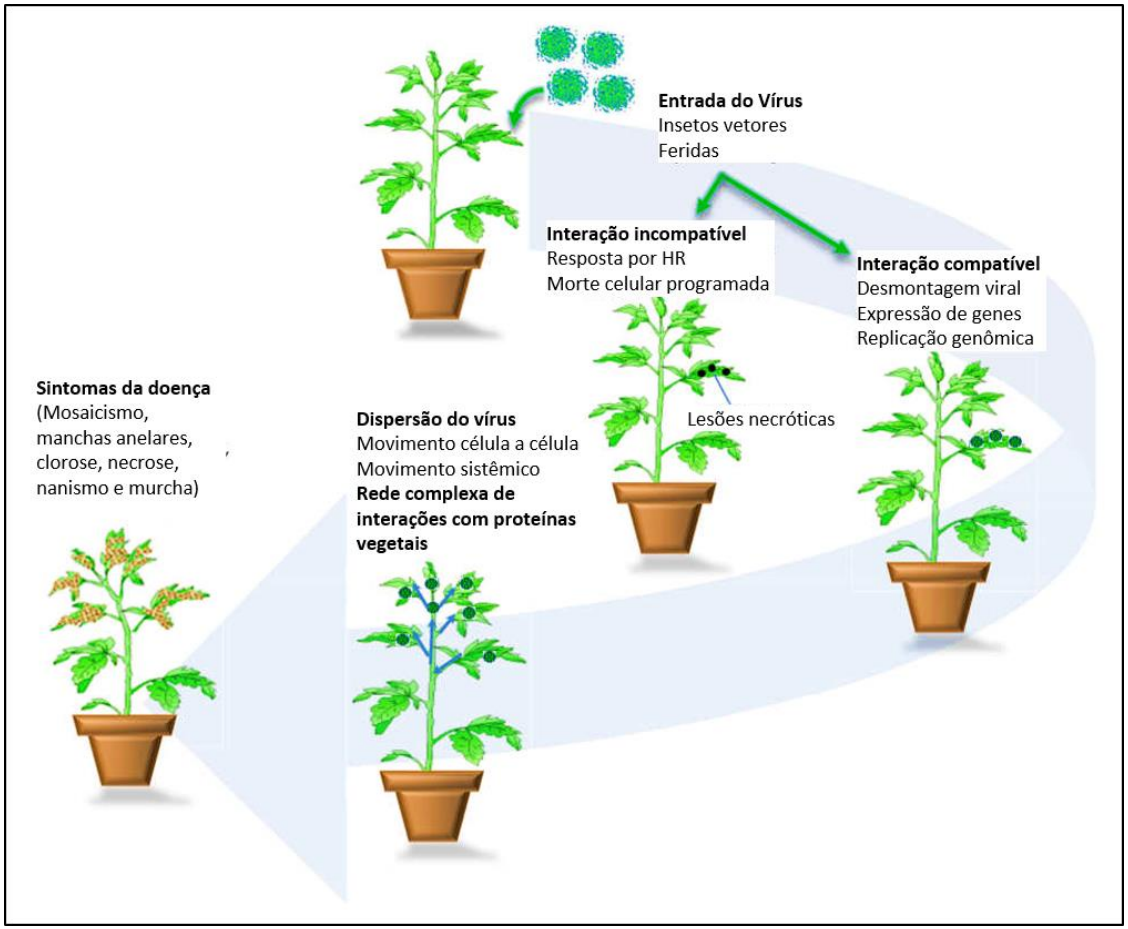

Figura 10. Representação esquemática da infecção viral em plantas. Vírus são parasitas intracelulares que precisam explorar a maquinaria metabólica da planta para sua replicação. Na maioria dos casos de interações incompatíveis, após a entrada do vírus, a planta produz uma resposta hipersensível localizada (HR), na qual as células infectadas rapidamente desenvolvem morte celular programada, prevenindo a dispersão do vírus. Em interações compatíveis, o vírus dribla as defesas da planta, se replica dentro das células e movendo-se, com sucesso, pela planta (movimento célula-célula/sistêmico), causando o desenvolvimento dos sintomas (DI CARLI; BENVENUTO; DONINI, 2012) adaptado.

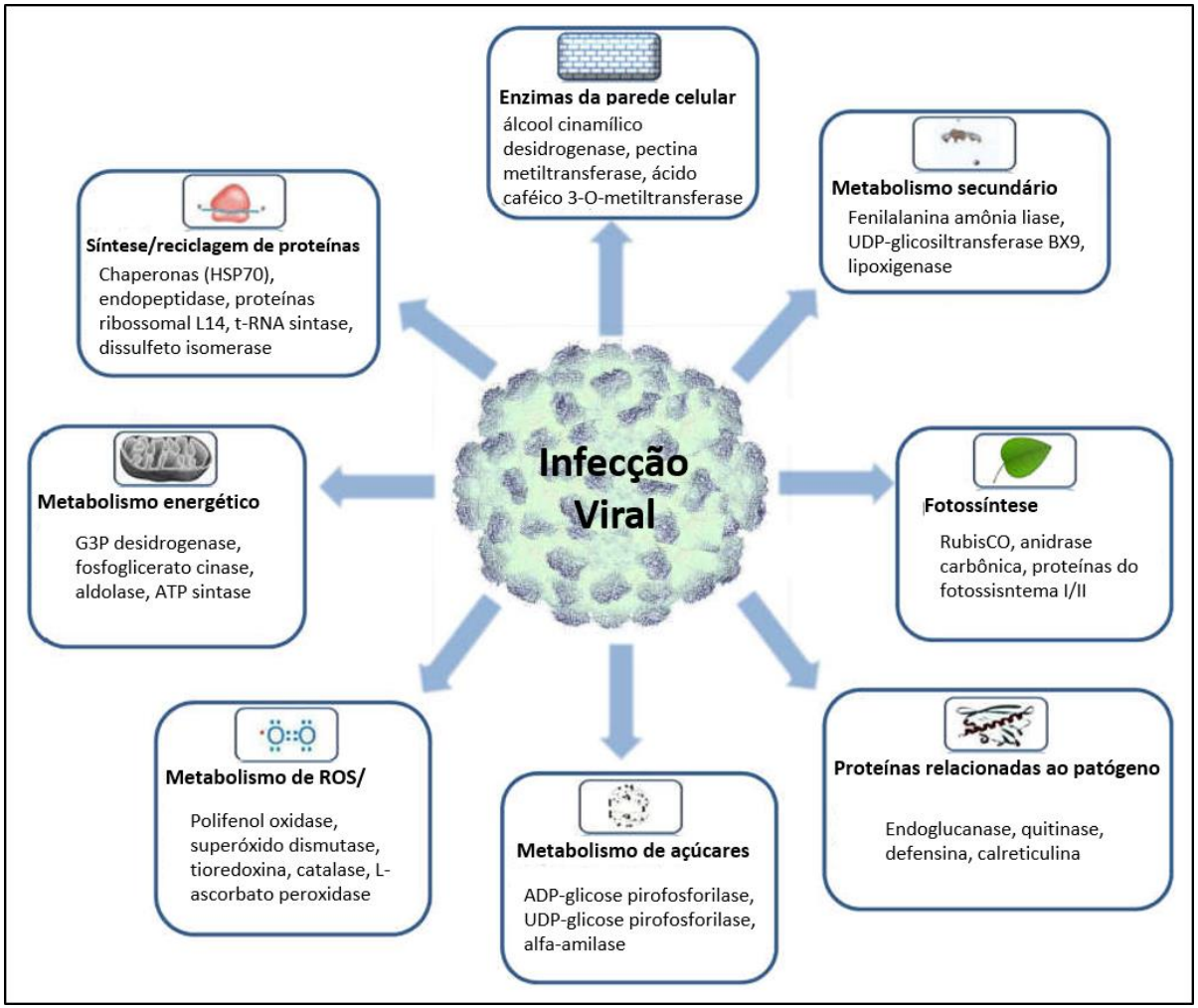

Figura 11. Visão esquemática de classes de proteínas que são moduladas após infecção por vírus. ROS, espécies reativas de oxigênio; G3P, gliceraldeído-3-fosfato; Rubisco, ribulose-1,5-bisfosfato carboxilase oxigenase (DI CARLI; BENVENUTO; DONINI, 2012) adaptado.

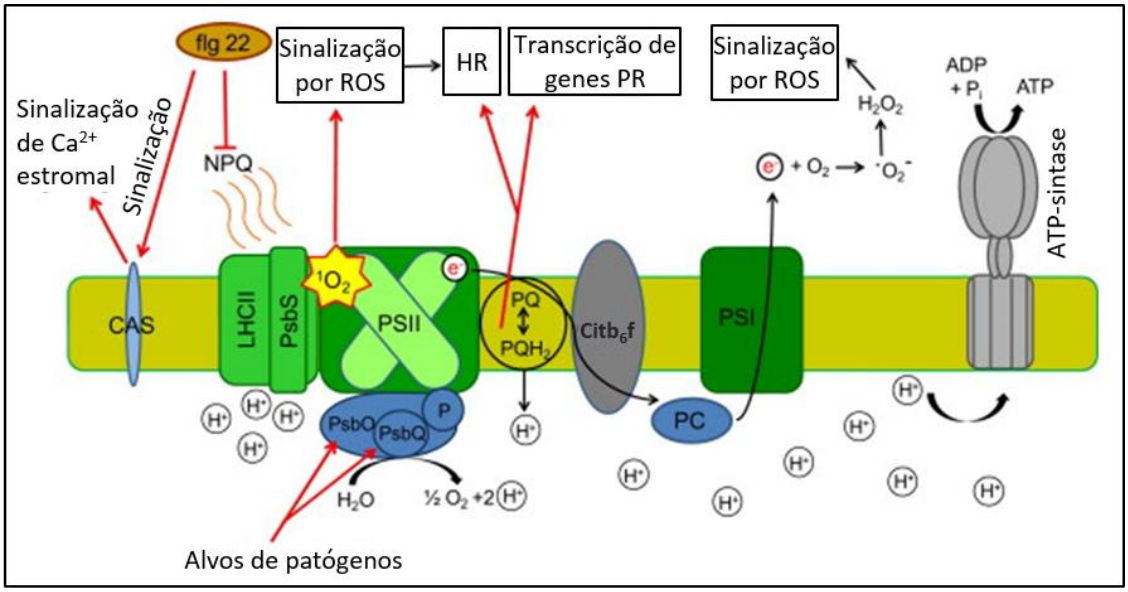

Figura 12. Reações luminosas da fotossíntese como uma fonte de sinais imunológicos em plantas. Redução do pool de plastoquinona (PQ) induzida pela luz, formação de oxigênio singleto ($^1O_2$) no fotossistema II (PSII) e/ou geração de superóxido ($\cdot O_2$) e peróxido de hidrogênio (H_2O_2) através do fotossistema I (PSI) podem disparar uma indução de genes relacionados à patogênese e reação hipersensível (HR) sobre os desafios bióticos. Para evocar tais sinais redox, as plantas podem intencionalmente modular o estado ativo dos mecanismos fotoprotetores. A percepção do peptídeo flagelina (flg22) no apoplasto dispara um sinal cálcio-dependente e uma down-regulação da extinção de energia não fotoquímica (NPQ) no cloroplasto. O enfraquecimento de NPQ pode promover redução do pool de plastoquinona e formação de $^1O_2$ no PSII. Acidificação do lúmen do tilacóide promove NPQ, mas também ativa o controle fotossintético, que limita o transporte de elétrons através do complexo do citocromo b6f (Citb6f), promovendo redução do pool de plastoquinona, mas aliviando a formação de ROS no PSI. Diferentes patógenos vegetais tentam anular a produção de ROS e consequentemente a formação de sinais de defesa no cloroplasto. Tanto bactérias, quanto vírus são conhecidos por deteriorar o complexo de evolução do oxigênio do PSII para este propósito (KANGASJÄRVI et al., 2014) adaptado.

A participação das reações luminosas da fotossíntese nos processos imunológicos vegetais se dá pela produção de ROS, induzindo a formação de oxigênio singleto ($^1O_2$) no fotossistema II (PSII) e/ou geração de superóxido ($\cdot O_2$) e peróxido de hidrogênio (H_2O_2) através do fotossistema I (PSI) que atuam, após percepção de patógeno, na sinalização para indução de genes relacionados à patogênese e reação hipersensível (HR). Uma forma de evocar estes mecanismos é a modulação intencional da atividade do sistema fotoprotetor. Um exemplo deste mecanismo é a percepção do peptídeo flagelina (flg22) no apoplasto, que dispara um sinal cálcio-dependente gerando uma diminuição da extinção de energia não fotoquímica (NPQ), promovendo assim a redução do pool de plastoquinona e formação de $^1O_2$ no PSII. Outra forma de evocação destes mecanismos é a limitação da atividade do complexo do citocromo b6f (Cytb6f), que interrompe o fluxo de elétrons para PSI com consequente diminuição na formação de formação de ROS no PSI. Diferentes patógenos vegetais tentam

anular a produção de ROS e consequentemente a formação de sinais de defesa no cloroplasto. Tanto bactérias, quanto vírus são conhecidos por deteriorar o complexo de evolução do oxigênio do PSII com este propósito (KANGASJÄRVI et al., 2014).

1.5. Sistema ubiquitina/proteassomo 26S na interação planta-vírus

Todos os processos celulares, desde a divisão à morte, necessitam em alguma etapa de degradação proteica. Proteólise, em eucariotos, é predominantemente controlada pelo sistema ubiquitina/proteassomo 26S (UPS) (DREHER; CALLIS, 2007). O proteassomo 26S consiste de: uma partícula central (CP ou 20S), que possui dois anéis externos composto por sete subunidades α e dois anéis centrais contendo sete subunidades β; e uma partícula reguladora (RP ou 19S), que associada a uma ou ambas extremidades de CP compõe os subcomplexos base e tampa (Figura 13). De maneira geral, a proteólise via UPS tem início com a marcação de proteínas alvo para degradação Ub-dependente, onde a ubiquitina (Ub) se liga com a enzima “Ub activating” (E1). Ub ativada é então transferida para a enzima “Ub conjugating” (E2), que junto com a “Ub ligase” (E3) catalisa a ligação do monômero Ub com o alvo (SMALLE; VIERSTRA, 2004). Existe ainda a possibilidade de desligamento da cadeia de poliubiquitnina das proteínas alvo, catalisado por proteases “Ub-specific” (UBPs), prevenindo a degradação das proteínas alvo. Estudos recentes mostram que 20SP e 26SP podem degradar algumas proteínas sem a cauda Ub (KUREPA; SMALLE, 2008).

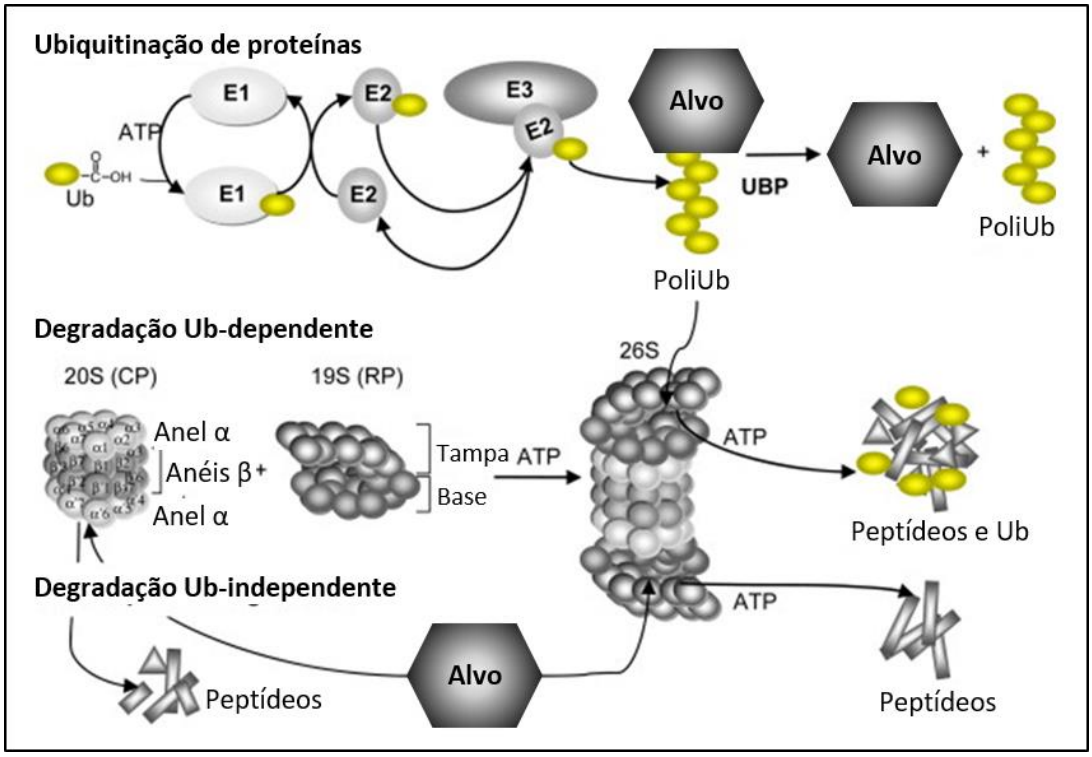

Figura 13. Estrutura de UPS e tipos de proteólises proteassomo-dependente. A marcação de proteínas para degradação Ub-dependente tem início com a ubiquitina (Ub) que se liga com a enzima "Ub activating" (E1). Ub ativada é então transferida para a enzima "Ub conjugating" (E2), que junto com a "Ub ligase" (E3) catalisa a ligação do monômero Ub com o alvo. O desligamento da cadeia de poliubiquitnina previne a degradação do alvo e esta reação é catalisada por proteases "Ub-specific" (UBPs). O proteassomo 26S consiste de uma partícula central (CP ou 20S) e uma partícula reguladora (RP ou 19S). CP possui dois anéis externos compostos por sete subunidades α e dois anéis centrais com sete subunidades β. RP associada a uma ou ambas extremidades de CP compõe os subcomplexos base e tampa. Estudos recentes mostram que 20SP e 26SP podem degradar algumas proteínas sem a cauda Ub (KUREPA; SMALLE, 2008) adaptado.

Com a possibilidade de promover grandes modificações no padrão de acúmulo de proteínas via degradação das mesmas, o UPS é um elemento chave nos mecanismos de interação planta-patógeno (DELAURÉ et al., 2008), sendo as mudanças nos níveis de Ub, E1 e E2 de amplo efeito na reprogramação celular durante a defesa em plantas. Entretanto, E3 possui uma atuação mais direta na interação planta-patógeno, por ser o elemento chave na especificidade dos alvos do UPS, possibilitando respostas de defesa precoce e indução de resistência a doenças (ZENG et al., 2006). UPS desempenha dois papéis distintos e fundamentais às células: atua como controle de qualidade, ao degradar proteínas mal formadas, mal enoveladas ou danificadas (GOLDBERG, 2003); ou atua como um sistema regulatório, ao degradar proteínas portadoras de sinais específicos de degradação como a poliubiquitinação (KUREPA; SMALLE, 2008). UPS atua no desenvolvimento vegetal, incluindo: desenvolvimento vascular (JIN; LI; VILLEGAS, 2006); controle do ciclo celular (JURADO et al., 2008);

morte celular programada (ENDO; DEMURA; FUKUDA, 2001); e sinalização hormonal. A atuação de UPS na sinalização hormonal já foi demonstrada para etileno (BINDER et al., 2007), ácido jasmônico (THINES et al., 2007) e ácido salicílico (YAENO; IBA, 2008).

Entretanto, não é somente a planta que controla e se beneficia da atividade proteassomal. Vírus foram observados inibindo a atividade proteassomal via proteína HcPro (*helper component proteinase*) (PLISSON et al., 2003) ou sequestrando o UPS para benefício próprio ao alterar o ciclo celular do hospedeiro, como é o caso da proteína Clink, codificada por um nanovirus, que interage com a proteína retinoblastoma-related (pRB) afetando o ciclo celular da planta (LAGEIX et al., 2007). Adicionalmente, vírus são capazes de marcar proteínas de resistência do hospedeiro para serem degradadas, como é o caso do supressor de silenciamento (P0) direcionando a proteína argonauta (AGO1) para degradação (BAUMBERGER et al., 2007), resultando na inibição da resistência mediada por RNAi (*post-transcriptional gene silencing*, PTGS). Sendo assim, a atividade proteassomal é utilizada durante a interação planta-patógeno tanto pela planta, em sua maquinaria de defesa, quanto pelo vírus, inibindo a atividade proteassomal ou usurpando a atividade proteassomal para benefício próprio. A atividade proteassomal na interação planta-patógeno constitui um verdadeiro jogo de esconde-esconde sem fim (DIELEN; BADAOUI; CANDRESSE, 2010).

1.6. Parede celular e o processo infeccioso

A parede celular é composta por microfilamentos de celulose, que são sintetizados por grandes complexos hexaméricos situados na membrana plasmática, além de hemiceluloses e pectinas, que compõe a matriz de polissacarídeos e são sintetizadas no aparato de Golgi e depois depositadas, por vesículas, na superfície da parede celular (Figura 14) (COSGROVE, 2005). Parede celular consiste na primeira barreira (física) contra o ataque de patógenos e possui as mais distintas funções, sendo a função primária a de dar forma e resistência mecânica (potencial de parede, PP) à célula, evitando assim a ruptura celular (WALLS; KEEGSTRA, 2010), principalmente durante os processos que envolvem modificações no potencial osmótico superiores às suportadas pelas membranas plasmáticas. Processos de desequilíbrio osmótico não são raros em plantas doentes, como o caso de meleira do mamoeiro que provoca uma elevação nos níveis de fósforo, potássio e água nos laticíferos (DE ARAÚJO et al., 2007).

Porém a parede celular possui muitas outras funções, mais complexas e de mecanismos refinados, tais como: adesão célula-célula; regulação do desenvolvimento e expansão celular (WAGNER; KOHORN, 2001); além de absorção e translocação de água, nutrientes e outras moléculas via apoplasto. A parede celular possui ainda participação ativa na imunidade vegetal (MALINOVSKY; FANGEL; WILLATS, 2014), incluindo a função de sinalização celular, uma vez que a mesma estabelece contato íntimo e primário com patógenos. A fragmentação de componentes da parede celular fornece moléculas capazes de evocar respostas celulares específicas que são consideradas moléculas de sinalização (MALINOVSKY; FANGEL; WILLATS, 2014; WOLF; HÉMATY; HÖFTE, 2012).

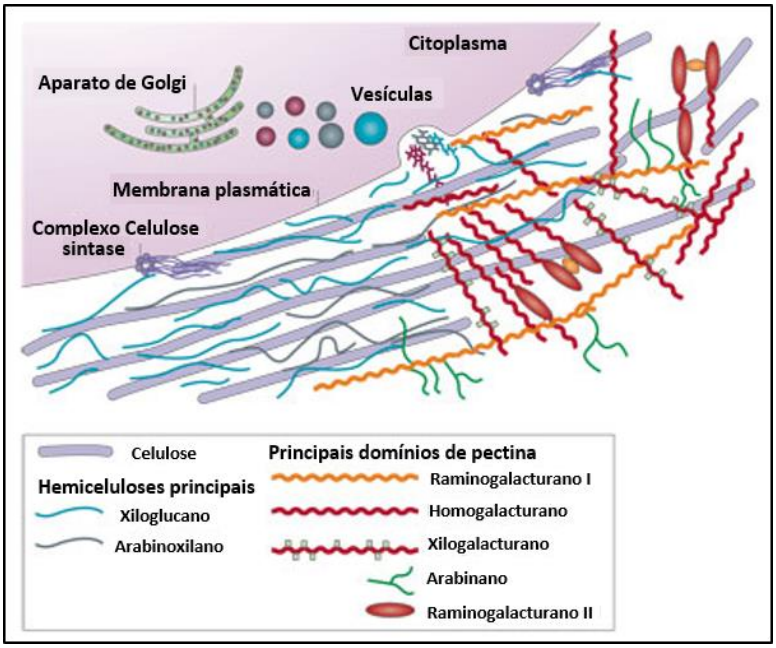

Figura 14. Estrutura da parede celular primária. Microfilamentos de celulose (bastões roxos) são sintetizados por grandes complexos hexaméricos na membrana plasmática, enquanto hemiceluloses e pectinas, que compõe a matriz de polissacarídeos, são sintetizados no aparato de Golgi e são depositados, por vesículas, na superfície da parede. Para esclarecer, a rede de hemicelulose-celulose está representada na parte esquerda da parede celular sem pectinas, que são enfatizadas na parte direita da figura. Na maioria das espécies vegetais, a hemicelulose predominante é xiloglucano (azul), enquanto hemiceluloses como arabinoxylanos (cinza) e mananas (não representada) são encontradas em menor frequência. Os polissacarídeos principais incluem ramnogalacturonano I e homogalaturonano, com quantidades menores de xilogalacturonano, arabinano, arabinogalactano I (não representado) e ramnogalacturonano II. Acredita-se que domínios de pectina são covalentemente ligados entre si e se ligam à xiloglucano de forma covalente e não covalente. Polissacarídeos neutros de pectina (verde) são também capazes de se ligar à superfícies de celulose (COSGROVE, 2005) adaptado.

A deposição de calose faz parte de um controle refinado no transporte celular via plasmodesmas, limitando a dimensão das partículas capazes de serem translocadas (*size exclusion limit*, SEL) (VERMA; HONG, 2001). Este mecanismo é comumente utilizado para evitar a movimentação célula-célula do vírus (LUCAS, 2006).

1.7. Proteômica quantitativa "*Gel-free, label-free*"

Proteínas são as moléculas que realizam a maioria das funções celulares em organismos vivos (DERACINOIS et al., 2013), cuja imprecisa correlação com os níveis de mRNA torna inviável uma predição no padrão de acúmulo de proteínas baseada no padrão de expressão de mRNA (GUO et al., 2008; GYGI et al., 1999). Desta forma, a análise qualitativa e quantitativa do padrão de acúmulo de proteínas (proteômica) é a metodologia que permite uma maior aproximação entre modificações a nível molecular com seus efeitos fenotípicos em células e organismos.

A marcha analítica da proteômica é constituída de quatro etapas principais (Figura 15), iniciando-se pelo acondicionamento da amostra (experimento, coleta e armazenamento da amostra e disponibilização das proteínas), seguido do preparo da amostra (extração, concentração, purificação e armazenamento das proteínas), que tem continuidade por métodos de separação (eletroforese ou cromatografia) e se finaliza-se com a quantificação (com ou sem gel) e identificação das proteínas via espectrometria de massas (BODZON-KULAKOWSKA et al., 2007)

O processo de separação pode ser realizado com as proteínas inteiras, com a preferência pela eletroforese, ou com os peptídeos derivados da digestão enzimática, com preferência por cromatografia líquida (AEBERSOLD; MANN, 2003). Já o processo de quantificação pode ser realizado de forma colorimétrica ou fluorescente em gel, ou por espectrometria de massas, sendo esta última proporcionadora de maior cobertura, precisão e exatidão (PATEL et al., 2009). Similarmente ao processo de separação, a identificação pode ser realizada com base em proteínas inteiras (*top-down*) ou com os peptídeos derivados da digestão enzimática (*bottom-up*), mas sempre via espectrometria de massas. Tendo em vista a redução nos custos, facilitação no processo e incremento de cobertura, a estratégia de *bottom-up* prevalece nos estudos de proteômica. A utilização da separação baseada em peptídeos combinada com a quantificação por espectrometria de massas e identificação *bottom-up* é denominada *shotgun* e permite a realização destes três

processos simultaneamente via cromatografia líquida acoplada à espectrometria de massas em tandem (LC-MS/MS).

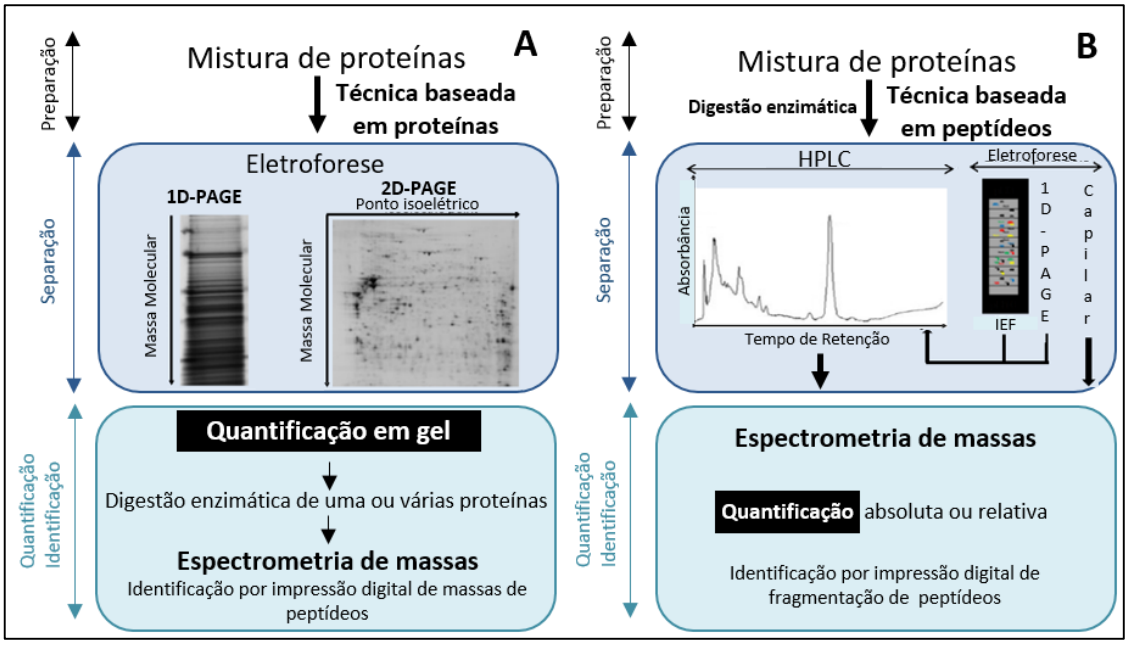

Figura 15. Fluxograma das técnicas mais utilizadas em proteômica comparativa e quantitativa. (A) Técnica baseada em proteínas (*top-down*); (B) técnica baseada em peptídeos (*bottom-up*). A análise proteômica consiste de quatro etapas: (i) condicionamento das amostras; (ii) preparação das amostras; (iii) separação; e (iv) quantificação/identificação das proteínas. A separação pode ser realizada para proteínas ou peptídeos e via eletroforese ou cromatografia. A quantificação é possível com ou sem gel, enquanto a identificação sempre ocorre via espectrometria de massas. Cromatografia líquida acoplada à espectrometria de massas em tandem (LC-MS/MS); Cromatografia líquida de alta performance (HPLC); Focalização isoelétrica (IEF); Eletroforese em gel de poliacrilamida (PAGE); Impressão digital de massas de peptídeos (PMF); Impressão digital de fragmentação de peptídeos (PFF) (DERACINOIS et al., 2013) adaptado.

A estratégia *shotgun* permite a quantificação baseada em marcação com isótopos estáveis (*stable-isotope labelling*) ou livre de marcação (*label-free*), cuja diferença consiste primordialmente na utilização de isótopos estáveis para marcar peptídeos oriundos de amostras distintas (Figura 16). A marcação permite a comparação direta da abundância dos peptídeos de diferentes amostras em uma mesma análise, enquanto a estratégia *label-free* necessita de uma análise para cada amostra com a comparação de abundâncias posteriori, elevando o tempo demandado pelo processo (ZHU; SMITH; HUANG, 2010). Por sua vez, o processo de marcação não possui eficiência de 100%, resultando em peptídeos que não recebem a marcação, o que faz da estratégia *label-free* a proporcionadora de uma maior cobertura proteômica tanto

para identificação quanto para quantificação , além de uma maior precisão e acurácia (WANG; ALVAREZ; HICKS, 2012).

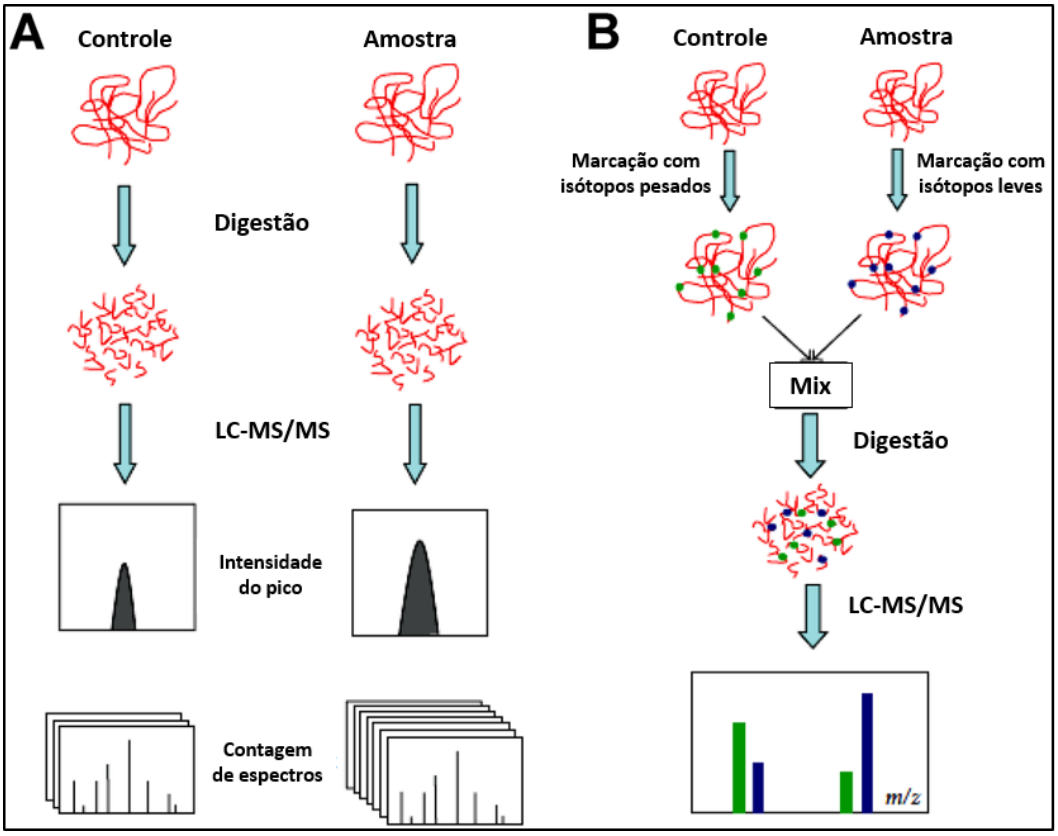

Figura 16. Diferenças entre proteoma quantitativo com e sem marcação. (A) Quantificação livre de marcação (*label-free*); (B) quantificação baseada em marcação com isótopo estável (*stable-isotope labelling*). A quantificação livre de marcação consiste de duas análises independentes a priori da comparação, enquanto a marcação permite a comparação direta dos pares de peptídeos marcados com isótopos estáveis. (DERACINOIS et al., 2013) adaptado.

2. OBJETIVOS

2.1. Objetivo Geral

Qualificar e quantificar o perfil de acúmulo de proteínas de *Carica papaya L.* em estádio de prefloração e pós-floração em resposta à meleira do mamoeiro e avaliar o envolvimento destas proteínas no fenômeno de resistência ao surgimento dos sintomas de meleira.

2.2. Objetivos Específicos

- Identificar as proteínas diferencialmente acumuladas em resposta à infecção por PMeV em estádio de prefloração de *Carica papaya L*;
- Estabelecer o perfil proteômico de folhas de *Carica papaya L.* sadias ou infectadas por PMeV+PMeV2 em quatro idades diferentes (3, 4, 7 e 9 meses pós germinação);
- Discutir o papel das proteínas diferencialmente acumuladas no processo de interação PMeV+PMeV2-*C. papaya* em estádio de prefloração;

- Discutir a relevância das proteínas diferencialmente acumuladas no fenômeno de resistência ao surgimento dos sintomas de meleira em estádios anteriores ao florescimento.

3. ARTIGOS DERIVADOS DA TESE

3.1. Manuscrito 1

Manuscrito aceito para publicação na revista *Journal of Proteomics* (ISSN: 1874-3919; I.F.: 3.888; Qualis A2 Biotecnologia). http://dx.doi.org/10.1016/j.jprot.2016.06.025

Label-free quantitative proteomic analysis of pre-flowering PMeV-infected *Carica papaya L.*

Eduardo de A. Soares[a], Emily G. Werth[b], Leidy J. Madroñero[a], José A. Ventura[a,c], Silas P. Rodrigues[a,d]*, Leslie M. Hicks[b], Patricia M.B. Fernandes[a]

[a]Núcleo de Biotecnologia, Universidade Federal do Espírito Santo, Av. Marechal Campos, 1498, Vitória, ES 29040-090, Brazil

[b]Department of Chemistry, University of North Carolina at Chapel Hill, 125 South Road, Chapel Hill, NC 27599, USA

[c]Instituto Capixaba de Pesquisa, Assistência Técnica e Extensão Rural, Rua Afonso Sarlo 160, Vitória, ES 29052-010, Brazil

[d]Unidade de Espectrometria de Massas e Proteômica e Núcleo Multidisciplinar de Pesquisa [e]Extensão de Xerém, Universidade Federal do Rio de Janeiro, Av. Carlos Chagas Filho 373, CCS Bloco H2 Sala 04, Rio de Janeiro, RJ 21941-902, Brazil

*Corresponding author: S.P.Rodrigues, e-mail: srodrigues@xerem.ufrj.br, Phone: +55 21 3938 6782

Keywords: Label-free quantitative proteomics, mass spectrometry, *Papaya meleira vírus*

ABSTRACT

Papaya meleira virus (PMeV) infects papaya (*Carica papaya L*.) and leads to Papaya Sticky Disease (PSD) or "Meleira", characterized by a spontaneous exudation of latex from fruits and leaves only in the post-flowering developmental stage. The latex oxidizes in contact with air and accumulates as a sticky substance on the plant organs, impairing papaya fruit's marketing and exportation. To understand pre-flowering *C. papaya* resistance to PMeV, an LC-MS/MS-based label-free proteomics approach was used to assess the differential proteome of PMeV-infected pre-flowering *C. papaya vs.* uninfected (control) plants. In this study, 1,333 proteins were identified, of which 111 proteins showed a significant abundance change (57 increased and 54 decreased) and supports the hypothesis of increased photosynthesis and reduction of 26S-proteassoma activity and cell-wall remodeling. All of these results suggest that increased photosynthetic activity has a positive effect on the induction of plant immunity, whereas the reduction of caspase-like activity and the observed changes in the cell-wall associated proteins impairs the full activation of defense response based on hypersensitive response and viral movement obstruction in pre-flowering *C. papaya* plants.

1. INTRODUCTION

Papaya meleira virus (PMeV) infects papaya (*Carica papaya L*.) and leads to Papaya Sticky Disease (PSD) or "Meleira" [1]. PSD is characterized by a spontaneous exudation of latex from fruits and leaves [2] which oxidizes in contact with air and accumulates as a sticky substance on the plant organs [3]. PSD is officially reported to occur in Brazil and Mexico, two major papaya fruit producing countries [4].

PMeV has been observed in the laticifers of *C. papaya* [3] where it induces an extensive production of H_2O_2 [5]. The analysis of PMeV-infected latex samples has previously allowed inferences about other local PMeV-associated effects such as higher levels of potassium, phosphorus and water, likely associated with an osmotic imbalance in PMeV-infected laticifers [5], along with reduced cysteine-protease abundance and activity [6]. In parallel, the accumulation of H_2O_2 in the phloem [5] and the increased activity of ROS-detoxifying enzymes peroxidase and superoxide dismutase in sticky-diseased *C. papaya* leaves suggested a systemic response in the plant [2]. MicroRNA coding genes predicted to target proteasome-related proteins, for instance ubiquitin-3-ligases, also accumulated in *C. papaya* sticky-diseased leaves suggesting their involvement in the control of protein turnover [7]. However, limited knowledge about key players of the PMeV x *C. papaya* interaction mechanism impairs the development of virus resistant plant genotype(s) and a differential proteomic study investigating the effects of infection at the protein level could be of value to this effort.

In Brazil, Sunrise Solo and Golden are the two economically relevant *C. papaya* cultivars. Interestingly, they can host high PMeV load and remain asymptomatic until flowering, which occurs about 3-4 months after seed germination. This suggests the existence of *C. papaya* resistance to PMeV prior to flowering. In plants, there is an intimate relationship between development and innate immunity [8], and several age-related resistance (ARR) phenotypes are reported [9–15]. Although ARR is not related to a particular developmental stage, the flowering transition has an important effect on resistance development, as reported for maize, tobacco and Arabidopsis [16–19]. The sink-source transition, which is accompanied by changes in cellular structure and

photoassimilate flux, is associated with turnip and Arabidopsis ARR to *Cauliflower mosaic virus* [20,21].

Previous proteomic studies have been applied to the analysis of latex and leaves of *C. papaya* Golden adult plants displaying typical sticky-disease symptoms. These studies have revealed accumulation of calreticulin, 20S proteasome b subunit, and PRs, *e.g.* endochitinase and PR-4 [22], while latex samples show lower abundance of chymopapain cysteine proteases and a latex serine proteinase inhibitor [6]. Together, this data indicates the existence of systemic acquired resistance (SAR) response in PSD symptomatic plants. Similarly, tobacco plants develop ARR against fungus, which involves the cell wall strengthening and the activation of SAR [23]. However, the involvement of SAR or other plant stress response mechanism(s) with the pre-flowering *C. papaya* resistance to PMeV is unknown.

In the present study, LC-MS/MS-based proteomics was used to investigate the proteome of pre-flowering PMeV-infected *C. papaya* leaf tissue samples. In total, 1,333 proteins were confidently identified, including mainly proteins involved with metabolism, stress response and cellular organization. Using label-free quantification, 111 proteins showed abundance differences, *i.e.* 57 increased and 54 decreased in abundance in PMeV-infected plants. The modulation trend of the proteins was compared with a recently obtained high-throughput shotgun RNA sequencing (RNA-Seq) dataset from equivalent pre-flowering Golden *C. papaya* plant samples. In total, fifteen and zero genes showed the same or opposite regulation trend, respectively, at the protein and the transcript levels. Ninety-six genes were modulated only at the protein level. The relevance of the differently accumulated proteins is discussed in the context of the PSD symptoms development in *C. papaya*.

2. MATERIAL AND METHODS

2.1. Plant Material

Carica papaya L. (cv. Golden) seedlings (n=6) were planted at INCAPER experimental farm located at North of Espírito Santo State, Brazil, thirty-days after germination. After two months, the plants (three biological replicates, n=3) were injected at the leaf petiole either with 1 mL of suspension of (1:1, v/v) latex collected from papaya sticky-diseased fruits in 50 mM sodium phosphate buffer, pH 7.0 (treatment), or with 1 mL of (1:1, v/v) ultrapure water in 50 mM sodium phosphate buffer, pH 7.0 (control). One-month after injection, when the plants were four months old and had formed floral buds, second fully expanded leaf samples were collected and immediately frozen in liquid nitrogen. The tissues were ground, freeze-dried and stored at -80 °C until use.

2.2. Protein Extraction

The tissue powder (10 mg) was submitted to total protein extraction as previously described [25]. Briefly, each sample received 600 µL of 10 mM Tris pH 8.8-buffered phenol and 600 µL of extraction buffer (100 mM Tris-HCl, pH 8.0, 2% (w/v) SDS, 0.9 M sucrose, 10 mM EDTA, and the Roche mini complete EDTA-free protease inhibitor cocktail, Roche, Indianapolis, IN). After 10 min of mixing and a 10 min centrifugation

at 5,000 × *g*, the phenol phase was collected for each sample. An additional extraction was performed using 400 µL of phenol and the phenolic phases (~700 µL) were combined for each sample. Following collection, the extracted proteins were precipitated with 4 mL of 0.1 M ammonium acetate in methanol for 10 hours at -20 °C. The proteins, collected by centrifugation (10 min, 20,000 × *g*, 4 °C), were sequentially washed twice with 1.5 mL of 0.1 M ammonium acetate in methanol, once with 1.5 mL of 80% acetone, and once with 1.5 mL of 70% methanol. Each wash step was followed by centrifugation. The concentration of proteins resuspended in 180 µL of resuspension buffer (50 mM Tris-HCl, pH 8.0, 8 M urea and 2 M thiourea) was determined using the CB-X protein assay (Genotech, St. Louis, MO).

2.3. Protein Digestion

The proteins were sequentially incubated in a compact Thermomixer (Eppendorf, Hamburg, Germany) with 5 mM dithiothreitol (DTT) at 37 °C for 45 min and 100 mM iodoacetamide at 25 °C for 40 min in darkness. The samples were then diluted to 1 M urea with 50 mM Tris-HCl, pH 8.8 prior to trypsin digestion (Sigma, St. Louis, MO) at 1:50 enzyme:substrate ratio. The reaction mixture was incubated at 37 °C for 16 h at 800 rpm and received formic acid to a final concentration of 2% following digestion. Prior to LC-MS/MS analysis, the resulting peptides were desalted using a PepClean C18 spin column (Thermo Scientific, Rockford, lL) and resuspended in 150 µL of 0.1% formic acid (FA)/5% acetonitrile (ACN).

2.4. LC-MS/MS Analysis

Samples were analyzed using a NanoAcquity UPLC system (Waters, Milford, MA) coupled to a TripleTOF 5600 MS/MS (AB SCIEX, Framingham, MA). The peptide mixtures (1µg) were loaded onto a trap column (NanoAcquity UPLC 2G-W/M Trap 5 µm Symmetry C18, 180 µm × 20 mm) at 5 µL/min for 3 min. The peptide separation was carried out in a C18 capillary column (NanoAcquity UPLC 1.8 µm HSS T3, 75 µm × 250 mm) at 300 nL/min. Solvent A constituted 0.1% FA in water and solvent B constituted 0.1% FA in ACN. The peptides were separated using a 90 min linear gradient from 5% to 40% of solvent B, followed by a column cleaning (5 min from 40% to 85% of solvent B and 10 min at 85% of solvent B) and re-equilibration (2 min from 85% to 5% of solvent B and 13 min at 5% of solvent B). The mass spectrometer was operated in positive ionization and high sensitivity mode. The MS survey spectrum was accumulated from 350 to 1600 *m/z* for 250 ms and the first 20 features with a charge state of +2 to +5 and exceeding a 150 count threshold were selected for information dependent acquisition (IDA) MS/MS experiments, each 87.5 ms in length. The fractionation was performed using ±5% rolling collision energy and precursor *m/z* were included on an 8 s dynamic exclusion list after MS/MS selection. A reference sample constituted of equivalent peptide amounts from all replicates was also analyzed and used for label-free protein quantification. An instrument automatic calibration was performed every three samples (6 h) to assure high mass accuracy in both MS and MS/MS acquisition.

2.5. Protein identification and label-free quantification

Raw files (.wiff) acquired from the TripleTOF 5600 were imported into Progenesis QI for proteomics v2.0 (NonLinear Dynamics). Two-dimensional ion intensity maps of features eluting between 25 and 105 min were submitted to automatic reference assignment and alignment of spectra. The alignment was validated (≥ 80% score) and the peak picking parameters were set to “Automatic”. Peak list files (.mgf) were used to interrogate a custom database (27,898 sequences total, May 2015) containing all *C. papaya* protein entries available on Phytozome 10.2 (27,775 sequences, May 2015) [26,27] combined with NCBI *C. papaya* organelle (123 sequences, May 2015) using a Mascot server v.2.2.2 (Matrix science Inc., Boston, MA). The protein identification parameters included +2 to +4 charge state, two missed cleavages, precursor and fragment mass tolerance of ± 20 ppm and ± 0.05 Da, respectively. The variable modifications included acetylation at peptide N-term, carbamidomethylation at cysteine, deamidation at asparagine or glutamine, and oxidation at methionine. An XML file containing the results following Mascot percolation and an FDR < 1% was re-imported to Progenesis QI for peptide quantification and identification. The protein quantification was performed using the normalized abundances of Hi-3 (up to 3) peptides [28] of infected and control samples filtering for Mascot peptide scores ≥ 13 ($p \leq 0.05$) [29]. The abundances of peptides occurring in all three control and PMeV-infected biological replicates were compared by one-way ANOVA test and the protein list was filtered based on $p \leq 0.05$ and a Log_2 fold change (FC) of ±0.58.

2.6. Differential abundance analysis and protein functional classification

All identified proteins were submitted to gene ontology (GO) analysis using Blast2GO (www.blast2go.org). The identified protein sequences were blasted against the NCBI non-redundant (nr) database. Only positive blast hits (E-value 10^{-10} and the first ranked hit) were further used. The GOslim analysis was selected for functional plant class filtering and GO enrichment for up- and down-accumulated protein sets using a Fisher's Exact test with the multiple testing correction FDR option selected [30]. A heat map of differently accumulated proteins was obtained using XLSTAT (www.xlstat.com/en/). The proteins were grouped by their Log_2 fold change.

3. RESULTS

3.1. Proteomic analysis of pre-flowering *C. papaya* leaf

A total of 125,048 MS/MS spectra (~20,841 per sample) (Table 1) were obtained from *C. papaya* leaf samples and searched against a *C. papaya* protein database using Mascot. 24,578 MS/MS (~6,036 per sample) (Table 1 and Supplemental Table S1) were assigned to 4,289 unique peptides (Supplemental Table S2), corresponding to 1,333 identified proteins (Supplemental Table S3). Out of those, 1,330 (99.8%) proteins had at least one positive Blast2GO hit (Supplemental Table S3). The most

represented GO biological processes were cellular metabolic process (690 proteins), organic substance metabolic process (651 proteins) and primary metabolic process (651 proteins) (Figure 1). A total of 228 identified proteins (17%) were associated to the response to stress GO term, which includes biotic/abiotic stress and immune response (Figure 1 and Supplemental Table S3). Some proteins in this group are already known to be involved with *C. papaya* x PMeV interaction such as 26s proteasome regulatory subunit, calreticulin and acidic endochitinase (Supplemental Table S3) [6,22]. The group represents a main source of other proteins potentially involved with plant responses to viruses. The Supplemental Figure S1 A and B demonstrate the protein grouping according to their associated GO cellular components and molecular processes, respectively.

3.2. Differential proteome of pre-flowering PMeV-infected *C. papaya vs.* control plants

The proteins showed average coefficient of variation (CV) of 24% (20% CV median) (Supplemental Table S4 and Supplemental Figure S2), and 1,257 (94%) (Table 1) proteins were considered for protein abundance comparisons between pre-flowering PMeV-infected and control *C. papaya* leaf samples. A total of 111 proteins, 57 up- and 54 down-accumulated, showed significant abundance changes ($p \leq 0.05$); FC of at least ±0.58 (Figure 2 and Table 2). The proteins with highest change in abundance levels were haloacid dehalogenase-like hydrolase family protein 2 (2.94 FC), alpha-glucan phosphorylase 2 (2.88 FC) and gamete expressed protein 1 (2.29 FC), while the lowest accumulation levels were observed for glycosyl hydrolase 9B13 (-3.93 FC), subtilase 1.3 (-2.41 FC), vacuolar membrane ATPase 10 (-2.19 FC) (Figure 2 and Table 2).

After Blast2GO analysis, at least one positive hit was obtained for each of the differential proteins (Figure 3, Supplemental Figure S3 and S4). Thirty-two GO terms were found enriched ($p \leq 0.05$), ten and twenty-two within the proteins with increased or reduced abundance in the PMeV-infected *C. papaya* samples, respectively (Supplemental Table S5). The most prevalent processes within proteins with increased abundances were photosynthesis and redox-regulation, whereas catabolic process and cell wall were prevalent within proteins with lower abundances. In parallel, of the 54 proteins showing reduced levels in PMeV-infected *C. papaya*, 14 were predicted to be involved with cell wall remodeling (*e.g.* beta-D-xylosidase 4, NAD(P)-binding Rossmann-fold superfamily protein and reversibly glycosylated polypeptide 3) and proteolysis (*e.g.* subtilase 1.3, xylem cysteine peptidase 1 and serine carboxypeptidase-like 33).

4. DISCUSSION

The availability of the *C. papaya* genome [26] has facilitated the utilization of proteomics to understand different biological aspects of the species. To our knowledge, previously published studies have used gel (1- and 2-DE and DIGE)-based separations of *C. papaya* proteins followed by peptide mass spectrometry analysis. In summary, the total number of identified proteins per sample type is 76 from somatic embryos [31], 54 from papaya fruit pulp [32,33], 71 from leaves [22], 186 from latex [6,34] and 1,581 proteins from isolated chromoplasts [35]. In this study, field-grown pre-flowering *C. papaya* plants' leaf samples were submitted to protein extraction and in-solution digestion, and the resulting peptides were analyzed using an LC-MS/MS based approach. As expected for this kind of approach [36,37], consistent proteomic coverage was obtained as 1,333 unique proteins were identified. The GO-based grouping of the identified proteins showed they were largely associated with

metabolism, stress responses and cellular organization. *C. papaya* proteins known to be differentially accumulated in sticky-diseased papaya leaf [22] and latex [6] samples, for instance tubulin beta, HSP70 and latex serine protease inhibitor, were among the identified proteins, suggesting the obtained dataset likely includes other proteins relevant to the pathosystem.

The comparison between infected and healthy control plants resulted in 111 proteins with abundance differences, *i.e.* 57 increased and 54 decreased in abundance in PMeV-infected plants. The list of differently accumulated proteins (Table 2) was compared with a recently obtained RNA-Seq dataset from equivalent pre-flowering Golden PMeV-infected *C. papaya* plant samples (Madroñero et al. [24], Submitted manuscript, please see Reviewers-only Supplemental Table). A total of 15 genes presented the same regulation trend at the transcript level. Zero genes showed opposite regulation trend in both datasets, while 96 genes were modulated only at the protein level. The last group of genes include those coding for proteins known to be involved with plant-virus interaction and plant immunity, *e.g.* 26S proteasome regulatory subunits [38] and photosystem II proteins [39]. Thus, understanding the effects of PMeV on pre-flowering *C. papaya* at the protein level may reveal resistance genes different or complementary to those discovered based on transcript analysis.

Photosynthesis largely contributes to the general cellular energy state and redox balance by providing NADPH, ATP and carbon skeletons, which support plant growth and fuels the initiation and maintenance of responses against external stress factors [39]. Changes in photosynthetic components may trigger and fine-tune plant responses to biotic stress. Thus, several photosynthesis-related proteins, for example PsbO [40], PSI proteins and ATP synthase [41], have been shown to be responsive to viral infection. The silencing of the gene encoding to 33K subunit of the oxygen-evolving complex of photosystem II, enhanced the replication of *Tobacco mosaic virus* (TMV) and other viruses in *Nicotiana benthamiana* [42]. This suggests the proper photosynthetic activity, especially at the light-driven reactions level, is important in plant response against viruses.

Photosynthesis-related proteins were found to be more abundant in the pre-flowering PMeV-infected *C. papaya* samples implicating a role for photosynthesis in *C. papaya* response to PMeV infection. The increased levels of oxygen evolving complex-related

proteins, *e.g.* photosystem II subunit R (10 kDa), favors an increased water-derived electron input in PSII. Accordantly, chloroplast electron transfer chain-related proteins, *i.e.* photosystem II protein V and photosystem II protein H, were also increased in abundance in infected samples. A higher electron flow ratio increases the reduced plastoquinone (PQ) pool, which is correlated with the activation of defense-related genes and the development of HR upon biotic stresses [43], and potentially leads to the production of ROS. This group of molecules has signaling effects in the chloroplast itself and in other cell parts, often involving hormonal cross-talk regulating the activation of defense [44]. ROS may induce the production of stress-related hormones in plants [44–46]. Although some proteins, *e.g.* ethylene-forming enzyme, allene oxide cyclase 3, and sterol methyltransferase 2, involved with the metabolism of ethylene, jasmonic acid and brassinosteroid respectively, were present in our dataset, they did not change in abundance in PMeV-infected *C. papaya*. This suggests that the analyzed plants were at the beginning of the stress response or, they had more likely developed a partial activation of stress response pathways upon PMeV infection.

Opposite to what was previously observed for adult and sticky-diseased *C. papaya* plants [22], pre-flowering PMeV-infected *C. papaya* leaves showed lower levels of 26S proteasome-related proteins. In plants, the 26S proteasome system is essential to regulate proteolysis and control the abundance of crucial cellular regulators in response to distinct environmental and developmental cues, including virus infection [47,48]. In *N. benthamiana*, the use of virus-induced gene silencing targeting the α6 subunit and the RPN9 subunit of the 20S and 19S proteasome, respectively, increased the levels of polyubiquitinated proteins resulting in increased programed cell death (PCD) [49]. Reduction in the levels of proteasome related proteins in pre-flowering PMeV-infected *C. papaya* is likely associated with the activation of defense response in the plant. The full activation of defenses involves the activity of caspase-like serine proteases [49,50], such as subtilase 1.3, whose levels were reduced in PMeV-infected *C. papaya*. This may contribute to reduce not only the resistance based on 26S proteasome-related proteins but also the overall resistance of pre-flowering *C. papaya* against PMeV.

The 26S proteasome affects the vascular development of plants, with negatively impacts the systemic transport of viruses. In *N. benthamiana*, the down-regulation of RPN9 compromises the development of phloem, but not xylem, resulting in resistance

to TMV and *Turnip mosaic virus* (TuMV) movement [38]. Besides phloem and xylem, *C. papaya* possesses laticifers, a system of interconnected cells spread in the whole plant body. However, the effects of 26S proteasome in *C. papaya* vascular cells and laticifers development are unknown. There may be a link between the lower abundance of 26S proteasome at early stages of PMeV infection and the development of *C. papaya* laticifers, maybe causing osmotic imbalance in those cells [5]. If changes in 26S proteassome levels affect the laticifers or vascular cells of *C. papaya,* the alteration must be at the cellular level since the analysis of leaf and petiole tissues of PSD symptomatic and asymptomatic plants using light microscopy conducted in our laboratory did not reveal any consistent difference in laticifers or phloem/xylem cells (data not shown). Although PMeV has been observed only in *C. papaya* laticifers [3], its movement through phloem or xylem cells must be considered [5].

Callose (1,3-β-glucan polymer) deposition either in the plasmodesmata (PD) or in the cell wall of phloem cells is a plant resistance mechanism to cell-to-cell and long-distance virus movement, respectively [51,52]. In response to the reduction in the size exclusion limit (SEL) of PD cytoplasmic sleeve, some viruses have evolved the capability of altering the SEL in favor of their spread in the plant [55]. For example, class I β-1,3-glucanase (GLU I)-deficient TAG4.4 tobacco mutant has a PD SEL reduced by increased callose deposition, which delayed intercellular virus trafficking via PD, decreasing the susceptibility to TMV, potexvirus, and *Cucumber mosaic virus* [51]. The down-regulation of several cell-wall associated proteins, *e.g.* reversibly glycosylated polypeptide 3 and NAD(P)-binding Rossmann-fold superfamily protein, may be involved with plant resistance against PMeV movement. Cell-wall proteins are not only considered host factors affecting the host susceptibility but also mediate the local and systemic translocation of viruses [54,55]. These results suggest that reduced levels of cell wall proteins in PMeV-infected pre-flowering *C. papaya* precede the sticky disease symptoms development.

5. CONCLUSION

This study reports the identification of 1,333 proteins from *C. papaya*. Significant abundance changes were observed for 111 proteins (57 increased and 54 decreased in abundance) in pre-flowering PMeV-infected *C. papaya*. The obtained data supports the assumption of increased photosynthesis and reduction of 26S-proteassoma activity and cell-wall remodeling. Based on the available information about the PMeV vs. *C. papaya* interaction and the knowledge from other models, increased photosynthetic activity has a positive effect on the induction of plant immunity. In parallel, the reduction in the caspase-like activity and the observed changes in the cell-wall associated proteins impairs the full activation of defense response based on hypersensitive cell death and viral movement obstruction in pre-flowering plants. Together, these effects contribute to *C. papaya* resistance against PMeV at the pre-flowering stage of the plant development.

ACKNOWLEDGMENTS

This work was supported by grants from FINEP (Financiadora de Estudos e Projetos), CNPq (Conselho Nacional de Desenvolvimento Científico e Tecnológico), CAPES (Coordenação de Aperfeiçoamento de Pessoal de Nível Superior) and FAPES (Fundação de Amparo à Pesquisa do Estado do Espírito Santo).

SUPPLEMENTARY DATA

Soares et al., 2016_Supplemental Tables.xlsx

Soares et al., 2016_Supplemental Figures.pdf

Table 1. Proteomic coverage of pre-flowering PMeV-infected and control *C. papaya* leaf samples.

Sample	Total number of MS/MS spectra[1]	Total number of ions[2]	Number of quantified proteins[3]
Control 1	24335	6070	1301
Control 2	24116	6068	1302
Control 3	14441	6035	1293
Infected 1	18053	5981	1289
Infected 2	23318	6012	1301
Infected 3	20785	6048	1296
Mean	20841	6036	1297
Total	**125048**	**24578**	**1257**

[1]Number of MS/MS spectra obtained using TripleTOF 5600.

[2]Number of peptide-assigned ions.

[3]Number of quantified proteins.

Table 2. Differently accumulated proteins in pre-flowering PMeV-infected *C. papaya* leaf.

Phytozome/NCBI Accession[1]	Description[2]	Confidence score[3]	Anova (p)[4]	Fold change[5]
Up-accumulated proteins				
PACid:16420809	haloacid dehalogenase-like hydrolase family protein	52.48	0.018	2.94
PACid:16405967	alpha-glucan phosphorylase 2	17.32	0.032	2.88
PACid:16406350	gamete expressed protein 1	19.33	0.002	2.29
PACid:16421050	nitrate reductase 2	39.8	0.016	1.62
PACid:16431468	alkenal reductase	142.47	0.033	1.59
PACid:16412285	photosystem I subunit O	82.63	0.024	1.55
PACid:16417715	alanine-2-oxoglutarate aminotransferase 2	844.87	0.046	1.48
PACid:16409579	chloroplast outer envelope protein 37	107.65	0.014	1.43
PACid:16419415	Eukaryotic aspartyl protease family protein	105.25	0.020	1.37
PACid:16405950	None	181.1	0.024	1.35
PACid:16421146	Mog1/PsbP/DUF1795-like photosystem II reaction center PsbP family protein	42.52	0.014	1.32
PACid:16416428	30S ribosomal protein, putative	248.82	0.022	1.30
PACid:16418757	Pseudouridine synthase/archaeosine transglycosylase-like family protein	86.15	0.007	1.27
PACid:16405684	None	108.06	0.026	1.27
PACid:16428298	Rhodanese/Cell cycle control phosphatase superfamily protein	132.8	0.014	1.27
PACid:16412313	None	39.08	0.021	1.26
PACid:16418903	FKBP-like peptidyl-prolyl cis-trans isomerase family protein	75.14	0.034	1.23
GI:167391793	ATP synthase CF0 A subunit (chloroplast)	72.79	0.001	1.21
PACid:16418478	Insulinase (Peptidase family M16) family protein	126.19	0.001	1.18
PACid:16419064	rubredoxin family protein	131.92	0.030	1.18
PACid:16415363	fatty acid biosynthesis 1	127.66	0.026	1.15
PACid:16425469	Mitochondrial substrate carrier family protein	190.84	0.004	1.14
PACid:16416362	None	41.27	0.037	1.14
PACid:16430998	photosystem II subunit R	163.23	0.037	1.13
PACid:16405384	None	74.07	0.025	1.13
GI:167391835	photosystem II protein H (chloroplast)	47.22	0.012	1.11
PACid:16412470	NAD(P)-linked oxidoreductase superfamily protein	432.71	0.033	1.11
PACid:16421240	Thioredoxin family protein	47.74	0.042	1.08
GI:167391811	ATP synthase CF1 epsilon subunit (chloroplast)	560.2	0.028	1.05
PACid:16424321	long chain acyl-CoA synthetase 9	77.16	0.033	1.04
PACid:16425458	Phosphoenolpyruvate carboxylase family protein	40.59	0.010	1.04
PACid:16415093	glyceraldehyde-3-phosphate dehydrogenase B subunit	1058.51	0.035	1.02
PACid:16413741	carbonic anhydrase 1	1158.5	0.038	1.01
PACid:16411817	Citrate synthase family protein	72.24	0.010	1.01
PACid:16429120	PsbQ-like 1	42.11	0.024	1.00

PACid:16425084	glycine decarboxylase P-protein 1	1306.07	0.039	0.98
PACid:16415334	thioredoxin M-type 4	325.81	0.022	0.98
PACid:16424704	uridylyltransferase-related	244.64	0.014	0.97
PACid:16426635	photosystem I subunit l	61.79	0.044	0.96
PACid:16410085	glutamine synthetase 2	749.17	0.022	0.87
PACid:16413084	pyrophosphorylase 6	297.23	0.002	0.85
PACid:16409157	lipoamide dehydrogenase 2	684.33	0.013	0.85
PACid:16425317	glyceraldehyde 3-phosphate dehydrogenase A subunit	1260.62	0.040	0.83
PACid:16427275	beta glucosidase 34	373.93	0.045	0.76
PACid:16430304	FtsH extracellular protease family	155.82	0.012	0.72
PACid:16428265	None	118.93	0.013	0.71
PACid:16428426	glycine decarboxylase complex H	142.36	0.015	0.67
PACid:16420953	thylakoid lumen 18.3 kDa protein	370.34	0.032	0.67
PACid:16412072	Chalcone-flavanone isomerase family protein	61.06	0.015	0.66
PACid:16417556	non-intrinsic ABC protein 7	48.5	0.025	0.65
PACid:16420444	chloroplast thylakoid lumen protein	218.14	0.021	0.65
PACid:16405665	ribulose-bisphosphate carboxylases	188.43	0.027	0.65
PACid:16424915	beta carbonic anhydrase 4	44.32	0.030	0.64
PACid:16432002	photosystem II protein V (chloroplast)	124.02	0.012	0.63
PACid:16422806	fructokinase-like 1	14.18	0.015	0.60
PACid:16404531	P-loop containing nucleoside triphosphate hydrolases superfamily protein	176.12	0.040	0.60
PACid:16422008	FtsH extracellular protease family	240.57	0.009	0.58
	Down-accumulated proteins			
PACid:16409537	glycosyl hydrolase 9B13	62.2	0.012	-3.93
PACid:16419256	subtilase 1.3	39.27	0.023	-2.41
PACid:16424681	vacuolar membrane ATPase 10	112.72	0.016	-2.19
PACid:16430034	Eukaryotic aspartyl protease family protein	218.19	0.030	-2.12
PACid:16420814	importin alpha isoform 4	76.58	0.005	-1.99
PACid:16411484	AMP-dependent synthetase and ligase family protein	215.65	0.016	-1.92
PACid:16416704	beta-6 tubulin	520.05	0.013	-1.90
PACid:16421623	acyl-CoA dehydrogenase-related	122.02	0.017	-1.90
PACid:16420458	hydroxycinnamoyl-CoA shikimate/quinate hydroxycinnamoyl transferase	148.57	0.005	-1.86
PACid:16429527	xylem cysteine peptidase 1	744.8	0.023	-1.85
PACid:16427373	Leucine-rich repeat (LRR) family protein	138.2	0.038	-1.85
PACid:16419512	Eukaryotic aspartyl protease family protein	527.01	0.001	-1.79
PACid:16405998	tubulin beta 8	908.72	0.004	-1.77
PACid:16429251	beta-galactosidase 2	79.49	0.018	-1.76
PACid:16423878	S-adenosyl-L-methionine-dependent methyltransferases superfamily protein	221.12	0.015	-1.73
PACid:16407258	Protein of unknown function, DUF642	50	0.032	-1.66
PACid:16406833	HIS HF	36.67	0.042	-1.57
PACid:16428909	regulatory particle AAA-ATPase 2A	130.86	0.028	-1.55
PACid:16417516	regulatory particle triple-A ATPase 5A	153	0.023	-1.51
PACid:16416562	Enolase	89.25	0.014	-1.46

PACid:16416090	xylem cysteine peptidase 1	814.17	0.042	-1.44
PACid:16426335	regulatory particle non-ATPase 12A	79.24	0.007	-1.42
PACid:16430932	O-fucosyltransferase family protein	69.34	0.047	-1.35
PACid:16428927	RNA-binding KH domain-containing protein	35.12	0.030	-1.31
PACid:16413069	ribophorin II (RPN2) family protein	57.41	0.027	-1.22
PACid:16404978	Glycosyl hydrolase family protein	344.76	0.015	-1.19
PACid:16413321	homolog of nucleolar protein NOP56	123.63	0.016	-1.14
PACid:16413698	annexin 2	300.66	0.016	-1.08
PACid:16403847	beta-D-xylosidase 4	309.11	0.013	-1.04
PACid:16431432	Microsomal signal peptidase 25 kDa subunit (SPC25)	19.26	0.017	-1.01
PACid:16409224	pathogenesis-related 4	108.41	0.017	-0.93
PACid:16414807	regulatory particle triple-A 1A	112.4	0.005	-0.92
PACid:16412735	sorting nexin 2A	50.82	0.041	-0.89
PACid:16429378	Phosphofructokinase family protein	272.49	0.013	-0.87
PACid:16405986	proliferating cell nuclear antigen 2	50.7	0.011	-0.82
PACid:16428304	serine carboxypeptidase-like 33	170.19	0.029	-0.82
PACid:16430896	annexin 8	164.29	0.008	-0.77
PACid:16423532	catalase 2	1602.63	0.017	-0.77
PACid:16427183	HXXXD-type acyl-transferase family protein	205.93	0.030	-0.75
PACid:16407705	calnexin 1	173.11	0.029	-0.75
PACid:16416571	ribosomal protein S13A	161	0.003	-0.75
PACid:16414081	ubiquitin-specific protease 21	25.59	0.033	-0.74
PACid:16405397	fibrillarin 2	31.61	0.018	-0.73
PACid:16416653	kunitz trypsin inhibitor 1	34.09	0.044	-0.72
PACid:16406190	acetyl Co-enzyme a carboxylase biotin carboxylase subunit	453.07	0.013	-0.68
PACid:16413146	poly(A) binding protein 2	143.5	0.047	-0.68
PACid:16408020	Ribosomal L28e protein family	31.37	0.026	-0.67
PACid:16411483	AMP-dependent synthetase and ligase family protein	62.2	0.016	-0.67
PACid:16428160	NAD(P)-binding Rossmann-fold superfamily protein	77.86	0.030	-0.62
PACid:16405062	Eukaryotic aspartyl protease family protein	90.65	0.029	-0.61
PACid:16432172	O-fucosyltransferase family protein	27.71	0.007	-0.60
PACid:16405578	reversibly glycosylated polypeptide 3	613.23	0.038	-0.60
PACid:16406570	tubulin alpha-3	966.21	0.004	-0.60
PACid:16425256	chaperonin 10	26.37	0.048	-0.59

[1]Phytozome or NCBI gene identification number.

[2]Phytozome or NCBI gene description.

[3]Quality assurance scores for protein identification by Progenesis QI.

[4]Analysis of variance (ANOVA) based p value.

[5]Log_2 fold change of protein abundances comparing PMeV-infected *vs.* control plants.

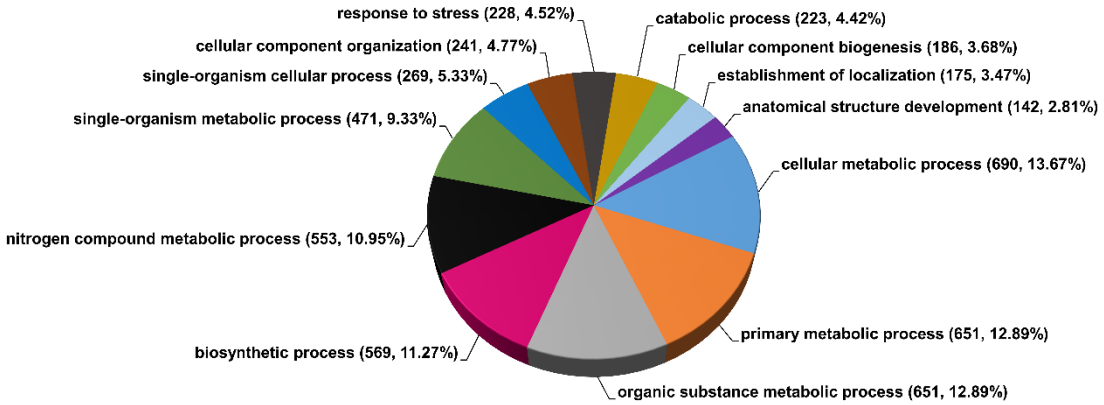

Figure 1. Gene Ontology (GO) grouping of PMeV-infected *C. papaya* leaf proteins according to their associated Biological Process at the third level using Blast2GO software. The numbers indicate the amount of sequences grouped in each GO term(s).

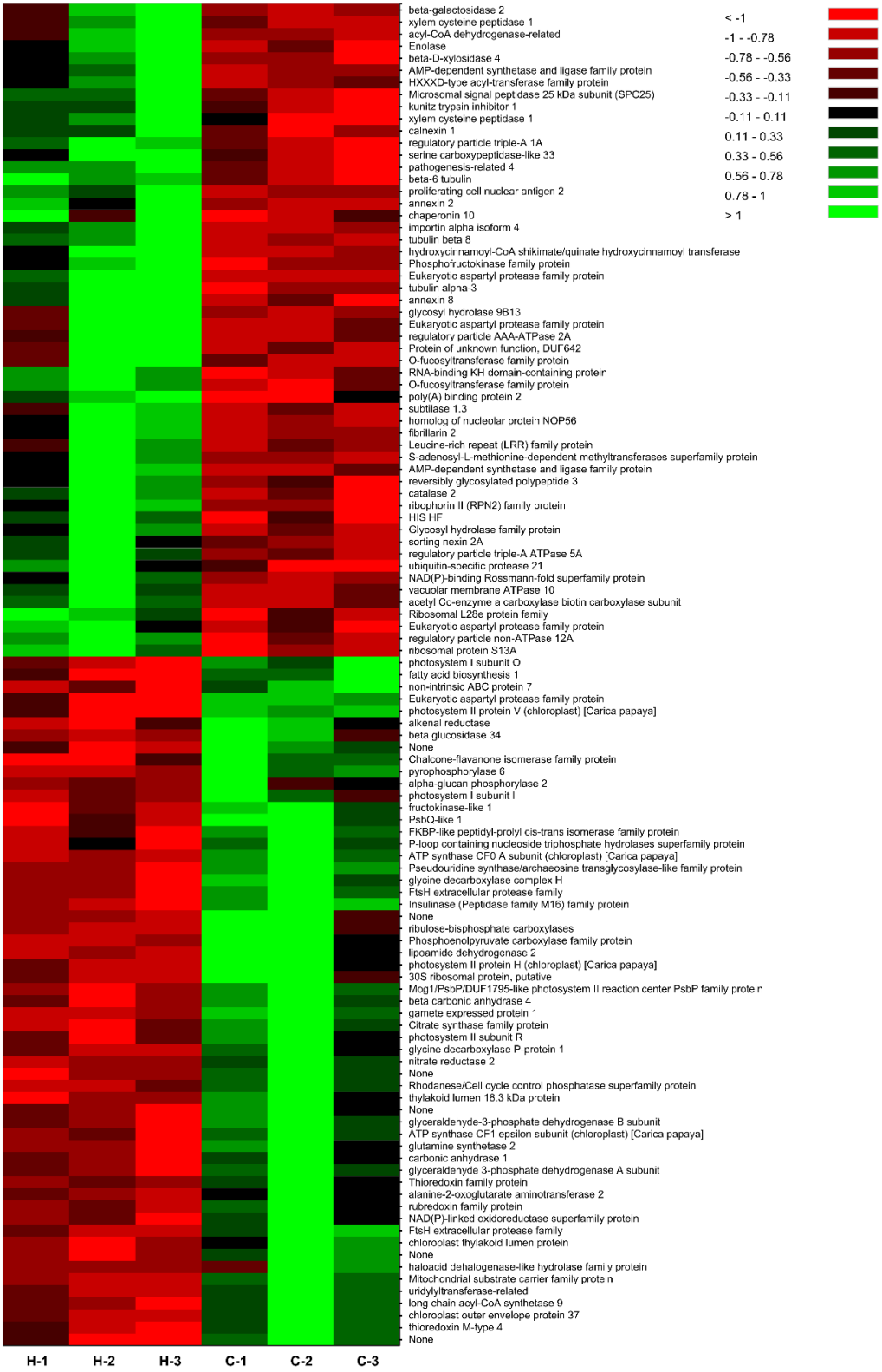

Figure 2. Heat map of the differently accumulated proteins in PMeV-infected *C. papaya* leaf samples. The proteins were ranked based on their Log2 fold change abundance values.

Figure 3. Gene Ontology (GO) multi-level bar chart displaying the GO terms percentage in Down-accumulated (green) and Up-accumulated (red) proteins. The proteins were grouped by their predicted GO Biological Process.

REFERENCES

[1] E. Maciel-Zambolim, S. Kunieda-Alonso, K. Matsuoka, M.G. De Carvalho, F.M. Zerbini, Purification and some properties of Papaya meleira virus, a novel virus infecting papayas in Brazil, Plant Pathol. 52 (2003) 389–394.

[2] D.S. Buss, G.B. Dias, M.P. Santos, J.A. Ventura, P.M.B. Fernandes, Oxidative stress defence response of Carica papaya challenged by nitric oxide, Papaya meleira virus and Saccharomyces cerevisiae, Open Nitric Oxide J. 3 (2011) 55–64.

[3] E.W. Kitajima, C.H. Rodrigues, J.S. Silveira, F. Alves, Association of isometric viruslike particles, restricted to lacticifers, with “meleira” (“sticky disease”) of papaya (Carica papaya), Fitopatol. Bras. 18 (1993) 118.

[4] D. Perez-Brito, R. Tapia-Tussell, A. Cortes-Velazquez, A. Quijano-Ramayo, A. Nexticapan-Garcez, R. Martín-Mex, First report of papaya meleira virus (PMeV) in Mexico, African J. Biotechnol. 11 (2012) 13564–13570.

[5] S.P. Rodrigues, M. Da Cunha, J. a Ventura, P.M.B. Fernandes, Effects of the Papaya meleira virus on papaya latex structure and composition, Plant Cell Rep. 28 (2009).

[6] S.P. Rodrigues, J. a. Ventura, C. Aguilar, E.S. Nakayasu, H. Choi, T.J.P. Sobreira, L.L. Nohara, L.S. Wermelinger, I.C. Almeida, R.B. Zingali, P.M.B. Fernandes, others, Label-free quantitative proteomics reveals differentially regulated proteins in the latex of sticky diseased Carica papaya L. plants, J. Proteomics 75 (2012) 3191–3198.

[7] P.M. V Abreu, C.G. Gaspar, D.S. Buss, J. a Ventura, P.C.G. Ferreira, P.M.B. Fernandes, Carica papaya microRNAs are responsive to Papaya meleira virus infection, PLoS One. 9 (2014) e103401.

[8] G. Wang, S. Seabolt, S. Hamdoun, G. Ng, J. Park, H. Lu, Multiple Roles of WIN3 in Regulating Disease Resistance , Cell Death , and Flowering Time in Arabidopsis, Plant. Physiol. 156 (2011) 1508–1519.

[9] G. Lazarovits, R. Stossel, E.W.B. Ward, Age-Related-Changes in Specificity and Glyceollin Production in the Hypocotyl Reaction of Soybeans to Phytophthora-megasperma mar-mojae, Phytopathology 71 (1981) 94–97.

[10] J. V Kus, K. Zaton, R. Sarkar, R.K. Cameron, Age-related resistance in Arabidopsis is a developmentally regulated defense response to Pseudomonas syringae, Plant Cell. 14 (2002) 479–490.

[11] J.D. Paxton, Chamberl.Dw, Phytoalexin production and disease resistance in soybeans as affected by age, Phytopathology. 59 (1969) 775–777.

[12] D.F. Bateman, R.D. Lumsden, Relation of calcium content and nature of pectic substances in bean hypocotyls of different ages to susceptibility to an isolate of Rhizoctonia solani, Phytopathology 55 (1965) 734–738.

[13] M.C. Heath, Genetics and cytology of age-related resistance in North-American

cultivars of cowpea (Vigna-unguiculata) to the cowpea rust fungus (Uromyces-vignae), Can. J. Bot. Can. Bot. 72 (1994) 575–581.

[14] P. Coelho, K. Bahcevandziev, L. Valerio, A. Monteiro, D. Leckie, D. Astley, I.R. Crute, I. Boukema, The relationship between cotyledon and adult plant resistance to downy mildew (Peronospora parasitica) in Brassica oleracea, Acta Horticulturae 459 (1997) 335–342.

[15] R.E. Hunter, J.M. Halloin, J.A. Veech, W.W. Carter, Terpenoid accumulation in hypocotyls of cotton seedlings during aging and after infection by Rhizoctonia-solani, Phytopathology 68 (1978) 347–350.

[16] B.G. Abedon, W.F. Tracy, Corngrass1 of maize (Zea mays L) delays development of adult plant resistance to common rust (Puccinia sorghi Schw) and European corn borer (Ostrinia nubilalis hubner), J. Hered. 87 (1996) 219–223.

[17] S.E. Wyatt, S.Q. Pan, J. Kuc, Beta-1,3-glucanase, chitinase, and peroxidase-activities in tobacco tissues resistant and susceptible to blue mold as related to flowering, age and sucker development, Physiol. Mol. Plant Pathol. 39 (1991) 433–440.

[18] K. Hugot, S. Aime, S. Conrod, A. Poupet, E. Galiana, Developmental regulated mechanisms affect the ability of a fungal pathogen to infect and colonize tobacco leaves, PLANT J. 20 (1999) 163–170.

[19] C. Rusterucci, Z. Zhao, K. Haines, D. Mellersh, A. Neumann, R.K. Cameron, Age-related resistance to Pseudomonas syringae pv. tomato is associated with the transition to flowering in Arabidopsis and is effective against Peronospora parasitica, Physiol. Mol. Plant Pathol. 66 (2005) 222–231.

[20] S.M. Leisner, R. Turgeon, S.H. Howell, others, Long distance movement of cauliflower mosaic virus in infected turnip plants, Mol. Plant-Microbe Interact. 5 (1992) 41–47.

[21] S.M. Leisner, R. Turgeon, S.H. Howell, Effects of host plant development and genetic-determinants on the long-distance movement of Cauliflower mosaic-virus in Arabidopsis, Plant Cell. 5 (1993) 191–202.

[22] S.P. Rodrigues, J. a. Ventura, C. Aguilar, E.S. Nakayasu, I.C. Almeida, P.M.B. Fernandes, R.B. Zingali, Proteomic analysis of papaya (Carica papaya L.) displaying typical sticky disease symptoms, Proteomics 11 (2011) 2592–2602.

[23] K. Hugot, M.-P. Rivière, C. Moreilhon, M. a Dayem, J. Cozzitorto, G. Arbiol, P. Barbry, C. Weiss, E. Galiana, Coordinated regulation of genes for secretion in tobacco at late developmental stages: association with resistance against oomycetes, Plant Physiol. 134 (2004) 858–870.

[24] J. Madroñero, S.P. Rodrigues, P.M. V Abreu, T.F.S. Antunes, J.A. Ventura, A.A.R. Fernandes, P.M.B. Fernandes, Transcriptome analysis of PMeV-infected C. papaya, Mol. Plant Pathol.

[25] H. Wang, S. Alvarez, L.M. Hicks, Comprehensive Comparison of iTRAQ and Label-free LC-Based Quantitative Proteomics Approaches Using Two Chlamydomonas reinhardtii Strains of Interest for Biofuels Engineering, J. Proteome Res. 11 (2012) 487–501.

[26] R. Ming, S. Hou, Y. Feng, Q. Yu, A. Dionne-Laporte, J.H. Saw, P. Senin, W. Wang, B. V. Ly, K.L.T. Lewis, S.L. Salzberg, L. Feng, M.R. Jones, R.L. Skelton, J.E. Murray, C. Chen, W. Qian, J. Shen, P. Du, M. Eustice, E. Tong, H. Tang, E. Lyons, R.E. Paull, T.P. Michael, K. Wall, D.W. Rice, H. Albert, M.-L. Wang, Y.J. Zhu, M. Schatz, N. Nagarajan, R.A. Acob, P. Guan, A. Blas, C.M. Wai, C.M. Ackerman, Y. Ren, C. Liu, J.J. Wang, J.J. Wang, J.-K. Na, E. V. Shakirov, B. Haas, J. Thimmapuram, D. Nelson, X. Wang, J.E. Bowers, A.R. Gschwend, A.L. Delcher, R. Singh, J.Y. Suzuki, S. Tripathi, K. Neupane, H. Wei, B. Irikura, M. Paidi, N. Jiang, W. Zhang, G. Presting, A. Windsor, R. Navajas-Pérez, M.J. Torres, F.A. Feltus, B. Porter, Y. Li, A.M. Burroughs, M.-C. Luo, L. Liu, D.A. Christopher, S.M. Mount, P.H. Moore, T. Sugimura, J. Jiang, M.A. Schuler, V. Friedman, T. Mitchell-Olds, D.E. Shippen, C.W. dePamphilis, J.D. Palmer, M. Freeling, A.H. Paterson, D. Gonsalves, L. Wang, M. Alam, others, The draft genome of the transgenic tropical fruit tree papaya (Carica papaya Linnaeus), Nature 452 (2008) 991–996.

[27] H. Nordberg, M. Cantor, S. Dusheyko, S. Hua, A. Poliakov, I. Shabalov, T. Smirnova, I. V Grigoriev, I. Dubchak, The genome portal of the Department of Energy Joint Genome Institute : 2014 updates, 42 (2014) 26–31.

[28] J.C. Silva, Absolute Quantification of Proteins by LCMSE: A Virtue of Parallel ms Acquisition, Mol. Cell. Proteomics 5 (2005) 144–156.

[29] M. Brosch, L. Yu, T. Hubbard, J. Choudhary, Accurate and sensitive peptide identification with Mascot Percolator, J. Proteome Res. 8 (2009) 3176–81.

[30] Y. Benjamini, Y. Hochberg, Controlling the False Discovery Rate: A Practical and Powerful Approach to Multiple Testing, J. R. Stat. Soc. Ser. B. 57 (1995) 289–300.

[31] E.D.M. Vale, A.S. Heringer, T. Barroso, A. Teixeira, M. Nunes, J. Enrique, A. Perales, C. Santa-catarina, V. Silveira, Comparative proteomic analysis of somatic embryo maturation in Carica papaya L, Proteome Science (2014) 12:37.

[32] J.Á. Huerta-Ocampo, J.A. Osuna-Castro, G.J. Lino-López, A. Barrera-Pacheco, G. Mendoza-Hernández, A. De León-Rodríguez, A.P. Barba de la Rosa, Proteomic analysis of differentially accumulated proteins during ripening and in response to 1-MCP in papaya fruit, J. Proteomics 75 (2012) 2160–2169.

[33] S.B. Nogueira, C.A. Labate, F.C. Gozzo, E.J. Pilau, F.M. Lajolo, J.R. Oliveira do Nascimento, Proteomic analysis of papaya fruit ripening using 2DE-DIGE, J. Proteomics 75 (2012) 1428–1439.

[34] R. Dhouib, J. Laroche-Traineau, R. Shaha, D. Lapaillerie, E. Solier, J. Ruaĺs, M. Pina, P. Villeneuve, F. Carrìre, M. Bonneu, V. Arondel, Identification of a putative triacylglycerol lipase from papaya latex by functional proteomics, FEBS J. 278 (2011) 97–110.

[35] Y.Q. Wang, Y. Yang, Z. Fei, H. Yuan, T. Fish, T.W. Thannhauser, M. Mazourek, L. V. Kochian, X. Wang, L. Li, Proteomic analysis of chromoplasts from six crop species reveals insights into chromoplast function and development, J. Exp. Bot. 64 (2013) 949–961.

[36] V.J. Patel, K. Thalassinos, S.E. Slade, J.B. Connolly, A. Crombie, J.C. Murrell,

J.H. Scrivens, A comparison of labeling and label-free mass spectrometry-based proteomics approaches, J Proteome Res. 8 (2009) 3752–3759.

[37] B. Deracinois, C. Flahaut, S. Duban-Deweer, Y. Karamanos, Comparative and Quantitative Global Proteomics Approaches: An Overview, Proteomes 1 (2013) 180–218.

[38] H. Jin, S. Li, A. Villegas, Down-regulation of the 26S proteasome subunit RPN9 inhibits viral systemic transport and alters plant vascular development, Plant Physiol. 142 (2006) 651–61.

[39] S. Kangasjärvi, M. Tikkanen, G. Durian, E.-M. Aro, Photosynthetic light reactions – An adjustable hub in basic production and plant immunity signaling, Plant Physiol. Biochem. 81 (2014) 128–134.

[40] C. Jang, E.-Y. Seo, J. Nam, H. Bae, Y.G. Gim, H.G. Kim, I.S. Cho, Z.-W. Lee, G.R. Bauchan, J. Hammond, H.-S. Lim, Insights into Alternanthera mosaic virus TGB3 Functions: Interactions with Nicotiana benthamiana PsbO Correlate with Chloroplast Vesiculation and Veinal Necrosis Caused by TGB3 Over-Expression, Front. Plant Sci. 4 (2013) 1–15.

[41] K. Lehto, M. Tikkanen, J.-B. Hiriart, V. Paakkarinen, E.-M. Aro, Depletion of the photosystem II core complex in mature tobacco leaves infected by the flavum strain of tobacco mosaic virus., Mol. Plant. Microbe. Interact. 16 (2003) 1135–44.

[42] T.E.M. Abbink, J.R. Peart, T.N.M. Mos, D.C. Baulcombe, J.F. Bol, H.J.M. Linthorst, Silencing of a gene encoding a protein component of the oxygen-evolving complex of photosystem II enhances virus replication in plants, Virology 295 (2002) 307–319.

[43] P. Muhlenbock, M. Szechynska-Hebda, M. Plaszczyca, M. Baudo, A. Mateo, P.M. Mullineaux, J.E. Parker, B. Karpinska, S. Karpinski, Chloroplast Signaling and LESION SIMULATING DISEASE1 Regulate Crosstalk between Light Acclimation and Immunity in Arabidopsis, Plant Cell 20 (2008) 2339–2356.

[44] S. Karpiński, M. Szechyńska-Hebda, W. Wituszyńska, P. Burdiak, Light acclimation, retrograde signalling, cell death and immune defences in plants, Plant. Cell Environ. 36 (2013) 736–744.

[45] H.-B. Shao, L.-Y. Chu, Z.-H. Lu, C.-M. Kang, Primary antioxidant free radical scavenging and redox signaling pathways in higher plant cells, Int. J. Biol. Sci. 4 (2008) 8–14.

[46] M. Szechyńska-Hebda, S. Karpiński, Light intensity-dependent retrograde signalling in higher plants, J. Plant Physiol. 170 (2013) 1501–1516.

[47] J.A. Sullivan, K. Shirasu, X.W. Deng, The diverse roles of ubiquitin and the 26S proteasome in the life of plants, Nat. Rev. Genet. 4 (2003) 948–958.

[48] D.H. Wolf, W. Hilt, The proteasome: A proteolytic nanomachine of cell regulation and waste disposal, Biochim. Biophys. Acta - Mol. Cell Res. 1695 (2004) 19–31.

[49] M. Kim, J.W. Ahn, U.H. Jin, D. Choi, K.H. Paek, H.S. Pai, Activation of the programmed cell death pathway by inhibition of proteasome function in plants, J. Biol. Chem. 278 (2003) 19406–19415.

[50] Y. Cai, P. Gallois, Programmed Cell Death Regulation by Plant Proteases with Caspase-Like Activity, Plant Program. Cell Death (2015) 191–202.

[51] V.A. Iglesias, F. Meins, Movement of plant viruses is delayed in β-1,3-glucanase-deficient mutant showing a reduced plasmodesmatal size exclusion limit and enhanced callose deposition, Plant J. 21 (2000) 157–166.

[52] J.E. Radford, R.G. White, Effects of tissue-preparation-induced callose synthesis on estimates of plasmodesma size exclusion limits, Protoplasma 216 (2001) 47–55.

[53] S. Su, Z. Liu, C. Chen, Y. Zhang, X. Wang, L. Zhu, L. Miao, X.-C. Wang, M. Yuan, Cucumber Mosaic Virus Movement Protein Severs Actin Filaments to Increase the Plasmodesmal Size Exclusion Limit in Tobacco, Plant Cell. 22 (2010) 1373–1387.

[54] S.H. An, K.H. Sohn, H.W. Choi, I.S. Hwang, S.C. Lee, B.K. Hwang, Pepper pectin methylesterase inhibitor protein CaPMEI1 is required for antifungal activity, basal disease resistance and abiotic stress tolerance, Planta 228 (2008) 61–78.

[55] V. Lionetti, A. Raiola, F. Cervone, D. Bellincampi, Transgenic expression of pectin methylesterase inhibitors limits tobamovirus spread in tobacco and Arabidopsis, Mol. Plant Pathol. 15 (2014) 265–74.

3.2. Manuscrito 2

Manuscrito em preparação a ser submetido à publicação.

Changes in *C. papaya* proteome induced by papaya sticky disease throughout the papaya's life cycle

Eduardo de A. Soares[a], Emily G. Werth[b], Leidy J. Madroñero[a], José A. Ventura[a,c], Silas P. Rodrigues[a,d]*, Leslie M. Hicks[b], Patricia M.B. Fernandes[a]

[a]Núcleo de Biotecnologia, Universidade Federal do Espírito Santo, Av. Marechal Campos, 1498, Vitória, ES 29040-090, Brazil

[b]Department of Chemistry, University of North Carolina at Chapel Hill, 125 South Road, Chapel Hill, NC 27599, USA

[c]Instituto Capixaba de Pesquisa, Assistência Técnica e Extensão Rural, Rua Afonso Sarlo 160, Vitória, ES 29052-010, Brazil

[d]Unidade de Espectrometria de Massas e Proteômica e Núcleo Multidisciplinar de Pesquisa e Extensão de Xerém, Universidade Federal do Rio de Janeiro, Av. Carlos Chagas Filho 373, CCS Bloco H2 Sala 04, Rio de Janeiro, RJ 21941-902, Brazil

*Corresponding author: S. P. Rodrigues, e-mail: srodrigues@xerem.ufrj.br, Phone: +55 21 3938 6782

Keywords: Label-free quantitative proteomics, mass spectrometry, *Papaya meleira virus,* PSD-Symptoms onset; *C. papaya* life cycle

ABSTRACT

A widely cultivated and consumed fruit around the word, papaya (*C. papaya L.*), have its production compromised by Papaya Sticky Disease (PSD) caused by the synergic infection of *Papaya meleira virus* (PMeV) and *Papaya meleira virus 2* (PMeV2). in post flowering *C. papaya* plants. This disease is characterized by a spontaneous exudation of the latex and a sticky aspect on fruits, making them unfit for marketing and exportation. There is no PSD-tolerant *C. papaya* genotype. To strengthen and deepen the knowledge about PMeV+PMeV2-*C. papaya* interaction and the post flowering symptoms onset phenomenon, the LC-MS/MS-based proteomics was used to reveal 1,623 papaya leaf proteins, assuredly identified through four different plant ages (3, 4, 7 and 9 months post germination, mpg) under PMeV+PMeV2-infection or control conditions. Of those proteins, 99 % (1,609 proteins) were label-free quantified and used to evaluate the modulation trends for each *C. papaya* plant age group. The proteins differently accumulated in the age groups showed the relevance of photosynthesis related proteins for the pre-flowering PSD symptoms tolerance phenomena and the molecular-phenotype connection between the proteasome, cell wall remodeling and other defense response related proteins with the PSD symptoms.

1. INTRODUCTION

Papaya (*C. papaya L.*) is a widely cultivated and consumed fruit around the word, with a global production of twelve million tons in 2013 [1], of which the major producers are India, Brazil, Indonesia, Nigeria and Mexico. Together, Brazil and Mexico contributed with 19% (2.3 million tons) of the papaya global production in 2013, which the future are at risk by the presence, officially reported, of the papaya sticky disease (PSD) [2,3], known to infects around 20% of the papaya plants, in Brazilian orchards rouging controlled, causing huge pre-harvest losses [4] and impairing the marketing and exportation of papaya fruit.

PMeV is a recently sequenced toti-like double-stranded RNA virus (dsRNA) [5], which naturally infects papaya by an unknown vector [6] and, in a newly described synergism with the umbra-like single-stranded *Papaya meleira virus 2* (ssRNA, PMeV2) leads to “Meleira”, also known as papaya sticky disease [7–9], for which there is not a tolerant genotype. The PMeV takes advantage of the peculiar papaya anatomical structure named laticifers (highly specialized cells producing mainly defense metabolites, i.e. cardenolides, alkaloids and natural rubber [10]), where it has been observed [2] inducing changes in latex structure and composition [11] and other features, such as increased production of H_2O_2 and osmotic disequilibrium (higher levels of potassium, phosphorus and water) [12].

The main PSD symptom is a plant spontaneous exudation of a watery latex mostly from fruits and leaves [13]. This latex fluidity delays its polymerization, leading to oxidation by prolonged contact with the air and accumulating, on the plant organs, as a sticky substance [2], making the fruit unfit for marketing. Besides the virus location in the plant, this disease peculiarity consists in the specific phenological stage needed to symptoms onset [14], the flowering, after which the first symptoms of small necrotic lesions on the tips of young leaves are observed [4]. As the papaya flowering takes place between three and four months post germination, asymptomatic plants can be hosting high viruses (PMeV+PMeV2) load, acting as a virus source, spreading the

disease through the orchard for a few months until the first symptoms are observed and the plant is discarded (rouging) [4].

The PSD symptoms onset phenological relationship resembles the intimate connection between development and innate immunity [15] reported for some plant-pathogen systems and generically known as age-related resistance (ARR) [16–22], which suggests the existence of age related mechanism(s) to prevent PSD symptoms prior to *C. papaya* flowering and/or to enable it after that. The ARR is a general phenomenon occurring at distinct developmental stage for each plant genotypes or pathogens, and the flowering transition is one of those affecting the resistance development, as reported for Arabidopsis, tobacco and maize [23–26]. Although not commonly observed in the plant-virus system, ARR has been reported for Arabidopsis and Turnip resistance to *Cauliflower mosaic virus*, which is attributed to the sink-source transition, accompanied by changes in cellular structure and photoassimilate flux throughout the plant development [27,28].

Although small, the current accumulated knowledge around the morphophysiological, biochemical and molecular changes undergone by the PSD diseased *C. papaya* directs for a control of protein turnover due to decreasing in microRNAs (miR162, miR398 and miR408) expression predicted to target proteasome-related proteins in plant diseased leaves compared with the pre-flowering asymptomatic infected plants [29], plus the proteasome-related proteins accumulation at the same phenological stage [30]. Additionally, microRNA analysis has shown the transcription modulation of several miRNAs involved in stress response pathways [29].

The proteomic field, in turn, indicates the existence of systemic acquired resistance (SAR) response in PSD symptomatic adult plants, since it has shown leaf accumulation of calreticulin, 20S proteasome b subunit, and PRs, *e.g.* endochitinase and PR-4 [30] combined with reduction of serine proteinase inhibitor and chymopapain cysteine proteases levels, both typically present in the papaya latex [31]. Nonetheless, neither SAR nor other plant stress response mechanism(s) explains the post flowering PSD symptoms onset, remaining limited the PMeV+PMeV2-*C. papaya* interaction mechanism knowledge, which weakens the chance of a virus resistant plant genotype(s) improvement.

Aiming to strengthen and deepen the knowledge about PMeV+PMeV2-*C. papaya* interaction, as well as the post flowering symptoms onset phenomenon, the LC-MS/MS-based proteomics was used to reveal 1,623 papaya leaf proteins, assuredly identified through four different plant ages (3, 4, 7 and 9 months post germination) under PMeV+PMeV2-infection or control conditions. Of which 99% (1,609 proteins) were label-free quantitative and used to modulation trends evaluation for each *C. papaya* plant age group, rendering 38 (12 up, 26 down) proteins differently accumulated in 3 mpg, 130 (63 up, 67 down) in 4 mgp, 160 (149 up, 11 down) in 5 mpg and 17 (11 up, 6 down) in 9 mpg *C. papaya* leaf sample groups. An individual investigation of differently accumulated proteins in each *C. papaya* age sample group, alongside the plant-pathogen/plant-virus interaction literature shows the involvement of these proteins with the PSD symptoms in a juvenile-adult transition symptoms onset perspective.

2. MATERIAL AND METHODS

2.1. Plant Material

Thirty-days post germination *Carica papaya L*. (6 seedlings of cv. Golden) were planted at the INCAPER experimental farm located at Sooretama-ES, Brazil, and cultivated for two months, when the plants received one of the two treatments: 3 plants (infected biological replicates) were PMeV+PMeV2 inoculated by 1 mL injection of papaya latex collected from sticky-diseased fruits in 50 mM sodium phosphate buffer, pH 7.0 suspension of (1:1, v/v) at the youngest leaf petiole. The other 3 papaya plants (control

biological replicates) were 1 mL injected with ultrapure water in 50 mM sodium phosphate buffer, pH 7.0 solution (1:1, v/v) at the same manner. Five minutes after experimental treatment, the second fully expanded leaf were collected of each plant and immediately frozen in liquid nitrogen, accounting for the three months post germination (mpg) with 0 days post infection (dpi) samples. The tissues were ground, freeze-dried and stored at -80 °C until use. The same collecting procedure were performed when the plants had completed four months post germination and were forming floral buds (pre-flowering, 30 dpi), seven months post germination and were forming fruits (post-flowering, 120 dpi) and nine months post germination (180 dpi).

2.2. Protein Extraction

The total protein were extracted from 10mg of leaf tissue powder as previously described [32]. Briefly, in each sample was added 600 µL of 10 mM Tris pH 8.8-buffered phenol and 600 µL of extraction buffer (100 mM Tris-HCl, pH 8.0, 2% (w/v) SDS, 0.9 M sucrose, 10 mM EDTA, and the Roche mini complete EDTA-free protease inhibitor cocktail, Roche, Indianapolis, IN). Samples were mixed for 10 min followed by 10 min centrifugation at 5,000 × *g* and storage of phenol phase for each sample. An additional 400 µL of phenol was added to remain tissue/buffer suspension and another extraction was performed with the phenolic phases (~700 µL) combined for each sample. The extracted proteins were cleaned by precipitation with 4 mL of 0.1 M ammonium acetate in methanol (10 hours at -20 °C) and centrifugation (10 min, 20,000 × *g*, 4 °C), then washed/centrifuged twice with 1.5 mL of 0.1 M ammonium acetate in methanol, once with 1.5 mL of 80% acetone, and once with 1.5 mL of 70% methanol. The cleaned proteins were resuspended in 180 µL of 50 mM Tris-HCl, pH 8.0, 8 M urea and 2 M thiourea and the concentration was determined using the CB-X protein assay (Genotech, St. Louis, MO).

2.3. Protein Digestion

Using a compact Thermomixer (Eppendorf, Hamburg, Germany), the proteins were incubated at 37 °C with 5 mM dithiothreitol (DTT) for 45 min and incubated in darkness at 25 °C with 100 mM iodoacetamide 40 min, followed by dilution to 1 M urea with 50 mM Tris-HCl, pH 8.8. The proteins were then trypsin digested for 16 h at 37°C and 800 rpm using a trypsin solution (Sigma, St. Louis, MO) at 1:50 enzyme/substrate ratio, which was quenched by formic acid addition to a final concentration of 2%. The resulting peptides were desalted in a PepClean C18 spin column (Thermo Scientific, Rockford, lL) and resuspended in 150 µL of 0.1% formic acid (FA)/5% acetonitrile (ACN).

2.4. LC-MS/MS Analysis

The analysis was performed in a NanoAcquity UPLC system (Waters, Milford, MA) coupled to a TripleTOF 5600 MS/MS (AB SCIEX, Framingham, MA) by loading the peptide mixtures (1µg) for 3 min onto a trap column (NanoAcquity UPLC 2G-W/M Trap 5 µm Symmetry C18, 180 µm × 20 mm) at 5 µL/min. The peptides were separated using a 90 min linear gradient from 5% to 40% of solvent B [solvent 0.1% FA in water (A), ACN (B)] in a C18 capillary column (NanoAcquity UPLC 1.8 µm HSS T3, 75 µm × 250 mm) at 300 nL/min. Column cleaning (5 min from 40% to 85% of solvent B; 10 min at 85% of solvent B) and re-equilibration (2 min from 85% to 5% of solvent B; 13 min at 5% of solvent B) were performed after each sample analysis. The mass spectrometer was operated in positive ionization and high sensitivity mode. The

features were selected for information dependent acquisition (IDA) MS/MS experiments based on MS survey spectrum accumulated from 350 to 1600 *m/z* for 250 ms, of witch the first 20 features with a charge state of +2 to +5 and exceeding a 150 count threshold were selected and included on an 8 s dynamic exclusion list prior to fractionation using ±5% rolling collision energy. A homogeneous mixture of equivalent peptide amounts from all replicates was also analyzed and used as a reference sample for label-free protein quantification. The high mass accuracy in both MS and MS/MS acquisition was assured by calibrating the instrument every three samples (6 h) automatically.

2.5. Protein identification and label-free quantification

Progenesis QI for proteomics v2.0 (NonLinear Dynamics) was used to generate two-dimensional ion intensity maps of features from the TripleTOF 5600 raw files (.wiff). The reference assignment, alignment (≥ 80% score) of spectra and the peak picking parameters were performed as automatic for the features eluting between 25 and 105 min. The protein identification was performed in a Mascot server v.2.2.2 (Matrix science Inc., Boston, MA) by interrogating the peak list file (.mgf) from Progenesis QI against a custom database (27,898 sequences total, May 2015) containing all *C. papaya* protein entries available on Phytozome 10.2 (27,775 sequences, May 2015) [33,34] combined with NCBI *C. papaya* organelle (123 sequences, May 2015). The parameters of +2 to +4 charge state, two missed cleavages, mass tolerance of ± 20 ppm and ± 0.05 Da for precursor and fragment ions, respectively, were considered for protein identification. Additionally, carbamidomethylation at cysteine, deamidation at asparagine or glutamine, oxidation at methionine and acetylation at peptide N-term were considered as variable modifications. Mascot percolator algorithm was used, providing an FDR < 1% prior to XML file exportation and Progenesis QI reimportation

for peptide quantification and identification. The protein quantification was performed using the normalized abundances of Hi-3 (up to 3) peptides [35] filtering for Mascot peptide scores ≥ 13. The abundances of proteins occurring in all three control and PMeV+PMeV2-infected biological replicates were compared by one-way ANOVA test and the protein list was filtered based on $p \leq 0.05$ and a Log_2 fold change (FC) of ±0.58.

2.6. Differential abundance analysis and protein functional classification

Gene ontology (GO) analysis of all identified proteins was performed in Blast2GO (www.blast2go.org) by blasting the identified protein sequences against the NCBI non-redundant (nr) database with an expected E-Value threshold of 10^{-10} and the first ranked hit was further used. The GO enrichment for up- and down-accumulated protein sets using a Fisher's Exact test with the multiple testing correction FDR option selected [36]. Additionally, the abundance changed proteins ($p \leq 0.05$; FC ±0.58) were submitted to *C. papaya* overview metabolic pathway mapping using the MapMan software (http://mapman.gabipd.org/web/guest/mapman).

3. RESULTS

3.1. Proteomic analysis of *C. papaya* leaf

The *C. papaya* leaf proteome comprising 1,623 proteins (Supplemental Table S1) was achieved by the Mascot search of 533,856 MS/MS spectra (~22,244 per sample) (Table 1) obtained from *C. papaya* leaf samples against a *C. papaya* protein database, rendering a total of 8,979 peptides (Table 1, Supplemental Table S2). Within that proteome, 99 % (1,609) were quantitative (Table 1) based on Progenesis QI analysis of 34,624 ions (Table 1, Supplemental Table S3). Of those quantitative proteins, 1,533 protein sequences (94%) had at least one Gene Ontology identification number (GO ID) attributed to it (Supplemental Table S1).

The proteome GO term grouping are exposed in Figure 1 based on biological process and in the Supplemental Figure S1 according to their associated molecular function (A) and cellular component (B). Cellular metabolic process (798 proteins), organic substance metabolic process (753 proteins) and primary metabolic process (453 proteins), were the most represented GO terms within the biological processes grouping, which also includes 256 proteins belonging to the response to stress GO term group (Figure 1). The response to stress GO term group comprise some proteins known to be modulated in the course of plant responses to viruses and even to PSD, which highlights this group as a good target.

3.2. Differential proteome of PMeV+PMeV2-infected *C. papaya* versus control plants within four developmental stages

The 1,609 quantified proteins (Table 1) comprising 1,242 proteins from 3 months post germination (mpg) samples, 1,454 from 4 mpg samples, 1,493 from 7 mpg samples, and 1,442 from 9 mpg samples with some overlapping (Figure 2), had an average coefficient of variance (CV) of 28.44% (22.55% CV median) (Table 1, Supplemental Figure S2) and were considered to correlate the protein abundances of PMeV+PMeV2-infected *C. papaya* leaf and control samples for each plant age group, to which the third level GO term grouping by biological process is shown in Figure 3 (A-D), by molecular function in Supplemental Figure S3 (A-D) and by cellular component in Supplemental Figure S4 (A-D).

3.2.1. Three months post germination (0 dpi)

The contribution of the 3 mpg plant group, including the group overlapping, was 77% (1,242 proteins) of the total quantified proteins (Figure 2) (Supplemental Figure S2) with a 36.56% CV mean (29.32% median) (Table 1, Supplemental Figure S2). Out of those, 38 proteins, 12 up- and 26 down-accumulated, showed significant abundance changes ($p \leq 0.05$); FC of at least ±0.58 (Table 2, Figure 2). The highest change in up-accumulation levels were observed in lipid transfer protein 4 (6.17 FC), AMP-dependent synthetase and ligase family protein (4.13 FC), and plastocyanin 1 (3.46 FC) whereas the highest change in down-accumulation levels were observed in uricase / urate oxidase / nodulin 35, putative (-∞ FC), Calcium-dependent lipid-binding

(CaLB domain) plant phosphoribosyltransferase family protein (-∞ FC), and eukaryotic translation initiation factor 2 beta subunit (-3.31 FC) (Table 2). The 3 mpg had no statistically significant (p≤0.05) GO term enriched (Supplemental Table S4). However, the *C. papaya* overview metabolic pathway mapping (Figure 4, Supplemental Table S5) shows reduction in the accumulation levels of protein related with the metabolism of proteins (*e.g.* eukaryotic translation initiation factor 2 beta subunit, methionyl-tRNA synthetase, putative / MetRS, putative, and ubiquitin-specific protease 21), RNA regulation of transcription related proteins (sequence-specific DNA binding transcription factors, Alba DNA/RNA-binding protein), cell wall degradation related protein (Glycosyl hydrolase family protein), and signaling related proteins (*e.g.* Calcium-binding EF-hand family protein, general regulatory factor 2), while proteins related with lipid metabolism (*e.g.* lipid transfer protein 4, AMP-dependent synthetase, ligase family protein) and organic acid transformations (Transketolase family protein, beta carbonic anhydrase 4) had the accumulation levels increased.

3.2.2. Four months post germination (30 dpi)

Based on the same criteria (p≤0.05, FC ±0.58), 130 proteins, 63 up- and 67 down-accumulated, were filtered out as significant abundance changed from the 1,454 proteins (90% of the total quantified proteins) belonging to the 4 mpg plant group (Table 3, Figure 2) which showed 25.60% CV mean (21.01% median) (Table 1, Supplemental Figure S2). Within the 63 positively regulated proteins, the haloacid dehalogenase-like hydrolase family protein (3.00 FC), sucrose phosphate synthase 3F (2.68 FC), and CAP (Cysteine-rich secretory proteins, Antigen 5, and Pathogenesis-related 1 protein) superfamily protein (2.67 FC) had the most significant change in accumulation levels, while the Subtilase family protein (-∞ FC), Reticulon family protein (-∞ FC), and P-loop containing nucleoside triphosphate hydrolases superfamily protein (-∞ FC) had the

most significant change in accumulation levels for the 67 negatively regulated (Table 3). Fifteen GO terms was found enriched (p≤0.05) within the 4 mpg *C. papaya* leaf proteins, of which eight were most represented among the up-regulated proteins, mainly related with photosynthesis and oxidoreductase activity, and seven GO terms was most represented among the down-accumulated proteins, comprising RNA binding, catabolic process and membranous cellular components (Supplemental Table S4). Furthermore, the MapMan reported, in its overview metabolic pathway, the up-accumulation of proteins related with photosynthesis (*e.g.* light harvesting complex photosystem II, photosystem I subunit l, high cyclic electron flow 1), carbohydrates metabolism (*e.g.* sucrose phosphate synthase 3F, NAD(P)-linked oxidoreductase superfamily protein), organic acid transformations (NAD-dependent malic enzyme 1, carbonic anhydrase 1), amino acid metabolism (threonine aldolase 1, glycine decarboxylase P-protein 1), and the down-accumulation of proteins related with cell wall (*e.g.* rhamnose biosynthesis 1, glycosyl hydrolase 9B13, beta-D-xylosidase 4), lipid metabolism (*e.g.* AMP-dependent synthetase and ligase family protein, acyl-CoA dehydrogenase-related), stress (*e.g.* pathogenesis-related 4, heat shock protein 101, S-adenosyl-L-methionine-dependent methyltransferases superfamily protein), RNA metabolism (*e.g.* NOP56-like pre RNA processing ribonucleoprotein, Eukaryotic aspartyl protease family protein, U2 snRNP auxilliary factor - large subunit - splicing factor), protein metabolism (*e.g.* myristoyl-CoA:protein N-myristoyltransferase, importin alpha isoform 4, eukaryotic translation initiation factor 3E) signaling (*e.g.* Calcium-binding EF-hand family protein, calnexin 1) and cell organization (*e.g.* tubulin beta 8, annexin 8) (Supplemental Figure S4, Supplemental Table S6).

3.2.3. Seven months post germination (120 dpi)

The 7 mpg plant group had the biggest contribution, 1,493 proteins (92%), for the total quantified proteome (Figure 2) with an average of 26.23%CV (20.71% median) (Table 1, Supplemental Figure S2) and 160 proteins, 149 up- and 11 down-accumulated, abundance changed (p≤0.05, FC ±0.58) (Table 4, Figure 2). The proteins alpha/beta-Hydrolases superfamily protein (4.18 FC), DEA(D/H)-box RNA helicase family protein (3.13 FC), and Adaptor protein complex AP-2, alpha subunit (2.87 FC) showed the most prominent levels of protein abundance change among the 149 up-accumulated proteins, and the proteins kunitz trypsin inhibitor 1 (-3.43 FC), non-photochemical quenching 1 (-2.98 FC), and the protein without description PACid:16430895 (-2.30 FC) among the 11 Down-accumulated (Table 4). The 7 mpg plant group had only photosynthesis as a GO term enriched (p≤0.05) most represented in down-accumulated proteins, while plastid, thylakoid and energy as a GO term enriched most represented in up-accumulated proteins (Supplemental Table S4). Additionally, the overview metabolic pathway has shown, among the up-accumulated, proteins related with carbohydrates metabolism (sucrose synthase 4, NAD(P)-linked oxidoreductase superfamily protein), glycolysis (*e.g.* triosephosphate isomerase, Pyruvate kinase family protein), oxidative pentose phosphate pathway (*e.g.* root FNR 1, Aldolase superfamily protein, glyoxylate reductase 1), organic acid transformation (*e.g.* Succinyl-CoA ligase - alpha subunit, aconitase 1, pyruvate dehydrogenase E1 alpha), mitochondrial proteins (gamma carbonic anhydrase 1, Cytochrome C1 family, ATP synthase alpha/beta family protein), cell wall (*e.g.* nucleotide-rhamnose synthase/epimerase-reductase, Glucose-1-phosphate adenylyltransferase family protein, UDP-glucose 6-dehydrogenase family protein), lipid metabolism (Pyruvate kinase family protein, Enoyl-CoA hydratase/isomerase family), amino acid metabolism (*e.g.* aspartate aminotransferase, delta 1-pyrroline-5-carboxylate synthase 2, urease accessory protein G), stress (*e.g.* HSP20-like chaperones superfamily protein, Disease resistance-responsive dirigent-like protein, mitochondrion-localized small heat shock protein 23.6), nucleotide metabolism (*e.g.* uracil phosphoribosyltransferase, uridine 5\'-monophosphate synthase / UMP synthase (PYRE-F) (UMPS), L-Aspartase-like family

protein), RNA metabolism (*e.g.* ureidoglycine aminohydrolase, glycine-rich RNA-binding protein 3, arginine/serine-rich splicing factor 35), DNA metabolism (*e.g.* gamma histone variant H2AX, RNAhelicase-like 8), protein metabolism (*e.g.* TCP-1/cpn60 chaperonin family protein, AAA-type ATPase family protein, MAP kinase 4), signaling (general regulatory factor 8, general regulatory factor 11), cell (*e.g.* Adaptor protein complex AP-2, alpha subunit, annexin 5), development (ARF-GAP domain 8, transducin family protein / WD-40 repeat family protein), transport (ATPase V1 complex subunit B, voltage dependent anion channel 2), and among those down-accumulated only photosynthesis (PsbQ-like 2, ribulose-bisphosphate carboxylases, Aldolase superfamily protein) was highlighted (Supplemental Figure S4, Supplemental Table S7).

3.2.4. Nine months post germination (180 dpi)

Featuring 26.59%CV mean (21.53% median) (Table 1, Supplemental Figure S2), the 1,442 proteins (89% of the total quantified proteins) (Figure 2) representatives of the 9 mpg plant group, the oldest group and longer infected, showed the smallest amount of abundance changed proteins ($p \leq 0.05$, FC ±0.58), 11 up- and 6 down-accumulated in a total of 17 modulated proteins. This small group of differentially accumulated proteins was headed by the proteins ATP-dependent caseinolytic (Clp) protease/crotonase family protein (2.13 FC), Cyclophilin-like peptidyl-prolyl cis-trans isomerase family protein (2.13 FC), and fumarase 1 (1.86 FC) as the top three in up-accumulation abundance changed levels, and the PLC-like phosphodiesterase family protein (-1.88 FC), P-loop containing nucleoside triphosphate hydrolases superfamily protein (-1.50 FC), and tryptophan biosynthesis 1 (-1.01 FC) as the top three proteins in down-accumulation abundance changed levels (Table 5). The 9 mpg had no statistically significant ($p \leq 0.05$) GO term enriched (Supplemental Table S4). The MapMan analysis

showed that up-accumulated proteins were mainly related with organic acid transformation (fumarase 1), RNA metabolism (Cleavage and polyadenylation specificity factor_CPSF_A subunit protein, ATPase E1, binding to TOMV RNA 1L), cell (Cyclophilin-like peptidyl-prolyl cis-trans isomerase family protein), and the down-accumulated were related with photosynthesis (P-loop containing nucleoside triphosphate hydrolases superfamily protein) and mitochondrial protein (alternative oxidase 2) (Supplemental Figure S4, Supplemental Table S8).

4. DISCUSSION

The proteomics analysis has been widely used in the characterization and quantification of plant proteins, from different organs and tissues, as a tool to elucidate phenotypic and phenological phenomena, plant-pathogens interaction mechanisms and to identify targets for induction of resistance or genetic breeding. Alexander and Cilia had shown in their recent review [37] that during plant-virus interaction the metabolic pathways targeted by viruses may vary according to the infection period and plant age, reflecting in proteome variations for each observed time point during the infection. Besides, the PSD is a phenological related disease, which the symptoms are observed only at the post-flowering. Aiming to understand the mechanisms involved in the PMeV+PMeV2-*C. papaya* interaction and the plant age contribution during this interaction, a quantitative label-free LC-MS/MS proteomic approach was used to analyze peptides from, in solution trypsin digested, proteins extracted from PMeV+PMeV2-infected and non-infected (control) *C. papaya* leaf samples, harvested at four different phenological stages (3, 4, 7 and 9 mpg) of experimental field grown *C. papaya* plants.

The *C. papaya* proteomic analysis based in different approaches provided the identification of 159 proteins from leaves [30], 160 from latex [31], 27 from fruit pulp [38,39], 1,581 proteins from isolated chromoplasts [40] and 76 from somatic embryos [41] at this chronological order. Known for its great coverage [42,43], the label-free proteomic approach, coupled with the availability of the *C. papaya* genome [33], afforded the identification of 1,623 *C. papaya* proteins. The Gene Ontology analysis of the identified proteins demonstrates the power of this study to elucidate the plant-pathogen interaction mechanisms by grouping 246 proteins as oxidoreductase activity molecular function, known to be involved with plant-virus interaction [44], and 256 proteins as response to stress biological process.

At the third month post germination, the *C. papaya* plants were injected with latex from papaya sticky-diseased fruits (treatment) or phosphate buffer (control) at the youngest leaf petiole and a different leaf (second fully expanded) was collected five minutes later, rendering 1,242 proteins quantified. However, only 38 proteins were differentially accumulated (12 up and 26 down) when comparing PMeV+PMeV2-infected *vs*. control samples. This result was expected since the broad plant systemic response against virus is commonly manifested much later during the infection [45]. Nevertheless, it is possible to notice the accumulation levels reduction of proteins related to metabolism of proteins, RNA regulation of transcription, cell wall degradation, and signaling, while the proteins related with lipid metabolism and organic acid transformations had the accumulation levels increased.

Based on the plant-virus productive cycle [46] and its intimate interaction with the host's metabolism and physiology [47], the down-accumulation of proteins related with RNA, protein and cell wall metabolism provides host's benefits, since the virus requires the gene transcription and translation plant's machineries and cell wall remodeling for replication and movement, respectively [48–50]. In addition, the up-accumulation of proteins related to lipid metabolism, of which derives much of signaling in plant defense [51] and the increase in organic acid transformations related proteins, needed to satisfy the requirement of cell for intermediate products of sugar metabolism and reductant [44,52] may contribute to pre-flowering *C. papaya* tolerance to PSD by delaying the viral replication and movement, increasing the defense signaling possibility and assuring the sugars needed for defense, growth and development. In contrast, the down-accumulation of signaling proteins, commonly attributed to viral-induced

changes to self-benefit [53], attenuate the downstream plant stress response [54]. Despite of the beneficial effect of viruses containment, the decreased in accumulation levels of cell wall remodeling proteins for a prolonged time may cause the weakening of cell walls. The cell wall weakened in PSD diseased *C. papaya* [55] combined with the osmotic imbalance of the latex vessels with increasing in potassium, phosphorus and water levels [12] are parts of an equation that can result in laticifers burst, spontaneously pouring the aqueous and fluid latex characteristic of the PSD.

Except for the proteins involved in lipid metabolism, the 4 mpg samples group showed the same accumulation trends of 3 mpg samples, *i.e.* proteins involved in the signaling, organic acid transformation and metabolism of: RNA; proteins; cell wall. At the same time, as expected for a latter asymptomatic infection stage, it was observed an increasing number of proteins differently accumulated and additional molecular functions attributed to it. The up-accumulation of proteins linked to photosynthesis, carbohydrates metabolism, nitrogen metabolism, and the decrease in accumulation levels of cell organization proteins contributes positively to the plant tolerance by biosynthesis of signaling molecules precursors and energy, carbohydrates supply, amino acid biosynthesis and hindering the virus movement, respectively [56–58]. However, the down-accumulation of lipid metabolism, stress and signaling related proteins observed at pre-flowering are chain reaction events, since the lipid metabolism is an important precursor of stress response and signaling over the plant defense [51], without which the *C. papaya* resistance or a lifetime tolerance against PSD becomes infeasible.

The 3 and 4 mpg samples correspond to the asymptomatic stage of the PMeV+PMeV2 infection prior to the flowering. Then, the observed protein modulation contributed to *C. papaya* tolerance against PSD or were not enough to PSD symptoms onset. At the seventh month post germination (120 dpi), with the flowering stage overcome, the PSD symptoms arose and the number of proteins differently accumulated reached its apex in these study, mostly up-accumulated. Among the 11 down-accumulated proteins there are six related to photosynthesis *i.e.* PsbQ-like 2, ribulose-bisphosphate carboxylases, aldolase superfamily protein, photosystem I P700 chlorophyll a apoprotein A2, cytochrome b6 and non-photochemical quenching 1. The down accumulation of these proteins decrease the reactive oxygen species (ROS) generation by photosystem I (PSI), while increase its formation by the oxygen evolving

complex of photosystem II (PSII) [59], which is more destructive and closely related with chlorosis. Moreover, the observed increase in the accumulation of proteins related to metabolism of carbohydrates, amino acid, proteins, nucleotide, and those involved with stress response, signaling, transport and cell wall supports the hypothesis that juvenile-adult transition add the lacking players to the pre-flowering incomplete tolerance. At the post-flowering, the tolerance is complete but uneffectiveness in the viruses confinement since the infection is already systemic. One of the possible consequences of this late activated immune response is the systemic necrosis [60].

The 9 mpg samples, besides the smallest number of differently accumulate proteins in this study, conserved some molecular functions pattern of differently accumulated proteins observed in 7 mpg samples (i.e. up-accumulation of RNA, cell, lipid and amino acid metabolism, organic acid transformation and the down-accumulation of photosynthesis related proteins), which was expected, since both correspond to the symptomatic (post-flowering) PSD stage. The decrease number of differently accumulated proteins in this group is not related to physiology diversification, commonly attributed to long time field grown plants, since it was the group with the smallest number of proteins with FC±0.58 and filtered out as a co-accumulated by the $p>0.05$. Nevertheless, only 133 proteins of this group felt in the filtered out situation, while the groups 3, 4 and 7 had 545, 318 and 382 filtered out proteins, respectively. Thus, the small number of differently accumulate proteins seen for the 9 mpg group may be induced by the *C. papaya* physiological depletion after 180 days of PMeV+PMeV2 struggle.

5. CONCLUSION

The PMeV+PMeV2-*C. papaya* interaction comprises a great virus-induced change in protein accumulation patterns. The identification of 1,623 and the label-free quantification of 1,609 *C. papaya* leaf proteins through the 3, 4, 7 and 9 mpg groups, linked to the PSD and plant-virus models knowledge, provided the picturing of some of the respective 38, 130, 160 and 17 differently accumulated proteins as involved in the pre-flowering PSD symptoms tolerance phenomena or its molecular-phenotype connection with the PSD symptoms. The results, enables the statement of pre-flowering increasing photosynthesis related proteins as beneficial for the pre-flowering PSD tolerance by ROS signaling, while the decreasing proteasome and cell wall proteins as disadvantageous for the papaya tree, by inhibit the cell death proteasome-mediated, viruses confinement mediated by callose deposition and contributing to the latex spontaneous exudation by weakens the latex vessels cell wall. Additionally, the post-flowering reversion in the protein accumulation trend may contribute for the excessive PSII ROS production, generating chlorosis and activation of programed cell death in already infected cells, leading to systemic necrosis.

ACKNOWLEDGMENTS

This work was supported by grants from FINEP (Financiadora de Estudos e Projetos), CNPq (Conselho Nacional de Desenvolvimento Científico e Tecnológico), CAPES (Coordenação de Aperfeiçoamento de Pessoal de Nível Superior) and FAPES (Fundação de Amparo à Pesquisa do Estado do Espírito Santo).

SUPPLEMENTARY DATA

Soares et. al., 2016-b_Supplemental Tables.xlsx

Soares et. al., 2016-b_Supplemental Figures.pdf

Table 1. Proteomic coverage of PMeV+PMeV2-infected and control *C. papaya* leaf samples.

Sample		MS/MS spectra[1]	Ions[2]	peptide[3]	Quantified proteins[4]	%CV mean	%CV median
3 mpg (0 dpi)	C - 1	21,793	26,275	8,316	1,569	36.56	29.32
	C - 2	22,608	25,928	8,317	1,580		
	C - 3	20,214	26,516	8,265	1,567		
	I - 1	23,147	26,659	8,394	1,577		
	I - 2	24,168	27,164	8,454	1,581		
	I - 3	20,299	20,532	6,205	1,262		
4 mpg (30 dpi)	C - 1	24,116	25,273	8,205	1,548	25.60	21.01
	C - 2	24,335	25,477	8,215	1,548		
	C - 3	14,441	25,740	8,208	1,558		
	I - 1	20,785	25,136	8,079	1,532		
	I - 2	23,318	24,006	7,968	1,520		
	I - 3	18,053	24,698	7,974	1,533		
7mpg (120 dpi)	C - 1	21,007	26,204	8,287	1,568	26.23	20.71
	C - 2	24,753	26,367	8,279	1,567		
	C - 3	24,398	25,567	8,183	1,560		
	I - 1	23,163	26,481	8,279	1,567		
	I - 2	23,422	26,661	8,260	1,559		
	I - 3	23,969	25,056	8,065	1,546		
9 mpg (180 dpi)	C - 1	21,607	25,056	8,089	1,528	26.59	21.53
	C - 2	23,909	25,221	8,027	1,529		
	C - 3	21,353	25,287	8,130	1,537		
	I - 1	23,355	26,116	8,246	1,560		
	I - 2	25,465	25,153	8,057	1,519		
	I - 3	20,178	24,821	8,062	1,542		
Mean		22,244	25,475	8,107	1,540	----	----
Total		**533,856**	**34,624**	**8,979**	**1,609**	28.44	22.55

[1]Number of MS/MS spectra obtained using TripleTOF 5600.

[2]Number of ions extracted from MS/MS spectra using Progenesis QI for proteomics.

[3]Number of peptides identified using Mascot.

[4]Number of proteins quantified using Progenesis QI for proteomics.

mpg - Months post germination

dpi - Days post infection

C - Control

I - Infected

Table 2. Proteins differently modulated in 3 months post germination (0 days post inoculation) *C. papaya* leaf.

Phytozome/NCBI Accession[1]	Description[2]	Confidence score[3]	Anova (p)[4]	FC[5]
Up-accumulated proteins				
PACid:16409811	lipid transfer protein 4	20.88	0.000	6.17
PACid:16408331	AMP-dependent synthetase and ligase family protein	39.4	0.029	4.13
PACid:16415201	plastocyanin 1	177.86	0.000	3.46
PACid:16405411	acyl-activating enzyme 7	35.54	0.044	3.40
PACid:16425995	methyl esterase 10	13.16	0.039	3.17
GI:167391859	photosystem I subunit VII (chloroplast) [Carica papaya]	87.72	0.002	3.16
PACid:16424915	beta carbonic anhydrase 4	44.03	0.002	2.57
PACid:16429310	Transketolase family protein	40.95	0.020	2.04
PACid:16411634	chitinase A	138.06	0.009	1.73
PACid:16413598	Ribosomal protein S11 family protein	51.01	0.004	1.62
PACid:16417715	alanine-2-oxoglutarate aminotransferase 2	525.52	0.039	1.25
GI:167391794	ribosomal protein S2 (chloroplast) [Carica papaya]	59.66	0.022	1.21
Down-accumulated proteins				
PACid:16422371	uricase / urate oxidase / nodulin 35, putative	19.62	0.040	-∞
PACid:16427270	Calcium-dependent lipid-binding (CaLB domain) plant phosphoribosyltransferase family protein	43.17	0.000	-∞
PACid:16412656	eukaryotic translation initiation factor 2 beta subunit	41.82	0.034	-3.31
PACid:16429295	glucose-6-phosphate dehydrogenase 2	14.94	0.045	-2.18
PACid:16427157	methionine--tRNA ligase, putative / methionyl-tRNA synthetase, putative / MetRS, putative	45.42	0.050	-2.16
PACid:16418818	D-3-phosphoglycerate dehydrogenase	103.61	0.004	-1.65
PACid:16412697	Alba DNA/RNA-binding protein	56.52	0.040	-1.48
PACid:16414081	ubiquitin-specific protease 21	24.89	0.026	-1.39
PACid:16414897	phospholipid:diacylglycerol acyltransferase	43.1	0.049	-1.38
PACid:16407009	UDP-glucosyl transferase 74D1	68.07	0.012	-1.37
PACid:16424332	Sec23/Sec24 protein transport family protein	43.77	0.032	-1.27
PACid:16427781	NAD(P)-binding Rossmann-fold superfamily protein	90.42	0.033	-1.09
PACid:16408289	Single hybrid motif superfamily protein	42.34	0.021	-1.09
PACid:16412334	annexin 8	127.72	0.040	-1.02
PACid:16411621	basic chitinase	87.11	0.022	-0.97
PACid:16408656	Glycosyl transferase, family 35	282.94	0.000	-0.94
PACid:16406935	ubiquitin family protein	14.98	0.042	-0.94

PACid:16425142	sodium/calcium exchanger family protein / calcium-binding EF hand family protein	42.94	0.018	-0.94
PACid:16411567	Calcium-binding EF-hand family protein	154.18	0.016	-0.91
PACid:16425236	sequence-specific DNA binding transcription factors	14.13	0.016	-0.87
PACid:16427718	HAD superfamily, subfamily IIIB acid phosphatase	94.1	0.034	-0.84
PACid:16408599	elongation factor Ts family protein	196.44	0.048	-0.83
PACid:16418358	general regulatory factor 2	482.89	0.030	-0.77
PACid:16404978	Glycosyl hydrolase family protein	288.12	0.025	-0.75
PACid:16403907	structural constituent of ribosome	119.06	0.020	-0.64
PACid:16423886	Ribosomal L29 family protein	89.28	0.004	-0.61

[1]Phytozome or NCBI gene identification number.

[2]Phytozome or NCBI gene description.

[3]Quality assurance scores for protein alignment by Progenesis QI.

[4]Analysis of variance (ANOVA) based p value ($p \leq 0.05$).

[5]Log_2 fold change of protein abundances comparing PMeV+PMeV2-infected vs. control plants.

Table 3. Proteins differently modulated in 4 months post germination (30 days post inoculation) PMeV+PMeV2-infected *C. papaya* leaf.

Phytozome/NCBI Accession[1]	Description[2]	Confidence score[3]	Anova (p)[4]	FC[5]
Up-accumulated proteins				
PACid:16420809	haloacid dehalogenase-like hydrolase family protein	22.7	0.017	3.00
PACid:16427159	sucrose phosphate synthase 3F	175.63	0.018	2.68
PACid:16413107	CAP (Cysteine-rich secretory proteins, Antigen 5, and Pathogenesis-related 1 protein) superfamily protein	44.08	0.030	2.67
PACid:16431468	alkenal reductase	113.47	0.023	1.73
PACid:16421050	nitrate reductase 2	49.95	0.014	1.67
PACid:16412313	None	37.08	0.014	1.64
PACid:16419415	Eukaryotic aspartyl protease family protein	89.58	0.024	1.51
PACid:16411922	light harvesting complex photosystem II	226.24	0.043	1.48
PACid:16405950	None	90.05	0.027	1.46
PACid:16421146	Mog1/PsbP/DUF1795-like photosystem II reaction center PsbP family protein	40.7	0.014	1.37
GI:167391793	ATP synthase CF0 A subunit (chloroplast) [Carica papaya]	44.2	0.003	1.31
PACid:16416428	30S ribosomal protein, putative	181.02	0.012	1.27
PACid:16409579	chloroplast outer envelope protein 37	43.14	0.033	1.26
PACid:16430998	photosystem II subunit R	165.42	0.041	1.23
PACid:16418478	Insulinase (Peptidase family M16) family protein	64	0.007	1.21
PACid:16412470	NAD(P)-linked oxidoreductase superfamily protein	389.37	0.026	1.20
PACid:16423768	TCP family transcription factor	16.26	0.022	1.19
PACid:16425469	Mitochondrial substrate carrier family protein	127.32	0.003	1.19
PACid:16416362	None	36.06	0.038	1.18
GI:167391835	photosystem II protein H (chloroplast) [Carica papaya]	66.82	0.013	1.15
PACid:16412285	photosystem I subunit O	62.54	0.003	1.14
PACid:16421240	Thioredoxin family protein	83.86	0.029	1.14
PACid:16413470	ubiquitin interaction motif-containing protein	16.45	0.018	1.13
PACid:16415334	thioredoxin M-type 4	183.49	0.039	1.11
PACid:16429120	PsbQ-like 1	42.69	0.010	1.11
PACid:16422090	NAD-dependent malic enzyme 1	24.09	0.048	1.10
PACid:16413741	carbonic anhydrase 1	880.96	0.047	1.09
PACid:16428298	Rhodanese/Cell cycle control phosphatase superfamily protein	134.49	0.010	1.06
PACid:16415093	glyceraldehyde-3-phosphate dehydrogenase B subunit	818.14	0.033	1.04

GI:167391811	ATP synthase CF1 epsilon subunit (chloroplast) [Carica papaya]	383.78	0.036	1.04
PACid:16406426	zeta-carotene desaturase	47.94	0.035	1.03
PACid:16425084	glycine decarboxylase P-protein 1	1172.08	0.039	1.03
PACid:16418225	PsbQ-like 2	31.23	0.050	1.01
PACid:16432002	photosystem II protein V (chloroplast) [Carica papaya]	57.98	0.005	1.01
PACid:16426635	photosystem I subunit l	43.58	0.036	1.00
PACid:16413139	Leucine-rich repeat (LRR) family protein	18.41	0.019	1.00
PACid:16423944	cyclase associated protein 1	43.57	0.024	0.98
PACid:16410085	glutamine synthetase 2	435.16	0.024	0.93
PACid:16424704	uridylyltransferase-related	172.33	0.015	0.92
PACid:16422798	high cyclic electron flow 1	369.94	0.040	0.92
PACid:16409157	lipoamide dehydrogenase 2	533.46	0.011	0.92
PACid:16429027	NADPH-dependent thioredoxin reductase C	76.97	0.022	0.91
PACid:16422277	Duplicated homeodomain-like superfamily protein	15.23	0.030	0.90
PACid:16427275	beta glucosidase 34	251.75	0.032	0.90
PACid:16425317	glyceraldehyde 3-phosphate dehydrogenase A subunit	852.26	0.034	0.88
PACid:16424321	long chain acyl-CoA synthetase 9	162.42	0.038	0.83
PACid:16406894	Ribonuclease E inhibitor RraA/Dimethylmenaquinone methyltransferase	27.44	0.043	0.82
PACid:16423870	polyamine oxidase 5	18.44	0.026	0.79
PACid:16404385	rubisco activase	2152.37	0.043	0.78
PACid:16422806	fructokinase-like 1	15.37	0.019	0.78
PACid:16430304	FtsH extracellular protease family	110.17	0.004	0.77
PACid:16428265	None	89.33	0.012	0.76
PACid:16420953	thylakoid lumen 18.3 kDa protein	265.04	0.031	0.75
PACid:16413084	pyrophosphorylase 6	283.99	0.010	0.73
PACid:16426854	rubisco activase	2131.37	0.038	0.71
PACid:16409145	Pectin lyase-like superfamily protein	14.5	0.039	0.70
PACid:16415075	Oxidoreductase family protein	24.07	0.044	0.70
PACid:16428426	glycine decarboxylase complex H	179.38	0.014	0.69
PACid:16405405	Class II aaRS and biotin synthetases superfamily protein	59.12	0.037	0.66
PACid:16412072	Chalcone-flavanone isomerase family protein	129.56	0.000	0.65
PACid:16420610	ribosomal protein L9	81.53	0.005	0.65
PACid:16426826	Cyclophilin-like peptidyl-prolyl cis-trans isomerase family protein	54.19	0.023	0.65
PACid:16424781	villin 2	172.37	0.050	0.65
Down-accumulated proteins				
PACid:16415919	Subtilase family protein	43.6	0.004	-∞
PACid:16416866	Reticulon family protein	80.91	0.000	-∞

PACid:16419589	P-loop containing nucleoside triphosphate hydrolases superfamily protein	18.55	0.018	-∞
PACid:16420361	Mitochondrial glycoprotein family protein	22.92	0.000	-∞
PACid:16424925	DC1 domain-containing protein	128.33	0.014	-3.20
PACid:16424926	DC1 domain-containing protein	120.88	0.007	-2.73
PACid:16409537	glycosyl hydrolase 9B13	124.9	0.024	-2.54
PACid:16429609	NOP56-like pre RNA processing ribonucleoprotein	116.83	0.007	-2.26
PACid:16411185	TCP-1/cpn60 chaperonin family protein	174.62	0.041	-2.23
PACid:16424681	vacuolar membrane ATPase 10	51.23	0.017	-2.11
PACid:16420814	importin alpha isoform 4	106.23	0.004	-2.10
PACid:16411576	eukaryotic translation initiation factor 3E	47.97	0.005	-2.05
PACid:16426387	O-Glycosyl hydrolases family 17 protein	64.88	0.037	-1.96
PACid:16426831	myristoyl-CoA:protein N-myristoyltransferase	20.45	0.034	-1.88
PACid:16419512	Eukaryotic aspartyl protease family protein	399.76	0.001	-1.87
PACid:16421623	acyl-CoA dehydrogenase-related	54.22	0.017	-1.87
PACid:16411484	AMP-dependent synthetase and ligase family protein	179.79	0.017	-1.84
PACid:16430034	Eukaryotic aspartyl protease family protein	376.91	0.027	-1.77
PACid:16408093	Nucleic acid-binding, OB-fold-like protein	64.92	0.031	-1.72
PACid:16423878	S-adenosyl-L-methionine-dependent methyltransferases superfamily protein	169.48	0.017	-1.70
PACid:16426399	UDP-Glycosyltransferase superfamily protein	40.53	0.011	-1.66
PACid:16405998	tubulin beta 8	956.15	0.005	-1.62
PACid:16416704	beta-6 tubulin	554.88	0.040	-1.60
PACid:16411299	beta-galactosidase 7	43.28	0.009	-1.56
PACid:16428151	poly(ADP-ribose) polymerase	14.3	0.049	-1.51
PACid:16404978	Glycosyl hydrolase family protein	288.12	0.020	-1.42
PACid:16417516	regulatory particle triple-A ATPase 5A	86.12	0.019	-1.40
PACid:16428909	regulatory particle AAA-ATPase 2A	191.73	0.037	-1.36
PACid:16422729	ATPase, AAA-type, CDC48 protein	240.43	0.000	-1.32
PACid:16430932	O-fucosyltransferase family protein	62.33	0.041	-1.26
PACid:16407727	Transcriptional coactivator/pterin dehydratase	40.13	0.041	-1.21
PACid:16418291	U5 small nuclear ribonucleoprotein helicase, putative	164.7	0.036	-1.20
PACid:16413069	ribophorin II (RPN2) family protein	65.96	0.029	-1.16
PACid:16426335	regulatory particle non-ATPase 12A	54.65	0.020	-1.11
PACid:16425490	P-loop containing nucleoside triphosphate hydrolases superfamily protein	69.33	0.036	-1.09
PACid:16416571	ribosomal protein S13A	84.32	0.001	-1.07
PACid:16427467	P-loop containing nucleoside triphosphate hydrolases superfamily protein	205.33	0.009	-1.06
PACid:16413762	PDI-like 1-4	121.19	0.045	-1.04
PACid:16420853	ATP-citrate lyase A-3	72.22	0.014	-1.04

PACid:16416709	Calcium-binding EF-hand family protein	80.77	0.029	-1.01
PACid:16431432	Microsomal signal peptidase 25 kDa subunit (SPC25)	34.83	0.015	-0.98
PACid:16409224	pathogenesis-related 4	207.21	0.007	-0.95
PACid:16413132	Cyclase family protein	34.03	0.029	-0.93
PACid:16412735	sorting nexin 2A	49.23	0.021	-0.92
PACid:16421699	rhamnose biosynthesis 1	67.78	0.026	-0.84
PACid:16428767	heat shock protein 101	77.65	0.025	-0.79
PACid:16427981	importin alpha isoform 1	70.78	0.014	-0.76
PACid:16431114	Serine protease inhibitor (SERPIN) family protein	65.7	0.037	-0.75
PACid:16403847	beta-D-xylosidase 4	252.22	0.038	-0.74
PACid:16413146	poly(A) binding protein 2	139.48	0.009	-0.74
PACid:16428304	serine carboxypeptidase-like 33	149.42	0.040	-0.71
PACid:16430896	annexin 8	124.55	0.005	-0.70
PACid:16423532	catalase 2	1306.22	0.021	-0.70
PACid:16407440	S-adenosyl-L-methionine-dependent methyltransferases superfamily protein	15.35	0.027	-0.69
PACid:16428198	pfkB-like carbohydrate kinase family protein	247.48	0.020	-0.69
PACid:16414807	regulatory particle triple-A 1A	90.4	0.003	-0.68
PACid:16413698	annexin 2	256.94	0.002	-0.67
PACid:16429726	threonine aldolase 1	43.42	0.017	-0.65
PACid:16408635	U-box domain-containing protein	77.45	0.049	-0.65
PACid:16414081	ubiquitin-specific protease 21	24.89	0.043	-0.64
PACid:16408020	Ribosomal L28e protein family	33.14	0.038	-0.64
PACid:16405397	fibrillarin 2	32.67	0.024	-0.63
PACid:16407705	calnexin 1	281.89	0.015	-0.62
PACid:16411594	GHMP kinase family protein	34.33	0.014	-0.62
PACid:16418246	U2 snRNP auxilliary factor, large subunit, splicing factor	61.69	0.050	-0.61
PACid:16432172	O-fucosyltransferase family protein	36.48	0.008	-0.61
PACid:16406190	acetyl Co-enzyme a carboxylase biotin carboxylase subunit	484.32	0.016	-0.60

[1]Phytozome or NCBI gene identification number.

[2]Phytozome or NCBI gene description.

[3]Quality assurance scores for protein alignment by Progenesis QI.

[4]Analysis of variance (ANOVA) based p value ($p \leq 0.05$).

[5]Log_2 fold change of protein abundances comparing PMeV+PMeV2-infected vs. control plants.

Table 4. Proteins differently modulated in 7 months post germination (120 days post inoculation) PMeV+PMeV2-infected *C. papaya* leaf.

Phytozome/NCBI Accession[1]	Description[2]	Confidence score[3]	Anova (p)[4]	FC[5]
Up-accumulated proteins				
PACid:16425167	alpha/beta-Hydrolases superfamily protein	70.84	0.005	4.18
PACid:16414854	DEA(D/H)-box RNA helicase family protein	78.53	0.012	3.13
PACid:16420664	Adaptor protein complex AP-2, alpha subunit	43.87	0.018	2.87
PACid:16426114	None	20.1	0.035	2.52
PACid:16425995	methyl esterase 10	13.16	0.031	2.37
PACid:16429356	Mov34/MPN/PAD-1 family protein	187.68	0.015	2.24
PACid:16410436	root FNR 1	37.56	0.042	2.23
PACid:16418327	general regulatory factor 11	206.53	0.039	2.23
PACid:16411641	MAP kinase 4	43.78	0.023	2.14
PACid:16429196	ureidoglycine aminohydrolase	43.92	0.002	2.05
PACid:16412227	60S acidic ribosomal protein family	180.19	0.007	1.92
PACid:16426518	UDP-glucosyl transferase 71B1	17.94	0.015	1.88
PACid:16428415	ARF-GAP domain 8	49.31	0.023	1.88
PACid:16420360	Glucose-1-phosphate adenylyltransferase family protein	22.02	0.015	1.87
PACid:16425098	gamma vacuolar processing enzyme	19.3	0.000	1.86
PACid:16425960	mitochondrial HSO70 2	156.04	0.023	1.84
PACid:16426929	SWAP (Suppressor-of-White-APricot)/surp RNA-binding domain-containing protein	19.5	0.025	1.81
PACid:16412697	Alba DNA/RNA-binding protein	56.52	0.037	1.79
PACid:16416617	mitochondrion-localized small heat shock protein 23.6	60.7	0.008	1.75
PACid:16411051	Tetratricopeptide repeat (TPR)-like superfamily protein	130.26	0.027	1.71
PACid:16423953	phenylalanyl-tRNA synthetase, putative / phenylalanine--tRNA ligase, putative	81.46	0.011	1.70
PACid:16427150	None	378.99	0.032	1.65
PACid:16423462	proteasome alpha subunit D2	169.49	0.038	1.60
PACid:16423092	D-isomer specific 2-hydroxyacid dehydrogenase family protein	55.58	0.017	1.59
PACid:16416992	serine hydroxymethyltransferase 3	48.69	0.041	1.59
PACid:16416747	transducin family protein / WD-40 repeat family protein	38.13	0.015	1.58
PACid:16428853	subtilisin-like serine protease 3	22.31	0.037	1.58
PACid:16416771	HSP20-like chaperones superfamily protein	27.8	0.011	1.56
PACid:16420148	Pyruvate kinase family protein	28.15	0.021	1.55
PACid:16422738	uracil phosphoribosyltransferase	47.85	0.044	1.53
PACid:16421573	glutathione S-transferase PHI 9	486.36	0.038	1.48

PACid:16410427	urease accessory protein G	201.03	0.019	1.44
PACid:16429423	pentatricopeptide (PPR) repeat-containing protein	13.75	0.048	1.44
PACid:16409579	chloroplast outer envelope protein 37	43.14	0.048	1.37
PACid:16425809	Nuclear transport factor 2 (NTF2) family protein with RNA binding (RRM-RBD-RNP motifs) domain	43.24	0.017	1.35
GI:167391831	ATP-dependent Clp protease proteolytic subunit (chloroplast) [Carica papaya]	226.37	0.003	1.35
PACid:16421838	GDSL-like Lipase/Acylhydrolase superfamily protein	243.83	0.004	1.33
PACid:16410318	RP non-ATPase subunit 8A	87.78	0.008	1.33
PACid:16425955	Leucine-rich repeat protein kinase family protein	15.13	0.005	1.30
PACid:16429335	TCP-1/cpn60 chaperonin family protein	338.47	0.009	1.30
PACid:16407544	peroxisomal NAD-malate dehydrogenase 1	311.43	0.012	1.28
PACid:16412645	regulatory particle triple-A ATPase 3	90.74	0.015	1.28
PACid:16428030	gamma histone variant H2AX	68.53	0.042	1.27
PACid:16411947	Ribosomal protein L10 family protein	303.53	0.009	1.26
PACid:16413034	aspartate aminotransferase	43.12	0.016	1.22
PACid:16415916	NagB/RpiA/CoA transferase-like superfamily protein	168.97	0.012	1.20
PACid:16416453	SPFH/Band 7/PHB domain-containing membrane-associated protein family	74.17	0.014	1.20
PACid:16428003	GTP binding Elongation factor Tu family protein	167.67	0.027	1.20
PACid:16420362	delta 1-pyrroline-5-carboxylate synthase 2	43.99	0.014	1.19
PACid:16407265	None	56.26	0.049	1.18
PACid:16427279	gamma histone variant H2AX	113.2	0.037	1.18
PACid:16412130	histone H2A 12	324.16	0.030	1.17
PACid:16408534	histidinol dehydrogenase	110.54	0.022	1.16
PACid:16404356	triosephosphate isomerase	587.62	0.035	1.16
PACid:16403829	Succinyl-CoA ligase, alpha subunit	48.28	0.026	1.16
PACid:16418455	Sugar isomerase (SIS) family protein	118.53	0.019	1.15
PACid:16427501	actin-11	555.43	0.012	1.15
PACid:16413596	KH domain-containing protein	23.68	0.046	1.15
PACid:16418661	methylthioadenosine nucleosidase 1	43.42	0.026	1.15
PACid:16426375	glyoxylate reductase 1	206.04	0.021	1.14
PACid:16422232	binding to TOMV RNA 1L (long form)	31.85	0.033	1.13
PACid:16415072	Photosystem II reaction center PsbP family protein	91.78	0.019	1.13
PACid:16427467	P-loop containing nucleoside triphosphate hydrolases superfamily protein	205.33	0.035	1.12
PACid:16428900	voltage dependent anion channel 4	125.12	0.014	1.09
PACid:16416231	nucleotide-rhamnose synthase/epimerase-reductase	96.38	0.004	1.08

PACid:16414029	uridine 5\'-monophosphate synthase / UMP synthase (PYRE-F) (UMPS)	20.29	0.006	1.07
PACid:16427399	Enoyl-CoA hydratase/isomerase family	39.94	0.044	1.07
PACid:16416361	glutamine synthase clone R1	203.95	0.031	1.04
PACid:16419957	Nucleotide-diphospho-sugar transferases superfamily protein	42.75	0.041	1.03
PACid:16417615	NAD(P)-linked oxidoreductase superfamily protein	178.46	0.002	1.03
PACid:16423410	NAD(P)-binding Rossmann-fold superfamily protein	37.01	0.002	1.03
PACid:16411964	L-Aspartase-like family protein	42.78	0.020	1.02
PACid:16406784	homolog of bacterial cytokinesis Z-ring protein FTSZ 1-1	205.63	0.042	1.02
PACid:16414159	aldehyde dehydrogenase 2C4	67.66	0.026	1.01
PACid:16421709	Phosphoribosyltransferase family protein	44.2	0.034	1.00
PACid:16409578	None	41.55	0.046	1.00
PACid:16415012	Disease resistance-responsive (dirigent-like protein) family protein	41.67	0.026	0.99
PACid:16431407	thioredoxin-dependent peroxidase 1	182.21	0.023	0.99
PACid:16416408	NagB/RpiA/CoA transferase-like superfamily protein	68.8	0.033	0.98
PACid:16405261	GroES-like zinc-binding alcohol dehydrogenase family protein	98.52	0.040	0.96
PACid:16422901	pyrophosphorylase 1	103.82	0.003	0.95
PACid:16412903	ATPase, V1 complex, subunit B protein	617.88	0.002	0.95
PACid:16425533	cinnamyl alcohol dehydrogenase 9	72.32	0.002	0.95
PACid:16423409	voltage dependent anion channel 2	85.1	0.017	0.94
PACid:16407928	prohibitin 3	149.49	0.044	0.92
PACid:16416152	Aldolase superfamily protein	81.89	0.040	0.91
PACid:16412620	None	114.86	0.045	0.90
PACid:16424190	proteasome beta subunit C1	196.55	0.041	0.90
PACid:16416071	Coatomer epsilon subunit	156.65	0.017	0.90
PACid:16425372	vacuolar ATP synthase subunit C (VATC) / V-ATPase C subunit / vacuolar proton pump C subunit (DET3)	174.93	0.046	0.90
PACid:16425539	Splicing factor, CC1-like	79.67	0.035	0.89
PACid:16427103	sucrose synthase 4	1393.58	0.026	0.86
PACid:16410071	alpha/beta-Hydrolases superfamily protein	296.24	0.012	0.86
PACid:16416941	clathrin adaptor complexes medium subunit family protein	176.42	0.020	0.86
PACid:16410388	RNA-binding (RRM/RBD/RNP motifs) family protein	43.17	0.046	0.86
PACid:16429310	Transketolase family protein	40.95	0.017	0.85
PACid:16406589	purin-rich alpha 1	27.95	0.017	0.85
PACid:16418604	proteasome alpha subunit D2	124.17	0.025	0.84
PACid:16404068	ATPase E1	43.25	0.013	0.84

PACid:16427505	Plastid-lipid associated protein PAP / fibrillin family protein	32.1	0.029	0.84
PACid:16423500	aconitase 1	386.92	0.030	0.84
PACid:16413063	mitochondrial HSO70 2	286.75	0.002	0.82
PACid:16425886	Alba DNA/RNA-binding protein	210.89	0.033	0.82
PACid:16416137	tetraticopeptide domain-containing thioredoxin	220.99	0.045	0.82
PACid:16417130	general regulatory factor 8	210.02	0.005	0.82
GI:224020956	ATP synthase F1 subunit 1 (mitochondrion) [Carica papaya]	379.58	0.022	0.82
PACid:16416032	Ribosomal protein S7e family protein	133.88	0.028	0.81
PACid:16405150	AAA-type ATPase family protein	191.65	0.047	0.80
PACid:16421200	Pyruvate kinase family protein	308.36	0.028	0.80
PACid:16418653	Class II aminoacyl-tRNA and biotin synthetases superfamily protein	214.67	0.045	0.80
PACid:16410367	Ribosomal protein L14	107.55	0.048	0.80
PACid:16411302	alpha/beta-Hydrolases superfamily protein	83.48	0.015	0.78
PACid:16431481	phosphomannomutase	43.6	0.038	0.78
PACid:16420035	nuclear transport factor 2B	88.57	0.010	0.78
PACid:16414185	ATP-dependent caseinolytic (Clp) protease/crotonase family protein	287.02	0.004	0.75
PACid:16418595	arginine/serine-rich splicing factor 35	72.74	0.049	0.75
PACid:16428797	glycine-rich RNA-binding protein 3	136.21	0.018	0.75
PACid:16424511	ATP synthase alpha/beta family protein	1236.99	0.018	0.74
PACid:16429306	delta(3,5),delta(2,4)-dienoyl-CoA isomerase 1	45.27	0.021	0.74
PACid:16404188	ABC transporter family protein	79.31	0.037	0.73
PACid:16410178	Cobalamin-independent synthase family protein	1605.03	0.009	0.72
PACid:16425443	2-isopropylmalate synthase 1	183.91	0.029	0.71
PACid:16427747	aconitase 3	595.98	0.028	0.71
PACid:16418905	Aldolase-type TIM barrel family protein	365.53	0.007	0.71
PACid:16413886	Nucleoside diphosphate kinase family protein	340.18	0.001	0.69
PACid:16423481	E3 ubiquitin ligase SCF complex subunit SKP1/ASK1 family protein	123.84	0.020	0.69
PACid:16411383	RNAhelicase-like 8	38.55	0.020	0.68
PACid:16420138	Pseudouridine synthase/archaeosine transglycosylase-like family protein	89.47	0.038	0.68
PACid:16417606	Nascent polypeptide-associated complex (NAC), alpha subunit family protein	302.44	0.032	0.68
PACid:16406013	Plastid-lipid associated protein PAP / fibrillin family protein	114.55	0.024	0.68
PACid:16409816	phytoene desaturase 3	41.46	0.042	0.67
PACid:16408660	UDP-glucose 6-dehydrogenase family protein	203.64	0.013	0.66
PACid:16414684	adenine phosphoribosyl transferase 1	190.56	0.020	0.66

PACid:16412214	pyruvate dehydrogenase E1 alpha	135.87	0.047	0.65
PACid:16416636	annexin 5	173.85	0.029	0.65
PACid:16429896	proteasome alpha subunit A1	63.64	0.022	0.65
PACid:16415884	eif4a-2	701.65	0.019	0.65
PACid:16410640	translation initiation factor 3B1	172.57	0.011	0.64
PACid:16412527	Small nuclear ribonucleoprotein family protein	42.37	0.011	0.63
PACid:16404756	ssDNA-binding transcriptional regulator	127.65	0.022	0.63
PACid:16412600	Phosphoglucomutase/phosphomannomutase family protein	651.19	0.002	0.62
PACid:16406115	Ribosomal protein S12/S23 family protein	48.56	0.018	0.62
PACid:16422265	GTP binding Elongation factor Tu family protein	554.87	0.040	0.62
PACid:16423313	gamma carbonic anhydrase 1	117.74	0.010	0.62
PACid:16411975	Ribosomal protein L35Ae family protein	117.63	0.030	0.61
PACid:16419278	phosphoglucomutase	82.81	0.003	0.60
PACid:16407915	Cytochrome C1 family	131.43	0.012	0.59
PACid:16431114	Serine protease inhibitor (SERPIN) family protein	65.7	0.016	0.58
PACid:16404753	ACT domain-containing protein	30.2	0.043	0.58
Down-accumulated proteins				
PACid:16426616	kunitz trypsin inhibitor 1	82.22	0.043	-3.43
PACid:16421897	non-photochemical quenching 1	41.64	0.006	-2.98
PACid:16430895	None	15.11	0.003	-2.30
PACid:16418225	PsbQ-like 2	31.23	0.041	-1.96
PACid:16425864	DnaJ/Hsp40 cysteine-rich domain superfamily protein	25.92	0.016	-1.84
PACid:16405665	ribulose-bisphosphate carboxylases	188.91	0.003	-1.69
PACid:16428787	histone deacetylase 5	56.63	0.045	-1.64
GI:167391804	photosystem I P700 chlorophyll a apoprotein A2 (chloroplast) [Carica papaya]	510.29	0.007	-0.90
GI:167391836	cytochrome b6 (chloroplast) [Carica papaya]	141.28	0.029	-0.79
PACid:16406942	Aldolase superfamily protein	336.7	0.038	-0.61
PACid:16415292	tubulin beta-1 chain	270.36	0.021	-0.60

[1]Phytozome or NCBI gene identification number.

[2]Phytozome or NCBI gene description.

[3]Quality assurance scores for protein alignment by Progenesis QI.

[4]Analysis of variance (ANOVA) based p value ($p \leq 0.05$).

[5]Log_2 fold change of protein abundances comparing PMeV+PMeV2-infected vs. control plants.

Table 5. Proteins differently modulated in 9 months post germination (180 days post inoculation) PMeV+PMeV2-infected *C. papaya* leaf.

Phytozome/NCBI Accession[1]	Description[2]	Confidence score[3]	Anova (p)[4]	FC[5]
Up-accumulated proteins				
PACid:16421621	ATP-dependent caseinolytic (Clp) protease/crotonase family protein	42.8	0.025	2.13
PACid:16426826	Cyclophilin-like peptidyl-prolyl cis-trans isomerase family protein	54.19	0.025	2.13
PACid:16409552	fumarase 1	27.17	0.019	1.86
PACid:16412603	ENTH/ANTH/VHS superfamily protein	14.61	0.043	1.56
PACid:16418772	Glycosyl hydrolase superfamily protein	83.32	0.010	1.50
PACid:16405045	Dihydroneopterin aldolase	86.91	0.027	1.44
PACid:16407797	GroES-like zinc-binding alcohol dehydrogenase family protein	44.76	0.049	1.15
PACid:16404068	ATPase E1	43.25	0.023	1.14
PACid:16422232	binding to TOMV RNA 1L (long form)	31.85	0.047	0.92
PACid:16404260	Cleavage and polyadenylation specificity factor (CPSF) A subunit protein	78.4	0.045	0.81
PACid:16426651	succinate dehydrogenase 5	118.62	0.035	0.70
Down-accumulated proteins				
PACid:16406769	PLC-like phosphodiesterase family protein	118.14	0.007	-1.88
PACid:16428931	P-loop containing nucleoside triphosphate hydrolases superfamily protein	41.36	0.010	-1.50
PACid:16432121	tryptophan biosynthesis 1	32.85	0.003	-1.01
PACid:16423549	None	66.82	0.024	-0.81
PACid:16419807	alternative oxidase 2	38.33	0.032	-0.77
PACid:16424172	thylakoidal ascorbate peroxidase	73.69	0.005	-0.59

[1]Phytozome or NCBI gene identification number.

[2]Phytozome or NCBI gene description.

[3]Quality assurance scores for protein alignment by Progenesis QI.

[4]Analysis of variance (ANOVA) based p value ($p \leq 0.05$).

[5]Log_2 fold change of protein abundances comparing PMeV+PMeV2-infected vs. control plants.

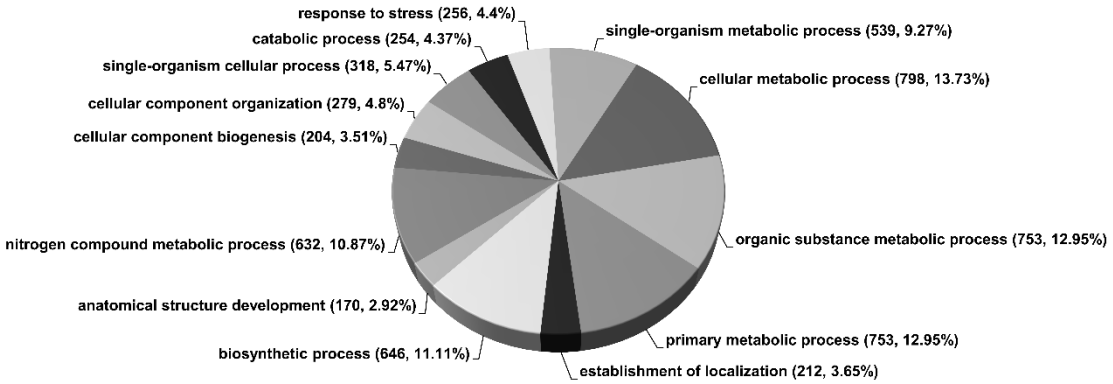

Figure 1. Gene Ontology (GO) grouping of PMeV+PMeV2-infected *C. papaya* leaf proteins according to their associated Biological Process at the third level using Blast2GO software. The numbers indicate the amount of sequences grouped in each GO term(s).

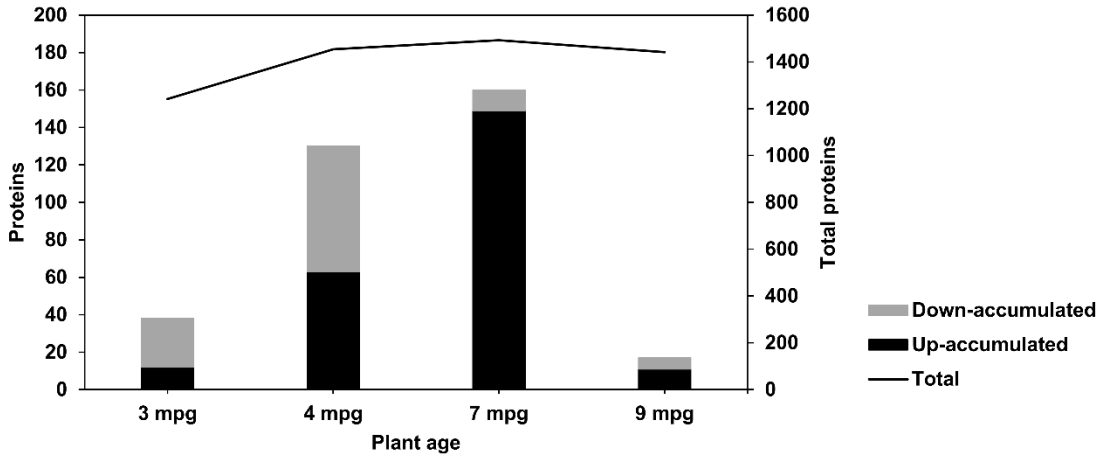

Figure 2. Label-free quantitative time course (months post germination, mpg) PMeV+PMeV2-infected *C. papaya* proteome coverage, considering as quantitative the proteins present in all three replicates with $p<0.05$ and as differentially accumulated proteins with ±0.58 fold change Log2(Infected/control).

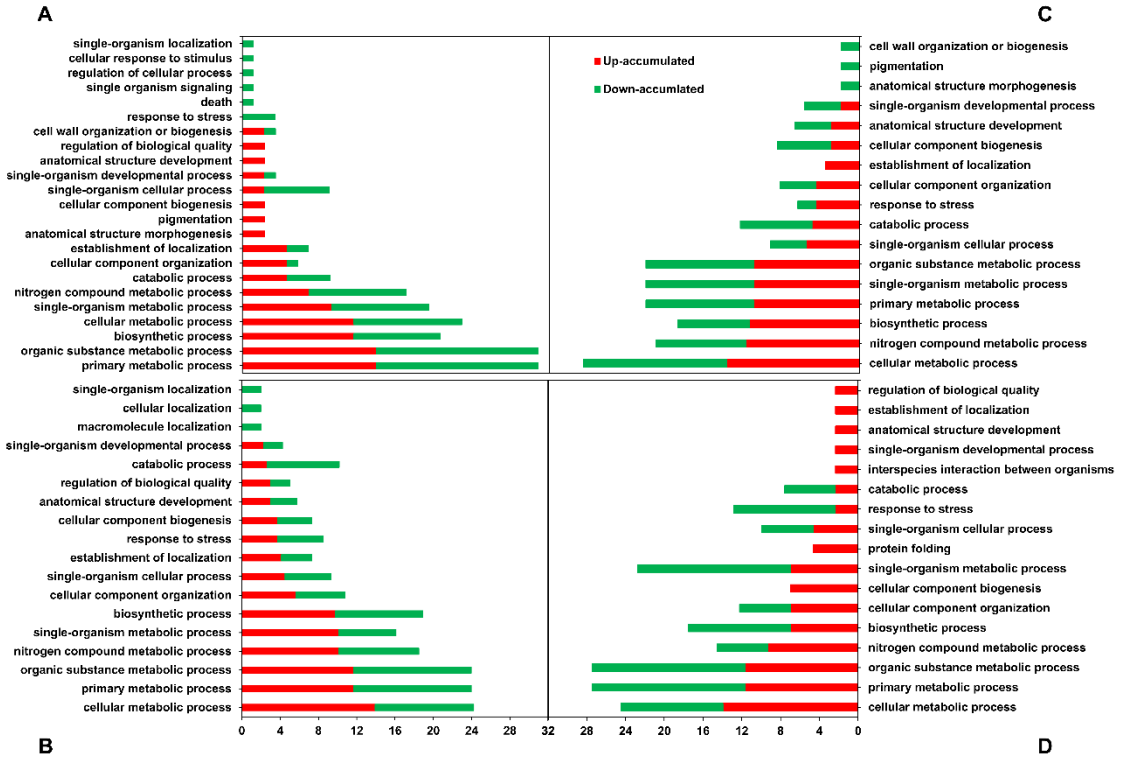

Figure 3. Gene Ontology (GO) bar chart displaying the third level GO terms percentage in up-accumulated (red) and down-accumulated (green) proteins. The proteins were grouped by their predicted GO Biological Process in 3 (A), 4 (B), 7 (C), 9 (D) months post germination (mpg).

MapMan Functional annotation	3 mpg		4 mpg		7 mpg		9 mpg	
	Up	Down	Up	Down	Up	Down	Up	Down
Photosynthesis	1	1	14	1	3	3		1
Major carbohydrates		1	2	1	1			
Minor carbohydrates			1		1			
Glycolysis					3			
Fermentation					1			
Gluconeogenesis/glyoxylate cycle					1			
Oxidative pentose phosphate pathway		1			5			
TCA cycle/organic acid transformations	2		3	1	5		1	
Mitochondrial electron transport/ATP synthesis					3			1
Cell wall		1	2	4	5			
Lipid metabolism	3	1	1	3	3		1	1
Nitrogen metabolism			2		1			
Amino acid metabolism	1	1	1	1	8		1	1
Sulphur assimilation			1		1			
Secondary metabolism			2	1	3	1		
Hormone metabolism				1				
Stress	1	1	1	4	5	1		
Redox			2	2	1			1
Nucleotide metabolism		1	1	1	7			
C1 metabolism			1		1		1	
Miscellaneous enzyme families	1	3	3	4	5		2	
RNA		2	3	7	16	1	3	
DNA		1	1	2	4			
Protein	1	8	6	21	3			
Signalling		3	1	2	2			
Cell		1	2	4	8	1	1	
Development					2	1		
Transport			1	1	5			
Not assigned		1	11	9	19	1	2	1

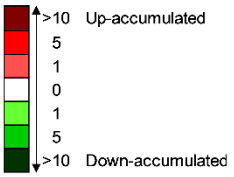

Figure 4. Heatmap of abundance changed proteins (p ≤0.05; FC ±0.58) displaying the number of up- (shades of red) and down-accumulated (shades of green) proteins mapped in each *C. papaya* overview metabolic pathway using MapMan software.

REFERENCES

[1] FAOSTAT, FAOSTAT Prod. (2016). http://faostat3.fao.org (accessed April 25, 2016).

[2] E.W. Kitajima, C.H. Rodrigues, J.S. Silveira, F. Alves, Association of isometric viruslike particles, restricted to lacticifers, with “meleira” (“ sticky disease”) of papaya (Carica papaya), Fitopatol. Bras. 18 (1993) 118.

[3] D. Perez-Brito, R. Tapia-Tussell, A. Cortes-Velazquez, A. Quijano-Ramayo, A. Nexticapan-Garcez, R. Martín-Mex, First report of papaya meleira virus (PMeV) in Mexico, African J. Biotechnol. 11 (2012) 13564–13570. doi:10.5897/AJB12.1189.

[4] J.A. Ventura, H. Costa, J. da S. Tatagiba, J. de S. Andrade, D. dos S. Martins, Meleira do mamoeiro: etiologia, sintomas e epidemiologia, Papaya Bras. Qual. Do Mamão Para O Merc. Interno. INCAPER, Vitória. (2003) 267–276.

[5] E.F.M. Abreu, C.B. Daltro, E.O.P.L. Nogueira, E.C. Andrade, F.J.L. Aragão, Sequence and genome organization of papaya meleira virus infecting papaya in Brazil, Arch. Virol. (2015) 1–5. doi:10.1007/s00705-015-2605-x.

[6] S.P. Rodrigues, J.S. Andrade, J. a. Ventura, G.G. Lindsey, P.M.B. Fernandes, Papaya meleira virus is neither transmitted by infection at wound sites nor by the whitefly Trialeurodes variabilis, J. Plant Pathol. 91 (2009) 87–91. doi:10.4454/jpp.v91i1.628.

[7] F.J.F. Correa, B. Franco, H.S. Watanabe, M.Y. Sakay, E.M.A. YAMASHITA, Estudo preliminar sobre exsudação do látex do mamoeiro-Teixeira de Freitas, Anais. 2 (1988) 409–428.

[8] J. Nakagawa, Y. Takayama, Y. Suzukama, Exudação de látex pelo mamoeiro. Estudo de ocorrência em Teixeira de Freitas, BA, in: Congr. Bras. Frutic., 1987: pp. 555–559.

[9] T.F. Sá Antunes, R.J.V. Amaral, J.A. Ventura, M.T. Godinho, J.G. Amaral, F.O. Souza, P.A. Zerbini, F.M. Zerbini, P.M.B. Fernandes, The dsRNA Virus Papaya Meleira Virus and an ssRNA Virus Are Associated with Papaya Sticky Disease, PLoS One. 11 (2016) e0155240. doi:10.1371/journal.pone.0155240.

[10] J.M. Hagel, E.C. Yeung, P.J. Facchini, Got milk? The secret life of laticifers, Trends Plant Sci. 13 (2008) 631–639.

[11] S.P. Rodrigues, M. Da Cunha, J. a Ventura, P.M.B. Fernandes, Effects of the Papaya meleira virus on papaya latex structure and composition, Plant Cell Rep. 28 (2009) 861–71. doi:10.1007/s00299-009-0673-7.

[12] M.M.M. de Araújo, É.T. Tavares, F.R. da Silva, V.L. de Almeida Marinho, M.T.S. Júnior, M.M.M. De Araújo, E.T. Tavares, F.R. Da Silva, V.L.D.A. Marinho, M.T.S. Júnior, Molecular detection of Papaya meleira virus in the latex of Carica papaya by RT-PCR., J. Virol. Methods. 146 (2007) 305–10. doi:10.1016/j.jviromet.2007.07.022.

[13] C.H. RODRIGUES, F.L. ALVES, S.L.D. MARIN, L.A. MAFFIA, J.A. VENTURA, A.S.D. GUTIERREZ, Meleira do mamoeiro no estado do Espírito Santo: enfoque fitopatológico, Meleira Do Mamoeiro No Estado Do Espírito St. Enfoque Fitopatológico. (1989).

[14] E. Maciel-Zambolim, S. Kunieda-Alonso, K. Matsuoka, M.G. De Carvalho, F.M. Zerbini, Purification and some properties of Papaya meleira virus, a novel virus infecting papayas in Brazil, Plant Pathol. 52 (2003) 389–394. doi:10.1046/j.1365-3059.2003.00855.x.

[15] G. Wang, S. Seabolt, S. Hamdoun, G. Ng, J. Park, H. Lu, Multiple Roles of WIN3 in Regulating Disease Resistance , Cell Death , and Flowering Time, 156 (2011) 1508–1519. doi:10.1104/pp.111.176776.

[16] G. LAZAROVITS, R. STOSSEL, E.W.B. WARD, AGE-RELATED-CHANGES IN SPECIFICITY AND GLYCEOLLIN PRODUCTION IN THE HYPOCOTYL REACTION OF SOYBEANS TO PHYTOPHTHORA-MEGASPERMA VAR-SOJAE, Phytopathology. 71 (1981) 94–97. doi:10.1094/Phyto-71-94.

[17] J. V Kus, K. Zaton, R. Sarkar, R.K. Cameron, Age-related resistance in Arabidopsis is a developmentally regulated defense response to Pseudomonas syringae, Plant Cell. 14 (2002) 479–490. doi:10.1105/tpc.010481.

[18] J.D. PAXTON, CHAMBERL.DW, PHYTOALEXIN PRODUCTION AND DISEASE RESISTANCE IN SOYBEANS AS AFFECTED BY AGE, Phytopathology. 59 (1969) 775–777.

[19] D.F. BATEMAN, R.D. LUMSDEN, RELATION OF CALCIUM CONTENT AND NATURE OF PECTIC SUBSTANCES IN BEAN HYPOCOTYLS OF DIFFERENT AGES TO SUSCEPTIBILITY TO AN ISOLATE OF RHIZOCTONIA SOLANI, Phytopathology. 55 (1965) 734–&.

[20] M.C. HEATH, GENETICS AND CYTOLOGY OF AGE-RELATED RESISTANCE IN NORTH-AMERICAN CULTIVARS OF COWPEA (VIGNA-UNGUICULATA) TO THE COWPEA RUST FUNGUS (UROMYCES-VIGNAE), Can. J. Bot. Can. Bot. 72 (1994) 575–581.

[21] P. Coelho, K. Bahcevandziev, L. Valerio, A. Monteiro, D. Leckie, D. Astley, I.R. Crute, I. Boukema, The relationship between cotyledon and adult plant resistance to downy mildew (Peronospora parasitica) in Brassica oleracea, in: Int. Symp. Brassica 97, Xth Crucif. Genet. Work. 459, 1997: pp. 335–342.

[22] R.E. HUNTER, J.M. HALLOIN, J.A. VEECH, W.W. CARTER, TERPENOID ACCUMULATION IN HYPOCOTYLS OF COTTON SEEDLINGS DURING AGING AND AFTER INFECTION BY RHIZOCTONIA-SOLANI, Phytopathology. 68 (1978) 347–350.

[23] B.G. Abedon, W.F. Tracy, Corngrass1 of maize (Zea mays L.) delays development of adult plant resistance to common rust (Puccinia sorghi Schw.) and European corn borer (Ostrinia nubilalis Hubner), J. Hered. 87 (1996) 219–223.

[24] S.E. WYATT, S.Q. PAN, J. KUC, BETA-1,3-GLUCANASE, CHITINASE, AND PEROXIDASE-ACTIVITIES IN TOBACCO TISSUES RESISTANT AND SUSCEPTIBLE TO BLUE MOLD AS RELATED TO FLOWERING, AGE AND SUCKER DEVELOPMENT, Physiol. Mol. Plant Pathol. 39 (1991) 433–440.

doi:10.1016/0885-5765(91)90009-7.

[25] K. Hugot, S. Aime, S. Conrod, A. Poupet, E. Galiana, Developmental regulated mechanisms affect the ability of a fungal pathogen to infect and colonize tobacco leaves, PLANT J. 20 (1999) 163–170. doi:10.1046/j.1365-313x.1999.00587.x.

[26] C. Rusterucci, Z. Zhao, K. Haines, D. Mellersh, A. Neumann, R.K. Cameron, Age-related resistance to Pseudomonas syringae pv. tomato is associated with the transition to flowering in Arabidopsis and is effective against Peronospora parasitica, Physiol. Mol. Plant Pathol. 66 (2005) 222–231. doi:10.1016/j.pmpp.2005.08.004.

[27] S.M. Leisner, R. Turgeon, S.H. Howell, others, Long distance movement of cauliflower mosaic virus in infected turnip plants, Mol. Plant-Microbe Interact. 5 (1992) 41–47.

[28] S.M. LEISNER, R. TURGEON, S.H. HOWELL, EFFECTS OF HOST PLANT DEVELOPMENT AND GENETIC-DETERMINANTS ON THE LONG-DISTANCE MOVEMENT OF CAULIFLOWER MOSAIC-VIRUS IN ARABIDOPSIS, Plant Cell. 5 (1993) 191–202.

[29] P.M. V Abreu, C.G. Gaspar, D.S. Buss, J. a Ventura, P.C.G. Ferreira, P.M.B. Fernandes, Carica papaya microRNAs are responsive to Papaya meleira virus infection, PLoS One. 9 (2014) e103401. doi:10.1371/journal.pone.0103401.

[30] S.P. Rodrigues, J. a. Ventura, C. Aguilar, E.S. Nakayasu, I.C. Almeida, P.M.B. Fernandes, R.B. Zingali, Proteomic analysis of papaya (Carica papaya L.) displaying typical sticky disease symptoms, Proteomics. 11 (2011) 2592–2602. doi:10.1002/pmic.201000757.

[31] S.P. Rodrigues, J. a. Ventura, C. Aguilar, E.S. Nakayasu, H. Choi, T.J.P. Sobreira, L.L. Nohara, L.S. Wermelinger, I.C. Almeida, R.B. Zingali, P.M.B. Fernandes, others, Label-free quantitative proteomics reveals differentially regulated proteins in the latex of sticky diseased Carica papaya L. plants, J. Proteomics. 75 (2012) 3191–3198. doi:10.1016/j.jprot.2012.03.021.

[32] H. Wang, S. Alvarez, L.M. Hicks, Comprehensive Comparison of iTRAQ and Label-free LC-Based Quantitative Proteomics Approaches Using Two Chlamydomonas reinhardtii Strains of Interest for Biofuels Engineering, J. Proteome Res. 11 (2012) 487–501. doi:10.1021/pr2008225.

[33] R. Ming, S. Hou, Y. Feng, Q. Yu, A. Dionne-Laporte, J.H. Saw, P. Senin, W. Wang, B. V. Ly, K.L.T. Lewis, S.L. Salzberg, L. Feng, M.R. Jones, R.L. Skelton, J.E. Murray, C. Chen, W. Qian, J. Shen, P. Du, M. Eustice, E. Tong, H. Tang, E. Lyons, R.E. Paull, T.P. Michael, K. Wall, D.W. Rice, H. Albert, M.-L. Wang, Y.J. Zhu, M. Schatz, N. Nagarajan, R.A. Acob, P. Guan, A. Blas, C.M. Wai, C.M. Ackerman, Y. Ren, C. Liu, J.J. Wang, J.J. Wang, J.-K. Na, E. V. Shakirov, B. Haas, J. Thimmapuram, D. Nelson, X. Wang, J.E. Bowers, A.R. Gschwend, A.L. Delcher, R. Singh, J.Y. Suzuki, S. Tripathi, K. Neupane, H. Wei, B. Irikura, M. Paidi, N. Jiang, W. Zhang, G. Presting, A. Windsor, R. Navajas-Pérez, M.J. Torres, F.A. Feltus, B. Porter, Y. Li, A.M. Burroughs, M.-C. Luo, L. Liu, D.A. Christopher, S.M. Mount, P.H. Moore, T. Sugimura, J. Jiang, M.A. Schuler, V. Friedman, T. Mitchell-Olds, D.E. Shippen, C.W. dePamphilis, J.D. Palmer, M. Freeling, A.H. Paterson, D. Gonsalves, L. Wang, M. Alam, others, The draft

genome of the transgenic tropical fruit tree papaya (Carica papaya Linnaeus), Nature. 452 (2008) 991–996. doi:10.1038/nature06856.

[34] H. Nordberg, M. Cantor, S. Dusheyko, S. Hua, A. Poliakov, I. Shabalov, T. Smirnova, I. V Grigoriev, I. Dubchak, The genome portal of the Department of Energy Joint Genome Institute : 2014 updates, 42 (2014) 26–31. doi:10.1093/nar/gkt1069.

[35] J.C. Silva, Absolute Quantification of Proteins by LCMSE: A Virtue of Parallel ms Acquisition, Mol. Cell. Proteomics. 5 (2005) 144–156. doi:10.1074/mcp.M500230-MCP200.

[36] Y. Benjamini, Y. Hochberg, Controlling the False Discovery Rate: A Practical and Powerful Approach to Multiple Testing, J. R. Stat. Soc. Ser. B. 57 (1995) 289–300. http://www.jstor.org/stable/2346101.

[37] M.M. Alexander, M. Cilia, A molecular tug-of-war: Global plant proteome changes during viral infection, Curr. Plant Biol. 5 (2016) 13–24. doi:10.1016/j.cpb.2015.10.003.

[38] J.Á. Huerta-Ocampo, J.A. Osuna-Castro, G.J. Lino-López, A. Barrera-Pacheco, G. Mendoza-Hernández, A. De León-Rodríguez, A.P. Barba de la Rosa, Proteomic analysis of differentially accumulated proteins during ripening and in response to 1-MCP in papaya fruit, J. Proteomics. 75 (2012) 2160–2169. doi:10.1016/j.jprot.2012.01.015.

[39] S.B. Nogueira, C.A. Labate, F.C. Gozzo, E.J. Pilau, F.M. Lajolo, J.R. Oliveira do Nascimento, Proteomic analysis of papaya fruit ripening using 2DE-DIGE, J. Proteomics. 75 (2012) 1428–1439. doi:10.1016/j.jprot.2011.11.015.

[40] Y.Q. Wang, Y. Yang, Z. Fei, H. Yuan, T. Fish, T.W. Thannhauser, M. Mazourek, L. V. Kochian, X. Wang, L. Li, Proteomic analysis of chromoplasts from six crop species reveals insights into chromoplast function and development, J. Exp. Bot. 64 (2013) 949–961. doi:10.1093/jxb/ers375.

[41] E.D.M. Vale, A.S. Heringer, T. Barroso, A. Teixeira, M. Nunes, J. Enrique, A. Perales, C. Santa-catarina, V. Silveira, Comparative proteomic analysis of somatic embryo maturation in Carica papaya L . Comparative proteomic analysis of somatic embryo maturation in Carica papaya L ., (2014).

[42] V.J. Patel, K. Thalassinos, S.E. Slade, J.B. Connolly, A. Crombie, J.C. Murrell, J.H. Scrivens, A comparison of labeling and label-free mass spectrometry-based proteomics approaches., J Proteome Res. 8 (2009) 3752–3759. doi:10.1021/pr900080y.

[43] B. Deracinois, C. Flahaut, S. Duban-Deweer, Y. Karamanos, Comparative and Quantitative Global Proteomics Approaches: An Overview, Proteomes. 1 (2013) 180–218. doi:10.3390/proteomes1030180.

[44] L. Wu, Z. Han, S. Wang, X. Wang, A. Sun, X. Zu, Y. Chen, Comparative proteomic analysis of the plant-virus interaction in resistant and susceptible ecotypes of maize infected with sugarcane mosaic virus, J. Proteomics. 89 (2013) 124–140. doi:10.1016/j.jprot.2013.06.005.

[45] K.K. Mandadi, K.-B.G.K.-B.G. Scholthof, Plant immune responses against viruses: how does a virus cause disease?, Plant Cell. 25 (2013) 1489–505.

doi:10.1105/tpc.113.111658.

[46] A. Maule, V. Leh, C. Lederer, The dialogue between viruses and hosts in compatible interactions, Curr. Opin. Plant Biol. 5 (2002) 279–284. doi:10.1016/S1369-5266(02)00272-8.

[47] R. Thyrhaug, A. Larsen, C.P.D. Brussaard, G. Bratbak, Cell cycle dependent virus production in marine phytoplankton, J. Phycol. 38 (2002) 338–343. <Go to ISI>://000175149000012.

[48] M. Heinlein, Plant virus replication and movement, Virology. 479-480 (2015) 657–671. doi:10.1016/j.virol.2015.01.025.

[49] V. Nicaise, Lost in translation: An antiviral plant defense mechanism revealed, Cell Host Microbe. 17 (2015) 417–419. doi:10.1016/j.chom.2015.03.009.

[50] J. Tilsner, O. Linnik, M. Louveaux, I.M. Roberts, S.N. Chapman, K.J. Oparka, Replication and trafficking of a plant virus are coupled at the entrances of plasmodesmata, J. Cell Biol. 201 (2013) 981–995. doi:10.1083/jcb.201304003.

[51] A. Kachroo, P. Kachroo, Fatty Acid – Derived Signals in Plant Defense, Annu. Rev. Phytopathol. 47 (2009) 153–176. doi:10.1146/annurev-phyto-080508-081820.

[52] K. Li, C. Xu, J. Zhang, Proteome profile of maize (Zea Mays L.) leaf tissue at the flowering stage after long-term adjustment to rice black-streaked dwarf virus infection, Gene. 485 (2011) 106–113. doi:10.1016/j.gene.2011.06.016.

[53] J.N. Culver, M.S. Padmanabhan, Virus-induced disease: altering host physiology one interaction at a time., Annu. Rev. Phytopathol. 45 (2007) 221–243. doi:10.1146/annurev.phyto.45.062806.094422.

[54] J.L. Dangl, J.D.G. Jones, Plant pathognes and integrated defence responses to infection, 411 (2001).

[55] A. Magaña-Álvarez, J. Vencioneck Dutra, T. Carneiro, D. Pérez-Brito, R. Tapia-Tussell, J. Ventura, I. Higuera-Ciapara, P. Fernandes, A. Fernandes, Physical Characteristics of the Leaves and Latex of Papaya Plants Infected with the Papaya meleira Virus, Int. J. Mol. Sci. 17 (2016) 574. doi:10.3390/ijms17040574.

[56] Y. Li, H. Cui, X. Cui, A. Wang, The altered photosynthetic machinery during compatible virus infection, Curr. Opin. Virol. 17 (2016) 19–24. doi:10.1016/j.coviro.2015.11.002.

[57] M.D. Bolton, Primary metabolism and plant defense--fuel for the fire., Mol. Plant. Microbe. Interact. 22 (2009) 487–497. doi:10.1094/MPMI-22-5-0487.

[58] U.F. Greber, M. Way, A superhighway to virus infection, Cell. 124 (2006) 741–754. doi:10.1016/j.cell.2006.02.018.

[59] S. Kangasjärvi, M. Tikkanen, G. Durian, E.-M. Aro, Photosynthetic light reactions – An adjustable hub in basic production and plant immunity signaling, Plant Physiol. Biochem. 81 (2014) 128–134. doi:10.1016/j.plaphy.2013.12.004.

[60] K. Komatsu, M. Hashimoto, J. Ozeki, Y. Yamaji, K. Maejima, H. Senshu, M. Himeno, Y. Okano, S. Kagiwada, S. Namba, Viral-induced systemic necrosis in plants involves both programmed cell death and the inhibition of viral

multiplication, which are regulated by independent pathways., Mol. Plant. Microbe. Interact. 23 (2010) 283–293. doi:10.1094/MPMI-23-3-0283.

4. CONSIDERAÇÕES FINAIS

Este estudo possibilitou a identificação de 1.623 e a quantificação de 1.609 proteínas, cuja comparação de abundâncias permitiu a análise de proteínas diferencialmente acumuladas nos períodos de prefloração e pós-floração. O estádio de prefloração revelou um acúmulo de proteínas relacionadas à fotossíntese e uma redução no nível de proteínas relacionadas ao proteassomo, de proteínas com atividade de caspase (caspase-like) e de proteínas relacionadas à formação e remodelamento de parede celular. A elevação nos níveis de proteínas relacionadas à fotossíntese possui um efeito positivo na indução resistência vegetal, com a produção de espécies reativas de oxigênio (ROS) para a sinalização celular do estresse biótico, ativando assim a maquinaria de defesa das demais células, enquanto a diminuição nos níveis de proteínas relacionadas ao proteassomo e à atividade de caspase limitam esta maquinaria de defesa ao minar a possibilidade de uma resposta hipersensível via proteassomo ou morte celular via vacúolo, mediada por atividade de proteínas caspase-like. Adicionalmente, a obstrução do movimento viral, via plasmodesmas, é impossibilitada pela diminuição dos níveis de proteínas relacionadas ao remodelamento da parede celular, limitando a deposição de calose.

O estádio de pós-floração das plantas infectadas e consequentemente sintomáticas revelou uma drástica mudança nos padrões de acúmulo de proteínas, apresentando uma redução no acúmulo de proteínas relacionadas à fotossíntese e elevação no acúmulo de proteínas relacionadas ao metabolismo de carboidratos, lipídeos, aminoácidos, proteínas, nucleotídeos e ácidos nucléicos. Foi observado ainda, elevação nos níveis de acúmulo de proteínas envolvidas em resposta a estresse, sinalização, transporte e parede celular. A redução nos níveis de proteínas relacionadas à fotossíntese, sobretudo àquelas responsáveis pelo acoplamento entre os fotossistemas II e I, proporciona uma elevada e descontrolada produção de ROS no complexo de evolução o oxigênio do fotossistema II.

As proteínas encontradas no período de pré florescimento, somadas as demais modificações descritas na literatura para as plantas infectadas e assintomáticas neste

estádio fenológico, nos permite inferir que o mamoeiro possui um mecanismo de tolerância à meleira anterior ao florescimento, com uma sinalização por ROS via cloroplasto. Porém, este mecanismo é insuficiente na contenção da infecção sistêmica provocada pela depleção da atividade caspásica, proteassomal, e de remodelamento de parede, todas necessárias para os mecanismos de morte celular programada e confinamento do vírus às células inicialmente infectadas. Este mecanismo de tolerância, incompleta no pré florescimento, ganha novos elementos com a transição juvenil-adulto, possibilitando uma ação mais efetiva por parte da planta na interação planta-vírus. Contudo, a efetividade destes mecanismos alcançada no mamoeiro adulto se dá de forma tardia com uma infecção sistêmica já instalada, resultando nos sintomas de resposta necrótica nas extremidades de folhas jovens e de resposta clorótica nos frutos.

Os processos de remodelamento da parede celular e a atividade do proteassomo 26S são necessários para um desenvolvimento saudável e para a manutenção das células dos vasos condutores vegetais durante o ciclo de vida da planta, principalmente no ciclo vegetativo, período no qual estes processos encontram-se inibidos, acarretando na formação de vasos condutores malformados e enfraquecidos. Uma das modificações observadas nos laticíferos é o desequilíbrio osmótico, que somado ao enfraquecimento das células destes vasos, acarreta o rompimento dos mesmos, com o extravasamento do látex aquoso, cuja elevada fluidez retarda sua polimerização e prolonga o tempo de exposição ao ar, promovendo oxidação deste látex e acúmulo desta substância pegajosa nos órgãos do mamoeiro, gerando o aspecto melado do mamoeiro doente, principal sintoma e origem de sua denominação.

Dada a importância do cultivo e magnitude dos prejuízos causados pela meleira, somadas a inexistência de genótipo de *C. papaya* resistente a esta doença, o entendimento das limitações na maquinaria de defesa aponta para um potencial biotecnológico promissor na construção de mamoeiros modificados para o aumento na atividade de proteínas caspase-like ou de proteínas de remodelamento de parede celular, sobretudo deposição de calose. Sendo ainda necessário um maior entendimento das implicações destas modificações no ciclo de vida e na produtividade do mamoeiro.

Tendo em visto que a sintomatologia da meleira do mamoeiro é dependente da transição juvenil-adulto e que o padrão de acúmulo de proteínas envolvidas nesta transição se dá, possivelmente, de forma constitutiva e independente de infeção, faz-se necessário e será conduzido um estudo do perfil proteômico do mamoeiro sadio ao longo do ciclo de vida com enfoque no padrão de acúmulo diferencial de proteínas envolvidas na transição juvenil-adulto e a possível correlação das mesmas com o sistema imune do mamoeiro e a sintomatologia da meleira do mamoeiro.

5. REFERÊNCIAS

ABREU, P. M. V et al. Molecular diagnosis of Papaya meleira virus (PMeV) from leaf samples of Carica papaya L. using conventional and real-time RT-PCR. **Journal of Virological Methods**, v. 180, n. 1-2, p. 11–17, 2012.

ABREU, P. M. V et al. Carica papaya microRNAs are responsive to Papaya meleira virus infection. **PloS one**, v. 9, n. 7, p. e103401, 2014.

ABREU, P. et al. A Current Overview of the Papaya meleira virus, an Unusual Plant Virus. **Viruses**, v. 7, n. 4, p. 1853–1870, 2015.

AEBERSOLD, R.; MANN, M. Mass spectrometry-based proteomics. **Nature**, v. 422, n. 6928, p. 198–207, 2003.

ALEXANDER, M. M.; CILIA, M. A molecular tug-of-war: Global plant proteome changes during viral infection. **Current Plant Biology**, v. 5, p. 13–24, 2016.

ARUMUGANATHAN, K.; EARLE, E. D. Nuclear DNA content of some important plant species. **Plant Mol Biol Report**, v. 9, n. 3, p. 208–218, 1991.

BAUMBERGER, N. et al. The Polerovirus Silencing Suppressor P0 Targets ARGONAUTE Proteins for Degradation. **Current Biology**, v. 17, n. 18, p. 1609–1614, 2007.

BINDER, B. M. et al. The Arabidopsis EIN3 binding F-Box proteins EBF1 and EBF2 have distinct but overlapping roles in ethylene signaling. **The Plant cell**, v. 19, n. 2, p. 509–523, 2007.

BODZON-KULAKOWSKA, A. et al. Methods for samples preparation in proteomic research. **Journal of Chromatography B: Analytical Technologies in the Biomedical and Life Sciences**, v. 849, n. 1-2, p. 1–31, 2007.

CORREA, F. J. F. et al. Estudo preliminar sobre exsudação do látex do mamoeiro-Teixeira de Freitas. **Anais**, v. 2, p. 409–428, 1988.

COSGROVE, D. J. Growth of the plant cell wall. **Nature reviews molecular cell biology**, v. 6, n. 11, p. 850–861, 2005.

DE ARAÚJO, M. M. M. et al. Molecular detection of Papaya meleira virus in the latex of Carica papaya by RT-PCR. **Journal of virological methods**, v. 146, n. 1-2, p. 305–10, 2007.

DELAURÉ, S. L. et al. Building up plant defenses by breaking down proteins. **Plant Science**, v. 174, n. 4, p. 375–385, 2008.

DERACINOIS, B. et al. Comparative and Quantitative Global Proteomics Approaches: An Overview. **Proteomes**, v. 1, n. 3, p. 180–218, 2013.

DI CARLI, M.; BENVENUTO, E.; DONINI, M. Recent insights into plant-virus

interactions through proteomic analysis. **Journal of Proteome Research**, v. 11, n. 10, p. 4765–4780, 2012.

DIELEN, A.; BADAOUI, S.; CANDRESSE, T. The ubiquitin / 26S proteasome system in plant – pathogen interactions : a never-ending hide-and-seek game SYSTEM TO REGULATE PROTEIN STABILITY. v. 11, p. 293–308, 2010.

DREHER, K.; CALLIS, J. Ubiquitin, hormones and biotic stress in plants. **Annals of Botany**, v. 99, n. 5, p. 787–822, 2007.

EDREVA, A. Generation and scavenging of reactive oxygen species in chloroplasts: A submolecular approach. **Agriculture, Ecosystems and Environment**, v. 106, n. 2-3 SPEC. ISS., p. 119–133, 2005.

ENDO, S.; DEMURA, T.; FUKUDA, H. Inhibition of proteasome activity by the TED4 protein in extracellular space: a novel mechanism for protection of living cells from injury caused by dying cells. **Plant & cell physiology**, v. 42, n. 1, p. 9–19, 2001.

FAOSTAT. Disponível em: <http://faostat3.fao.org>. Acesso em: 25 abr. 2016.

GOLDBERG, A. L. Protein degradation and protection against misfolded or damaged proteins. v. 426, n. December, 2003.

GUO, Y. et al. How is mRNA expression predictive for protein expression? A correlation study on human circulating monocytes. **Acta Biochimica et Biophysica Sinica**, v. 40, n. 5, p. 426–436, 2008.

GYGI, S. P. et al. Correlation between protein and mRNA abundance in yeast. **Molecular and cellular biology**, v. 19, n. 3, p. 1720–1730, 1999.

JIN, H.; LI, S.; VILLEGAS, A. Down-regulation of the 26S proteasome subunit RPN9 inhibits viral systemic transport and alters plant vascular development. **Plant physiology**, v. 142, n. 2, p. 651–61, 2006.

JONES, J. D. G.; DANGL, J. L. The plant immune system. **Nature**, v. 444, n. 7117, p. 323–329, 2006.

JURADO, S. et al. SKP2A, an F-box protein that regulates cell division, is degraded via the ubiquitin pathway. **Plant Journal**, v. 53, n. 5, p. 828–841, 2008.

KANGASJÄRVI, S. et al. Photosynthetic light reactions – An adjustable hub in basic production and plant immunity signaling. **Plant Physiology and Biochemistry**, v. 81, p. 128–134, 2014.

KIM, M. S. et al. Genetic diversity of Carica papaya as revealed by AFLP markers. **Genome / National Research Council Canada = Genome / Conseil national de recherches Canada**, v. 45, n. 3, p. 503–512, 2002.

KITAJIMA, E. W. et al. Association of isometric viruslike particles, restricted to lacticifers, with “meleira” (“sticky disease”) of papaya (Carica papaya). **Fitopatologia Brasileira**, v. 18, p. 118, 1993.

KUREPA, J.; SMALLE, J. A. Structure, function and regulation of plant proteasomes. **Biochimie**, v. 90, n. 2, p. 324–35, 2008.

LAGEIX, S. et al. The nanovirus-encoded Clink protein affects plant cell cycle regulation through interaction with the retinoblastoma-related protein. **Journal of**

virology, v. 81, n. 8, p. 4177–4185, 2007.

LUCAS, W. J. Plant viral movement proteins: Agents for cell-to-cell trafficking of viral genomes. **Virology**, v. 344, n. 1, p. 169–184, 2006.

MACIEL-ZAMBOLIM, E. et al. Purification and some properties of Papaya meleira virus, a novel virus infecting papayas in Brazil. **Plant Pathology**, v. 52, n. 3, p. 389–394, 2003.

MAGAÑA-ÁLVAREZ, A. et al. Physical Characteristics of the Leaves and Latex of Papaya Plants Infected with the Papaya meleira Virus. **International Journal of Molecular Sciences**, v. 17, n. 4, p. 574, 2016.

MALINOVSKY, F. G.; FANGEL, J. U.; WILLATS, W. G. T. The role of the cell wall in plant immunity. **Frontiers in plant science**, v. 5, n. 2014, p. 178, 2014.

MANDADI, K. K.; SCHOLTHOF, K.-B. G. K.-B. G. Plant immune responses against viruses: how does a virus cause disease? **The Plant cell**, v. 25, n. 5, p. 1489–505, 2013.

MING, R. et al. The draft genome of the transgenic tropical fruit tree papaya (Carica papaya Linnaeus). **Nature**, v. 452, n. 7190, p. 991–996, 2008.

MING, R.; YU, Q.; MOORE, P. H. Sex determination in papaya. **Seminars in Cell and Developmental Biology**, v. 18, n. 3, p. 401–408, 2007.

MUTHAMILARASAN, M.; PRASAD, M. Plant innate immunity: An updated insight into defense mechanism. **Journal of Biosciences**, v. 38, n. 2, p. 433–449, 2013.

NAKAGAWA, J.; TAKAYAMA, Y.; SUZUKAMA, Y. Exudação de látex pelo mamoeiro. Estudo de ocorrência em Teixeira de Freitas, BA. **Anais do Congresso Brasileiro de Fruticultura,** 1987

PATEL, V. J. et al. A comparison of labeling and label-free mass spectrometry-based proteomics approaches. **J Proteome Res**, v. 8, n. 7, p. 3752–3759, 2009.

PEREZ-BRITO, D. et al. First report of papaya meleira virus (PMeV) in Mexico. **African Journal of Biotechnology**, v. 11, n. 71, p. 13564–13570, 2012.

PLISSON, C. et al. Structural characterization of HC-Pro, a plant virus multifunctional protein. **Journal of Biological Chemistry**, v. 278, n. 26, p. 23753–23761, 2003.

RODRIGUES, C. H. et al. Meleira do mamoeiro no estado do Espírito Santo: enfoque fitopatológico. **Meleira do mamoeiro no estado do Espírito Santo: enfoque fitopatológico**, 1989.

RODRIGUES, S. P. et al. Papaya meleira virus is neither transmitted by infection at wound sites nor by the whitefly Trialeurodes variabilis. **Journal of Plant Pathology**, v. 91, n. 1, p. 87–91, 2009a.

RODRIGUES, S. P. et al. Effects of the Papaya meleira virus on papaya latex structure and composition. **Plant cell reports**, v. 28, n. 5, p. 861–71, 2009b.

RODRIGUES, S. P. et al. Proteomic analysis of papaya (Carica papaya L.) displaying typical sticky disease symptoms. **Proteomics**, v. 11, n. 13, p. 2592–2602, 2011.

RODRIGUES, S. P. et al. Label-free quantitative proteomics reveals differentially

regulated proteins in the latex of sticky diseased Carica papaya L. plants. **Journal of proteomics**, v. 75, n. 11, p. 3191–3198, 2012.

SÁ ANTUNES, T. F. et al. The dsRNA Virus Papaya Meleira Virus and an ssRNA Virus Are Associated with Papaya Sticky Disease. **Plos One**, v. 11, n. 5, p. e0155240, 2016.

SMALLE, J.; VIERSTRA, R. D. the Ubiquitin 26S Proteasome Proteolytic Pathway. **Annual Review of Plant Biology**, v. 55, n. 1, p. 555–590, 2004.

SPOEL, S. H.; DONG, X. How do plants achieve immunity? Defence without specialized immune cells. **Nature Reviews Immunology**, v. 12, n. 2, p. 89–100, 2012.

THINES, B. et al. JAZ repressor proteins are targets of the SCF(COI1) complex during jasmonate signalling. **Nature**, v. 448, n. 7154, p. 661–665, 2007.

VENTURA, J. A. et al. Meleira do mamoeiro: etiologia, sintomas e epidemiologia. **Papaya Brasil: Qualidade do mamão para o mercado interno. INCAPER, Vitória**, p. 267–276, 2003.

VENTURA, J. A.; COSTA, H.; PRATES, R. S. **Meleira do mamoeiro: uma ameaça à cultura,** Vitória-ES, DCM - Incaper, 2004.

VERMA, D. P. S.; HONG, Z. Plant callose synthase complexes. **Plant Molecular Biology**, v. 47, n. 6, p. 693–701, 2001.

WAGNER, T. A.; KOHORN, B. D. Wall-Associated Kinases Are Expressed throughout Plant Development and Are Required for Cell Expansion. v. 13, n. February, p. 303–318, 2001.

WALLS, P. C.; KEEGSTRA, K. Plant Cell Walls. **Plant Physiology**, v. 154, n. 2, p. 483–486, 2010.

WANG, H.; ALVAREZ, S.; HICKS, L. M. Comprehensive Comparison of iTRAQ and Label-free LC-Based Quantitative Proteomics Approaches Using Two Chlamydomonas reinhardtii Strains of Interest for Biofuels Engineering. **Journal of Proteome Research**, v. 11, n. 1, p. 487–501, 2012.

WHALEN, M. C. Host defence in a developmental context. **Molecular Plant Pathology**, v. 6, n. 3, p. 347–360, 2005.

WOLF, S.; HÉMATY, K.; HÖFTE, H. Growth Control and Cell Wall Signaling in Plants. **Annual Review of Plant Biology**, v. 63, n. 1, p. 381–407, 2012.

YAENO, T.; IBA, K. BAH1/NLA, a RING-type ubiquitin E3 ligase, regulates the accumulation of salicylic acid and immune responses to Pseudomonas syringae DC3000. **Plant physiology**, v. 148, n. 2, p. 1032–41, 2008.

ZENG, L.-R. et al. Ubiquitination-mediated protein degradation and modification: an emerging theme in plant-microbe interactions. **Cell research**, v. 16, n. 5, p. 413–426, 2006.

ZHU, W.; SMITH, J. W.; HUANG, C. Mass Spectrometry-Based Label-Free Quantitative Proteomics, 2010.

ANEXO 1

Protocolo detalhado de extração fenólica de proteínas.

PAPAYA LEAVES PROTEOMICS

for "S" samples

Material	Amount
1.5mL Tube	= S x 9
2.0mL Tube	= S x 3
5mL Tube	= S x 1
C18 Column	= S x 1
Cuvette	= S x 2
Vial	= S x 1

Phenol extraction process (2 tubes of 1.5mL and 1 tube of 5mL) approximately **2hours**

[Hurkman and Tanaka (1986) Plant Physiology 81:802-806]

Extraction buffer for "S" samples (**S x 1.0mL**)

(FRESH PREPARED)

Reagent	Concentration	Calculation
Tris-HCl (1M) pH8.0	100mM	= S x 0.1mL
SDS 10% w/v	2% w/v	= S x 0.2mL
Sucrose (342,24 $g.mol^{-1}$)	900mM	= S x 308mg
EDTA (292.24 $g.mol^{-1}$)	10mM	= S x 2.9mg
cOmplete, EDTA-free	0.1pills.mL^{-1}	= S x 0.1pills
H_2O milli-Q	q.s.	**~ = S x 1.0mL**

1- Weigh 0.01g of Lyophilized leaf tissue into a tube of 1.5mL (Tube 01)
2- Add approximately 0.01g of glass beads.
3- Add 150uL of extraction buffer
4- Grind with a 1.5 mL Pestle
5- Add more 450ul of extraction buffer (washing the pestle)
6- Add 600uL of 10 mM Tris pH 8.8-buffered Phenol pH8.8 (in the hood)

7- Vortex for 10min. at room temperature
8- Centrifuge for 10min. at 5000g and 4°C
9- Transfer the phenolic phase (top phase) for a new tube of 1.5mL (with pipette) and store (Tube 02)
10- Add 400uL of 10 mM Tris pH 8.8-buffered phenol pH8.8 into the tube with the left over aqueous phase (bottom phase) (Tube 01)
11- Vortex for 2min.
12- Centrifuge for 10min. at 5000g and 4°C
13- Transfer the phenolic phase (top phase) for the stored tube (Tube 02) with pipette
14- Centrifuge the mix of phenolic phases (Tube 02) for 10min. at 5000g and 4°C
15- Transfer the phenolic phase (top phase) for a new tube of 5mL (Tube 03) with pipette

Precipitation process (0 tubes) approximately **13hours**

16- Add 4mL of cold (-20°C) Methanolic Ammonium Acetate at 0.1M
17- Vortex quickly and incubate at -20°C overnight (12h)
18- Centrifuge for 10 min. at 20000g and 4°C
19- Discard supernatant

Washing process (1 tube of 2mL) approximately **3hours.**

20- Add 1.5mL of cold (-20°C) Methanolic Ammonium Acetate at 0.1M and homogenizer (Vortex, Pipette or Sonicator)
21- Transfer all solution for a new tube of 2mL (Tube 04)
22- Centrifuge for 10min. at 20000g and 4°C
23- Discard supernatant
24- Add 1.5mL of cold (-20°C) Methanolic Ammonium Acetate at 0.1M and homogenizer (Vortex, Pipette or Sonicator)
25- Centrifuge for 10min. at 20000g and 4°C
26- Discard supernatant
27- Add 1.5mL of cold (-20°C) Acetone 80% v/v and homogenizer (Vortex, Pipette or Sonicator)
28- Centrifuge for 10min. at 20000g and 4°C
29- Discard supernatant

30- Add 1.5mL of cold (-20°C) Methanol 70% v/v and homogenizer (Vortex, Pipette or Sonicator)
31- Centrifuge for 10min. at 20000g and 4°C
32- Discard supernatant
33- Centrifuge for 10min. at 20000g and 4°C
34- Discard supernatant by Pipette

Resuspension process (1 tube of 1.5mL) approximately **3hours.**

Resuspension buffer for "S" samples (**S x 200uL**)
(FRESH PREPARED)

Reagent	Concentration	Calculation
Tris-HCl (1M) pH8.0	50mM	= S x 10uL
Urea (60.07g.mol^{-1})	8M	= S x 96.1mg
Thiourea (76.12g.mol^{-1})	2M	= S x 30.4mg
H_2O milli-Q	q.s.	**~ = S x 200uL**

35- Add 180uL of resuspension buffer to dried precipitate (Tube 04)
36- Maximum homogenizer (4 x Pipette and 30min. on Thermomixer 25°C and 800 rpm), without heat to avoid bobbles and foam formation
37- Centrifuge at 16000g for 5min.
38- Transfer the supernatant for a new tube of de 1.5mL (Tube 05)

Quantification process in duplicate (2 tubes of 1.5mL and 2 Curvets of 1cm or a 96 well plate) approximately **20min.**
[CB-X kit]

39- Transfer 5uL of protein solution (Tube 05) for two new tubes of 1.5mL (Tubes 06 and 07)
40- Add 1mL of cold CB-X (-20°C) to quantifications´ aliquots (Tubes 06 and 07) and vortex
41- Centrifuge at 16000g for 5min.
42- Discard supernatant
43- Add 50uL of CB-X solubilization buffer I and 50uL of solubilization buffer II and vortex

44- Add 1mL of CB-X assay dye and vortex
45- Incubate for 5min. at room temperature
46- Read the absorbance at 595nm against water in a cuvette with 1cm optical path or in a 96 well plate with 200uL each well
47- Compare with the Table to calculate the concentration "C" in ug.uL^{-1} of protein solution.

Reduction process (2 tubes of 1.5mL) approximately **50min.**

48- Aliquot "V" uL, enough for 100ug of protein solution (Tube 05) in new tubes of 1.5mL (Tubes 08, 09) and **store tube 09 at -80°C** (V = 100 x C^{-1})
49- Add "X" uL of 500mM Dithiothreitol (DTT) to aliquot (Tube 08) enough to 5mM DTT concentration (X= 0.01 x V)
50- Incubate for 45min. at 37°C on Thermomixer at 800 rpm

Alkylation process (0 tubes) approximately **45min.**

51- Add "Y" uL of 500mM Iodoacetamide to reduced aliquots (Tube 08) enough to 100mM Iodoacetamide concentration (Y= 0.2 x V)
52- Incubate for 40 min. at 25°C on Thermomixer at 800 rpm, **protected from light**

Digestion process (0 tubes) approximately **17hours**

53- Add "A" uL of 50mM Tris-HCl pH8.8 to alkylated aliquot (Tube 08) to dilute to 1.0M Urea concentration (A = 7 x V)
54- Add "Z" uL of "W" ug.uL^{-1} Trypsin solution to 50:1 (Protein/Trypsin) (Z = 2 x W^{-1})
55- Incubate at 37°C for 16h on Thermomixer at 800 rpm.
56- Add "B" uL of 5% v/v Formic Acid enough to 0.2% v/v Formic Acid concentration to quench the digestion (B = 0.32 x V)
57- Check the pH of the samples by pH paper strips (need be ≤ 3).

Desalinization process (2 tubes of 2.0mL, 2 tubes of 1.5mL and 1 Pierce c18 spin column) approximately **2hours**

58- Check the volume of each peptide solution sample with pipet ("F" uL)

59- Take “G” uL of peptide solution enough to 30ug in a new 1.5mL tube (Tube 10). (G = 0.3 x F)
60- Add “H” uL of Sample solution (2% v/v Trifluoroacetic acid + 20% v/v Acetonitrile) (H = 0.33 x G)
61- Homogenize with pipet
62- Tap column to settle resin. Remove top and bottom cap. Place column into a new 2.0mL tube (Tube 11).
63- Add 200uL of Activation solution (50% v/v Methanol) by the walls to rinse.
64- Centrifuge at 1500g for 1min. and discard flow-through
65- Repeat the steps “63” and “64”.
66- Add 200uL of Equilibrate solution (0.5% v/v Trifluoroacetic acid + 5% v/v Acetonitrile)
67- Centrifuge at 1500g for 1min. and discard flow-through
68- Repeat the steps “66” and “67”.
69- Place the column in a new 2.0mL tube (Tube 12)
70- Load sample on top of resin bed
71- Centrifuge at 1500g for 1min. and **SAVE** flow-through
72- Load flow-through on top of resin bed.
73- Repeat the step “71”
74- Repeat the steps “72” and “73”. Store the flow-through at -80°C until confirm the desalinization successful.
75- Place the column in an old 2mL tube (Tube 11)
76- Add 200uL of Wash solution (0.5% v/v Trifluoroacetic acid + 5% v/v Acetonitrile)
77- Centrifuge at 1500g for 1min. and discard flow-through
78- Repeat the steps “76” and “77”
79- Repeat the step “78”
80- Place the column into a new 1.5mL tube (Tube 13)
81- Add **30uL** of Elution Buffer (70% v/v Acetonitrile + 0.1% v/v Formic acid)
82- Centrifuge at 1500g for 1min.
83- Repeat the steps “81” and “82”
84- Repeat the step “81”
85- Return the top and bottom cap to column. Store the column at -80°C until confirm the desalinization successful.
86- Freeze flow-through (Tube 13) at -80°C than dry in a vacuum evaporator (1hour)
87- Store at -80°C

LC/MS preparation process (1 Vial of 2mL) approximately **1hour**

88- Add 150uL of LC mobile phase (5% v/v Acetonitrile + 0.1% v/v Formic Acid) (Final concentration 0.2ug.uL^{-1})
89- Vortex quickly
90- Incubate for 10min. at 25°C in Thermomixer at 1000rpm
91- Centrifuge at 20000g for 5min. at 25°C
92- Transfer 20uL of the top phase to a new 2mL Vial (Pipet gently and by the walls to avoid bobbles)
93- Store the sample´s rest on -80°C
94- Close the Vail and Centrifuge (spin down) until 7000rpm on bench-top centrifuge.
95- Double check for little bobbles.

ANEXO 2

Protocolo detalhado de Cromatografia líquida acoplada à espectrometria de massas de peptídeos (LC-MS/MS).

LC-MS/MS parameters

- nanoAcquity UPLC (Waters) - nanoACQUITY Ultra Performance LC System
- TripleTOF 5600 (AB Sciex) – Triple quadrupole time-of-flight System
- NanoSpray III Ion Source and Heated Interface (AB Sciex)
- Analyst TF 1.5.1 software (AB Sciex)

Mass spectrometry parameters

	TOF MS (MS)	Product Ion (MS/MS)
MS		
Experiment	1	2
Scan Type	TOF MS	Product Ion
Accumulation time	0.249966 sec	0.085039 sec
Polarity	+	+
Duration	118.993 min	119.995 min
Cycle time	2.0021 sec	0.0021 sec
Cycles	3566	3566
Period	1	1
Delay Time	0 sec	0 sec
Experiment Type	IDA	IDA
TOF Masses (Da)	350-1600	100-1800
High Sensitivity	-------	✓
Advanced MS		
Auto Adjust with mass	✓	✓
Q1 Transition window	330.000 (Da); 100.0000%	80.000 (Da); 50.0415% 230.000 (Da); 49.9585%
Time bins to sum	4	4
TDC channels	1-4	1-4
Resolution	-------	UNIT
Setting time	0 ms	0 ms
Pause between mass ranges	1.068 ms	1.059 ms
Switch Criteria		
With charge state	2-5	2-5
which exceeds	150 cps	150 cps
Mass Tolerance	100 ppm	100 ppm
Candidate ions to monitor per cycle	20	20
Exclude former target ions for	8 sec	8 sec
IDA Advanced		
Rolling collision energy	✓	✓

ACQUITY UPL System

nACQUITY SM Method	nACQUITY BSM Method
- Loop Option: Partial Loop	- Application Mode: Single Pump Trapping
- Loop Offline: Disable	- Pump Type: BSM1
- Weak Wash Solvent Name: Water (+0.1% F. A.)	- Solvent Selection A: A1
- Weak Wash Volume: 600 uL	- Solvent Selection B: B1
- Strong Wash Solvent: Acetonitrile (+0.1% F. A.)	- Seal Wash: 5.0 min (Water + 10% ACN)
- Strong Wash Volume: 200 uL	- Switch 1: No Change
- Target Column Temperature: 45.0 C	- Switch 2: No Change
- Column Temperature Alarm Band: Disable	- Switch 3: No Change
- Full Loop Overvill Fractor: Automatic	- Chart Out 1: System Pressure
- Syringe Draw Rate: Automatic	- Chart Out 2: %B
- Needle Placement: Automatic	- Run Events: Yes
- Pre-Aspirate Air Gap: Automatic	- Analytical Low Pressure Limit: 0 psi
- Post-Aspirate Air Gap: Automatic	- Analytical High Pressure Limit: 10000 psi
- Column Temperature Data Channel: No	- Sample Loading Time: 3.00 min
- Ambient Temperature Data Channel: No	- Trapping Flow Rate: 5.000 uL/min
- Sample Temperature Data Channel: No	- Trapping %A: 99.9
- Sample Pressure Data Channel: No	- Trapping %B: 0.1
- Switch1: No Change	- Trapping Low Pressure Limit: 0 psi
- Switch2: No Change	- Trapping High Pressure Limit: 10000 psi
- Switch3: No Change	- Flow Rate A Data Channel: No
- Switch4: No Change	- Flow Rate B Data Channel: No
- Chart Out: Sample Pressure	- Solvent Name A: Water (+0.1% F. A.)
- Sample Temp Alarm: Disable	- Solvent Name B: Acetonitrile (+0.1% F. A.)
- Column Temp Alarm: Disable	- System Pressure Data Chanel: No
- Run Events: Yes	- Flow Rate Data Channel: No
- SampleLoop: 10.00	- %A Data Channel: No
- Saved as Trizaic: No	- Primary A Pressure Data Channel: No
- nanoTitle Cool Down: 2.4	- Accumulator A Pressure Data Channel: No
	- Primary B Pressure Data Channel: No
	- Degasser Pressure Data Channel: No

Run Time: 120.00 min

Gradient Table

Time	Flow Rate	%A	%B	Curve
Initial	0.300	95.0	5.0	------
90.00	0.300	60.0	40.0	6
95.00	0.300	15.0	85.0	6
105.00	0.300	15.0	85.0	6
107.00	0.300	95.0	5.0	6
120.00	0.300	95.0	5.0	6

ANEXO 3

Protocolo detalhado de quantificação (Progenesis QI for proteomics software) e identificação (Mascot software), livre de marcação, de proteínas.

Progenesis QI for proteomics

- Import Samples raw Data (.wiff)
- Apply mask (Masked Areas) one by one: (<25 min) and (>125 min)
- Review Alignment
    - Apply Manual Vectors and then align runs automatically (do that run by run)
    - Aligning enough to at least 80%
- Filtering: Inside Area: 25 to 105 min
    - Delete Non-Matching peptide ions
- Experiment Design Setup
    - Between-Subject Design
        - ➥ Name: Healthy or Diseased
- Review Peak Picking
- Peptide Ion Statistics
- Identify Peptides
    - Export MS/MS spectra to **Mascot**
    - Import Results from Mascot
- QC Metrics
    - * **Go to Refine Identification first**
    - Then, Report All Metrics
    - Experiment Metrics → Protein per condition → Add to Clip Gallery
- Refine Identifications
    - Apply filter **Score**: Less Than 13 (Based on p<0.05 of Mascot Percolator filter)
        - ➥ Delete Matching Search Results → Reset the Criteria
    - Apply filter **Hits**: Less Than 2
        - ➥ Delete Matching Search Results → Reset the Criteria
    - Apply filter Mass error (ppm): Greater than 20 (based on Calibration runs)
        - ➥ Delete Matching Search Results → Reset the Criteria
    - * **Go back to QC Metrics**
- Resolving Conflicts
    - Protein Options → Relative Quantification using Hi-N → 3
    - Employ protein grouping
- Review Proteins
    - Export Protein Measurements
    - Export Peptide Measurements
    - Export Peptide Ion data

Mascot MS/MS Ion Search

- Database: Papaya 2015
- Enzime: Trypsin
- Allow up to: 2 missed cleavages
- Quantification: None
- Taxonomy: All entries
- Fixed Modification: None selected
- Variable Modification:
  - ↳ Acetyl (Protein N-term)
  - ↳ Carbamidomethyl (C)
  - ↳ Deamidated (N Q)
  - ↳ Oxidation (M)
- Peptide tol.: ± 20 ppm
- # ^{13}C: 0
- MS/MS tol.: ± 0.05 Da
- Peptide charge: 2+, 3+ and 4+
- Monoisotopic: ✓
- Data File: from Progenesis (.mgf)
- Data format: Mascot Generic
- Precursor: ---- *m/z*
- Instrument: Default
- Decoy: ✓
- Report top: Auto hits

Protein family summary

- ↳ Significance threshold p<: 0.05
- ↳ Max. number of families: Auto
- ↳ Ion score or expected cut-off: 0
- ↳ Dendrograms cut at: 0
- ↳ Show percolator scores: ✓
- ↳ Preferred taxonomy: All entries

- Apply filter

➪ Export as : XML

Export search results

Export format: XML

Significance threshold p<: 0.05 at homology

Protein scoring: MudPIT

- ✓ Group protein families

Search information

- ✓ Holder
- ✓ Decoy
- ✓ Modification deltas
- ✓ Search parameters
- ✓ Format parameters

Protein Hit Information

- ✓ Score
- ✓ Description
- ✓ Mass (Da)
- ✓ Number of queries matched

Peptide Match Information

- ✓ Experimental Mr (Da)
- ✓ Experimental charge
- ✓ Calculated Mr (Da)
- ✓ Mass error (Da)
- ✓ Number of missed cleavages
- ✓ Score
- ✓ Expectation value
- ✓ Sequence
- ✓ Variable Modification
- ✓ Query title
- ✓ Show duplicate peptides

➪ Export search results